nagra National Cooperative for the Disposal of Radioactive Waste

TECHNICAL REPORT 95-08

The Radiolytic and Chemical Degradation of Organic Ion Exchange Resins under Alkaline Conditions: Effect on Radionuclide Speciation

September 1995

L.R. Van Loon
W. Hummel

PSI, Würenlingen and Villigen

Hardstrasse 73, CH-5430 Wettingen/Switzerland, Telephone +41-56-437 11 11

nagra National Cooperative for the Disposal of Radioactive Waste

TECHNICAL REPORT 95-08

The Radiolytic and Chemical Degradation of Organic Ion Exchange Resins under Alkaline Conditions: Effect on Radionuclide Speciation

September 1995

L.R. Van Loon
W. Hummel

PSI, Würenlingen and Villigen

Hardstrasse 73, CH-5430 Wettingen/Switzerland, Telephone +41-56-437 11 11

This report was prepared on behalf of Nagra. The viewpoints presented and conclusions reached are those of the author(s) and do not necessarily represent those of Nagra.

PREFACE

The waste Management Laboratory at the Paul Scherrer Institute is performing work to develop and test models as well as to acquire specific data relevant to performance assessment of Swiss nuclear waste repositories. These investigations are undertaken in close co-operation with, and with the partial financial support of, the National Cooperative for the Disposal of Radioactive Waste (Nagra). The present report is issued simultaneously as PSI-Bericht and Nagra Technical Report.

CONTENT

		Page
CONTENTS		I
ABSTRACT		III
RESUME		V
ZUSAMMENFASSUNG		VII
LIST OF FIGURES		IX
LIST OF TABLES		XIII
1	INTRODUCTION	1
2	THE DEGRADATION OF HEIGH MOLECULAR WEIGHT ORGANICS : GENERAL ASPECTS	3
2.1	Classification of polymers	3
2.2	Chemical (alkaline) degradation	4
2.3	Radiolytic degradation	4
3	THE DEGRADATION OF STRONG ACIDIC ION EXCHANGE RESINS	7
3.1	The ion exchange method to study metal-ligand interactions	7
3.1.1	The basic ion exchange method	7
3.1.2	The ion exchange method at different pH values	8
3.1.3	Titration of ligand L with metal M in presence of an ion exchange resin	10
3.2	Materials and methods	14
3.2.1	Irradiation of the ion exchange resins	14
3.2.2	pH-measurements	15
3.2.3	Organic and inorganic carbon measurements	15
3.2.4	Sulphate, Na^+ and oxalate	15
3.2.5	Cu-titrations	15
3.2.6	The ion exchange method with Ni^{2+}	16
3.3	Results and discussion	17
3.4	Conclusions	27
3.5	The influence of degradation products on Ni-speciation	27
3.5.1	Introduction	27
3.5.2	The thermodynamic data base	29

3.5.3	Oxalate	42
3.5.4	Ligand X	50
4	THE DEGRADATION OF STRONG BASIC ANION EXCHANGE RESINS AND MIXED BED ION EXCHANGE RESINS	58
4.1	Materials and methods	58
4.1.1	Irradiation of anion exchange resins	58
4.1.2	Irradiation of mixed bed ion exchange resins	59
4.1.3	Analytical procedures	59
4.1.4	Adsorption studies	60
4.2	Results and discussion	62
4.2.1	Degradation products of anion exchange resins	62
4.2.2	Degradation products of mixed bed resins	66
4.2.3	Adsorption of Eu on calcite	67
4.3	Speciation of radionuclides in the presence of degradation products	68
4.3.1	General overview	68
4.3.2	Speciation calculations for nickel and palladium	70
4.3.3	Detailed inspection of the system Pd(II)-H_2O-NH_3	72
5	GENERAL CONCLUSIONS	85
6	REFERENCES	88
7	ACKNOWLEDGEMENTS	96

ABSTRACT

The formation of water soluble organic ligands by the radiolytic and chemical degradation of several ion exchange resins was investigated under conditions close to those of the near field of a cementitious repository. The most important degradation products were characterised and their role on radionuclide speciation evaluated thoroughly.

Irradiation of strong acidic cation exchange resins (Powdex PCH and Lewatite S-100) resulted in the formation of mainly sulphate and dissolved organic carbon. A small part of the carbon (10-20 %) could be identified as oxalate. The identity of the remainder is unknown. Complexation studies with Cu^{2+} and Ni^{2+} showed the presence of two ligands: oxalate and ligand X. Although ligand X could not be identified, it could be characterised by its concentration ($[X]_T \sim 10^{-5} - 10^{-6}$ M), a deprotonation constant ($pK_H \sim 7.4$ at I = 0.1 M) and a complexation constant for the NiX complex ($\log K_{NiX} \sim 7.0$ at I = 0.1 M). The influence of oxalate and ligand X on the speciation of radionuclides is examined in detail. For oxalate no significant influence on the speciation of radionuclides is expected. The stronger complexing ligand X may exert some influence depending on its concentration and the values of other parameters. These critical parameters are discussed and limiting values are evaluated.
In the absence of irradiation, no evidence for the formation of ligands was found.

Irradiation of strong basic anion exchange resins (Powdex PAO and Lewatite M-500) resulted in the formation of mainly ammonia, amines and dissolved organic carbon. Up to 50 % of the carbon could be identified as methyl-, dimethyl- and trimethylamine. Complexation studies with Eu^{3+} showed that the complexing capacity under near field conditions was negligible. The speciation of cations such as Ag, Ni, Cu and Pd can be influenced by the presence of amines. The strongest amine-complexes are formed with Pd and therefore, as an example, the aqueous Pd-ammonia system is examined in great detail.
In the absence of irradiation, no evidence for the formation of ligands was found.

Irradiation of a mixed bed ion exchange resin (Amberlite MB-1) yielded small amounts of sulphate and amines, and a large amount of dissolved organic carbon. Only 3 % of the carbon could be identified as methyl-, dimethyl- and trimethylamine. The major part remained unknown. Complexation studies with Eu^{3+}, however, showed that the complexing capacity under near field conditions was negligible.

In the absence of irradiation, no evidence for the formation of ligands was found.

RESUME

La formation des ligands organiques solubles dans l'eau issus de la décomposition radiolytique et chimique de différentes résines échangeuses d'ions a été étudiée dans des conditions similaires à celles que l'on trouve dans le champs proche d'un dépôt de déchets radioactifs cimentés. Les principaux produits de la décomposition ont été caractérisés et leur rôle concernant la spéciation des radionucléides est discuté en détail.

L'irradiation des résines échangeuses de cations, à caractère très acide (Powdex PCH et Lewatit S-100), engendre principalement la formation de sulfate et de carbone organique dissouts. Seule une faible proportion de ce carbone (20 %) a pu être identifiée comme étant de l'oxalate alors que la majeure partie demeure encore non identifiée. Des études de complexation avec des cations tels que Cu^{2+} et Ni^{2+} ont révélés la présence de deux ligands: l'oxalate et un ligand X. Bien que le ligand X n' ait pu être identifié, sa concentration (10^{-5}-10^{-6} M), sa constante de déprotonation (pK_H ~ 7.4 pour I = 0.1 M) et sa constante de complexation avec Ni^{2+} ($\log K_{NiX}$ ~ 7 pour I = 0.1 M) ont pu être évaluées. L'influence sur la spéciation des nucléides de l'oxalate et du ligand X a été examinée en détail. En ce qui concerne l'oxalate cette dernière n'est pas significative. Par contre, le ligand X, fortement complexant, peut exercer une influence. Celle ci dépend de sa concentration et de certains paramètres tels que le pH, le P_{CO_2} et la complexation avec Ca^{2+} et Mg^{2+}. Les valeurs limites de ces paramètres ont été évaluées.
En l'absence d'irradiation aucune formation de ligand n'a été observée.

D'un autre côté, l'irradiation de résines échangeuses d'anions, à caractère très basique (Powdex PAO, Lewatit M-500), engendre principalement la formation d'ammoniaque, d'amines et de carbone organique dissout. 50 % de ce carbone a pu être identifié comme étant présent sous la forme de methyl-, dimethyl- et trimethylamine. Des études de complexation avec Eu^{3+} ont montré que la capacité de complexation des produits de dégradation était négligeable dans les conditions du champ proche d'un dépôt cimenté. Par ailleurs la spéciation de l' Ag^{+}, du Pd^{2+} et en moindre mesure celle du Ni^{2+} et du Cu^{2+} peut être influencée par la présence d'amines. Les complexes d'amine les plus stables sont formés avec le Pd^{2+}, c'est pourquoi le système aqueux Pd-ammoniaque a été étudié en détail.

En l'absence d'irradiation aucun ligand n'a été détecté.

L'irradiation d'une résine mixte échangeuse d'anion et de cation (Amberlite MB-1) produit une faible quantité de sulfate et d'amine pour une grande proportion de carbon organique dissout. Seulement 3 % de cette quantité de carbone ont pu être attribués à des methyl-, dimethyl- et trimethylamine alors que la majeure partie n'a pu être identifiée. Cependant, des essais de complexation avec Eu^{3+} ont montré que la capacité de complexation de ces produits était négligeable dans les conditions d'un dépôt cimenté.
En l'absence d'irradiation aucun ligand n'a été détecté.

ZUSAMMENFASSUNG

Ionentauscherharze können sich durch radioaktive Bestrahlung und chemische Angriffe bei hohem pH zersetzen und dabei wasserlösliche organische Liganden bilden. Diese Abbauvorgänge wurden unter Bedingungen untersucht, die denen nahekommen, die im Nahfeld eines zementhaltigen Endlagers herrschen. Die wichtigsten Abbauprodukte wurden charakterisiert und ihr Einfluss auf die Speziation von Radionukliden wird beleuchtet.

Bei der Bestrahlung stark saurer Kationentauscherharze (Powdex PCH und Lewatit S-100) bilden sich hauptsächlich Sulfat und löslicher organischer Kohlenstoff. Ein kleiner Teil dieses Kohlenstoffs (10-20%) liegt als Oxalsäure vor. Der grössere Teil gehört zu unbekannten Verbindungen. Untersuchungen zum Komplexierungsverhalten von Cu^{2+} und Ni^{2+} deuten auf die Anwesenheit zweier starker Liganden hin: Oxalsäure und ein unbekannter Ligand X. Dieser Ligand X wird bei den Versuchen in Konzentrationen von 10^{-5} bis 10^{-6} M gefunden, hat eine Deprotonierungskonstante von $pK_H \approx 7.4$ und eine Komplexierungskonstante mit Ni^{2+} von $\log K_{NiX} \approx 7$ (beide bei I = 0.1 M). Der Einfluss von Oxalsäure und Ligand X auf die Speziation von Radionukliden wird ausführlich abgehandelt. Es zeigt sich, dass für Oxalsäure kein Einfluss auf die Komplexbildung von Radionukliden zu erwarten ist. Der stärker komplexierende Ligand X hingegen kann einigen Einfluss ausüben, wobei dieser Einfluss von seiner Konzentration und anderen Parametern abhängt. Grenzwerte für diese Parameter werden angegeben.
Ohne Bestrahlung fanden sich keine komplexierenden Liganden in den Abbauprodukten.

Bei der Bestrahlung stark basischer Anionentauscherharze (Powdex PAO und Lewatit M-500) bilden sich hauptsächlich Ammoniak, Amine und löslicher organischer Kohlenstoff. Bis zu 50 % dieses Kohlenstoffs ist in Methyl-, Dimethyl- und Trimethylamin vorhanden. Versuche zur Komplexbildung mit Eu^{3+} zeigten, dass die Komplexbildungskapazität der Abbauprodukte unter den Bedingungen des Nahfeldes vernachlässigbar klein ist. Jedoch kann die Speziation von Ag und Pd, und in geringem Ausmass auch von Ni und Cu, durch Amine beeinflusst werden. Die stärksten Aminkomplexe bildet dabei

Pd, und deshalb wird als Beispiel das System Pd-Ammoniak-Wasser ausführlich abgehandelt.
Ohne Bestrahlung fanden sich keine komplexierenden Liganden in den Abbauprodukten.

Nach der Bestrahlung eines gemischten Kationen/Anionentauscherharzes (Amberlit MB-1) fanden sich kleine Mengen an Sulfat und Aminen und eine grosse Menge löslichen organischen Kohlenstoffs. Nur 3 % dieses Kohlenstoffs konnten Methyl-, Dimethyl- und Trimethylamin zugeordnet werden, während der grösste Teil zu unbekannten Verbindungen gehört. Versuche zur Komplexbildung mit Eu^{3+} zeigten jedoch, dass die Komplexbildungskapazität der Abbauprodukte unter den Bedingungen des Nahfeldes vernachlässigbar klein ist.
Ohne Bestrahlung fanden sich keine komplexierenden Liganden in den Abbauprodukten.

LIST OF FIGURES

page

Figure 1: Evolution of $K_d^o / K_d - 1$ as a function of the pH for different values of $\log K_H$ ($\log K_{ML} = 5$ and $\log L_T = -5$). 9

Figure 2: Evolution of $K_d^o / K_d - 1$ as a function of the total metal concentration in solution (M_T) for a ligand concentration of $\log L_T = -6$. 11

Figure 3: Evolution of $K_d^o / K_d - 1$ as a function of the total metal concentration (M_T) for a solution containing two ligands L_1 and L_2. 13

Figure 4: Titration of the Powdex PCH solutions (PB1 and PU1) with Cu^{2+} at pH = 6 and I = 0.1 M. 20

Figure 5: Titration of the Lewatite S-100 solutions (LB1 and LU1) with Cu^{2+} at pH = 6 and I = 0.1 M. 20

Figure 6: Evolution of $K_d^o / K_d - 1$ as a function of pH for an irradiated solution (Powdex = PB2 and Lewatite = LB2). 24

Figure 7: Evolution of $K_d^o / K_d - 1$ as a function of the total Ni-concentration in solution ($\log Ni_T$). 26

Figure 8: The Irving-Williams series for transition metal complexation (IRVING & WILLIAMS 1953). 30

Figure 9: Correlation of the stepwise formation constants of metal oxalate 1:1 and 1:2 complexes. 31

Figure 10: The first protonation constants of organic ligands plotted against the stability constants of their 1:1 Ni-organic complexes. 39

Figure 11: Stability constants of Ni and Ca 1:1 complexes with common organic oxo-ligands. 40

Figure 12a: Correlation of stepwise formation constants of 1:1 and 1:2 metal-organic complexes. 41

Figure 12b: Correlation of stepwise formation constants of 1:2 and 1:3 metal-ligand complexes. 42

Figure 13a: The influence of oxalate on the complexation of Ni in groundwaters at P_{CO_2} = 10^{-2} bar. For any given pH and Ca + Mg concentration the amount of oxalate shown by the surface is needed to reach 50% Ni-oxalate complexation. 43

Figure 13b: The influence of oxalate on the complexation of Ni in groundwaters at P_{CO_2} = 10^{-2} bar. The amount of oxalate needed to complex 50% Ni can be directly read from the contour lines. 44

Figure 14a: The influence of oxalate on the complexation of Ni in groundwater at [Ca + Mg] = 10^{-3} M. The 50% organic complexation surface is shown. 45

Figure 14b: The same results as Fig.14a but shown as contour plot. 46

Figure 15a: The influence of oxalate on the complexation of Ni in cement pore waters. The maximum values in Table 7 are used for the speciation calculations. The 50% organic complexation surface is shown. 48

Figure 15b: The same results as Fig.15a but shown as contour plot. 49

Figure 16a: The influence of ligand X on the complexation of Ni in groundwaters at P_{CO_2} = 10^{-2} bar. The maximum values in Table 7 are used for the speciation calculations. The 50% Ni-organic complexation surface is shown. 50

Figure 16b: The same results as Fig.16a but shown as contour plot. 51

Figure 17: The influence of estimated stability constants for ligand X on the complexation of Ni in groundwaters at P_{CO_2} = 10^{-2} bar. The 50% Ni-organic complexation surfaces are shown. 52

Figure 18: The influence of estimated stability constants for ligand X on the complexation of Ni in groundwaters. 50% contour lines are shown. 53

Figure 19a: The influence of ligand X on the complexation of Ni in cement pore waters. The maximum values in Table 7 are used for the speciation calculations. The 50% Ni-organic complexation surface is shown. 54

Figure 19b: The same results as Fig.19a but shown as contour plot. 55

Figure 20: The influence of estimated stability constants for ligand X on the complexation of Ni in cement pore waters. The 50% Ni-organic complexation surfaces are shown. 57

Figure 21: Schematic view of the degradation cell used for the radiolytic degradation of anion and mixed bed ion exchange resins. 60

Figure 22: Effect of radiolytic and chemical degradation products of anion and mixed bed resins on the adsorption of Eu on calcite at pH 12.6 and I = 0.1 M. 67

Figure 23: Selected stability constants of metal-amine complexes as a function of the number of methyl groups. 69

Figure 24: The influence of ammonia on the complexation of Ni and Pd in cement pore waters. The 50% metal-ammonia complexation surfaces are shown. 71

Figure 25: Predominance diagram of the system Pd(II)-H_2O-NH_3. The predominance areas of species are limited by 50% lines. 74

Figure 26: Predominance diagram of the system Pd(II)-H_2O-NH_3 including mixed ammonia-hydroxo complexes into the model. 76

Figure 27: Predominance diagram of the system Pd(II)-H_2O-NH_3. The consecutive formation constants of the mixed complexes are increased by one order of magnitude compared with Fig.26. 78

Figure 28: Predominance diagram of the system Pd(II)-H_2O-NH_3. Predicted hydrolysis constants of BROWN & WANNER (1987) are used instead of NABIVANETS & KALABINA (1970) data as in Figs. 25 to 27. 80

Figure 29: Solubility of "$Pd(OH)_2$", palladium oxide hydrate and PdO. 81

Figure 30: The concentration of ammonia needed in order to complex 50% Pd in solution (valid for $[Pd]_{total} \leq 10^{-6}$ M). 83

LIST OF TABLES

Table 1: Stability of common plastics. 5

Table 2: Characteristics of the irradiated and non-irradiated (cation) resin waters. 18

Table 3: Overview of the logK and $\log L_T$ values derived from the titrations of the resin-waters with Cu^{2+} at pH = 6 and I = 0.1 M. For comparison, results for bitumen and oxalate have been given. 21

Table 4: $K_d^o / K_d - 1$ and F values for the different concentrations of oxalate at different pH values. 21

Table 5: Parameters used to fit the experimental results of the pH experiment. 25

Table 6: Parameters used to fit the experimental results of the titration experiments with Ni^{2+}. 25

Table 7: Thermodynamic Database. 32

Table 8: Characteristics of the irradiated and non-irradiated (anion and mixed bed) resin waters. 63

Table 9: Measured and calculated total organic carbon content in irradiated Powdex PAO and Lewatite M-500 resin solutions. 65

Table 10: The stability of Pd(II) complexes with (poly)amine ligands. 77

1. INTRODUCTION

In Switzerland low- and intermediate level radioactive waste will be emplaced in an underground repository (SMA-repository) (NAGRA 1992). The use of large amounts of cement in constructing this repository causes an alkaline environment (pH of the cement porewater is 13.3). This ensures a slow release of most of the radionuclides because of their strong sorption on the cement phase (NAGRA 1994).

Low and intermediate level radioactive waste may contain substantial amounts of organic materials such as bitumen, cellulose, ion exchange resins, plastics and wood. Degradation of these organic waste forms under alkaline conditions, by radiolysis and by microbial action is a source of concern in radioactive waste management. It is possible that small water-soluble, organic ligands may be generated from these waste forms that could influence the chemistry of the near field resulting in a decrease of the sorption of radionuclides on the cement phase. This would enhance the release of radionuclides into the geosphere.

At the present state, the potential influence of these processes is still speculative because only a few experimental data are available.

Organic ion exchange resins form a large part of these organic waste forms: the total amount of resins to be disposed is estimated to be $2 \cdot 10^6$ kg (NAGRA 1994). Although the effect of radiation on ion exchange resins has been studied intensively, the work has focussed on the effect of radiation on the physical properties of the resins and on the generation of gaseous degradation products (MOHORCIC & KRAMER 1968, GANGWER et al. 1973, SEMUSHIN et al. 1979, BARLETTA et al. 1982, SWYLER et al. 1983, McCONNELL et al. 1993) and almost no information is available on the water soluble radiolytical degradation products.

In this work, we discuss the formation of water soluble organic ligands by irradiation of strong acidic, strong basic and mixed bed ion exchange resins under conditions close to those of the near field of a repository. The potential effect of the formed ligands on speciation of radionuclides and on their sorption behaviour will be discussed in detail.

In parallel, the alkaline degradation of the resins in absence of an irradiation field has been studied and evaluated.

The microbial degradation has not been treated in this study, although it has been shown recently that micro-organisms (bacteria) can survive under alkaline conditions (WENK 1993) so that their activity can't be ruled out.
The present level of knowledge in this field, however, does not allow more than guesses about possible microbiological effects and a more detailed study might be necessary.

2 THE DEGRADATION OF HEIGH MOLECULAR WEIGHT ORGANICS : GENERAL ASPECTS

2.1 Classification of polymers

The degradation of polymers under near field conditions can occur by two different mechanisms:

- radiolytic degradation
- chemical (alkaline) degradation

The former degradation is caused by the radiation field present in the repository, the latter is caused by the high pH of the cement pore water.
With respect to the alkaline degradation, polymers can be divided in two main classes:

- **"polymers insensitive to alkali"**. These are the so called addition polymers in which the monomers are molecules with multiple bonds which undergo true addition reactions (e.g. polystyrene, polyethylene, bitumen, natural rubber). These polymers have no functional groups in the main chain. Reaction (1) illustrates the addition reaction of n ethylene molecules to polyethylene:

$$n\ CH_2 = CH_2 \rightarrow [-CH_2-CH_2-CH_2-CH_2]_{n/2} \qquad (1)$$

- **"polymers sensitive to alkali"**. These are mainly condensation polymers in which a small molecule (usually water) is eliminated during condensation of any two monomer units (e.g. cellulose, polyester, nylon, proteins). These polymers contain regularly recurring functional group linkages in their main chain. Reaction (2) shows the condensation of n adipic acid and n hexamethylenediamine molecules to polyhexamethylene dipamide:

$$n\ HOOC-(CH_2)_4-COOH + n\ H_2N-(CH_2)_6-NH_2 \rightarrow [-NH-CO-(CH_2)_4-CO-NH-(CH_2)_6]_n + 2n\ H_2O \qquad (2)$$

2.2 Chemical (alkaline) degradation

The chemical structure of polymers control their stability to chemical attack. During alkaline degradation, the degradation reaction is initiated by a nucleophylic attack of the OH^- ion on the polymer chain or by a deprotonation reaction. The nucleophilic attack starts on a carbon atom with a partial positive charge. Such carbon atoms are in general not present in the typical addition polymers such as polystyrene and polyethylene, but abundant in condensation polymers such as cellulose. As already mentioned, addition polymers are insensitive to OH^-. Condensation polymers, on the other hand, will degrade to their composing monomers or to degradation products of these monomers, depending on the stability of the monomer under alkaline conditions. An overview of the stability of different polymers is given in Table 1.

2.3 Radiolytic degradation

Almost all organic substances are sensitive to irradation. The sensitivity, however, depends strongly on their chemical composition and on environmental factors such as the presence of oxygen. The chemical changes they undergo comprise

a) the formation of chemical bonds between different molecules
b) the irreversible cleavage of bonds resulting in fragmentation
c) the formation of unsaturated bonds
d) the disappearance of unsaturated bonds

In the case of polymers, process a) results in the so called intermolecular crosslinking whereas chain scission (process b) of main bonds leads to degradation (BOVEY 1958). Consequently, irradiation has a pronounced effect on the physical properties of polymers.
For the radiolytic degradation of polymers, process b) is very important. It is generally observed that irradiation of polymers leads to the production of small radicals such as $\cdot H$, $\cdot CH_3$, $\cdot CO$, $\cdot CO_2$. These radicals can recombine with the polymer itself or with each other, the latter resulting in the formation of H_2,

CH_4, C_2H_4. The irradiation of polymers (and organics in general) thus leads mainly to the formation of small gaseous products.

Table 1: Stability of common plastics (in SISMAN et al. 1963).

Material	polymer type[h]	heat stability[g]	Action by chemicals agents[a]		
			acids[b]	alkalies[b]	solvents
Phenol-formaldehyde:					
-unfilled or fabric filled	CP	220-250	A	A	N
-glass filled	CP	350-450	A[c]	A	N
Urea-formaldehyde:					
-cellulose filled	CP	170	A[d]	A	N
Melamine-formaldehyde	CP	210	A	A	N
Alkyds	CP	250[e]	A[c]	A	some
Polyamides	CP	270-300	A	N	N
Poly(vinyl chloride)	AP	120-160	N	N	some
Poly(vinyl acetate)	CP	f	A[d]	A	A
Poly(vinylidene chloride)	AP	160-200[e]	N	N	N
Polystyrene	AP	150-205	A[c]	N	some
Poly(methyl methacrylate)	AP	140-190	A[c]	N	A
Ethyl cellulose	CP	115-185	A	A	A
Cellulose acetate	CP	150-220[e]	A	A	some
Polyethylene	AP	212-250[e]	A[c]	N	A
Poly(tetrafluoroethylene)	AP	500[e]	N	N	N
Poly(chlorotrifluoroethylene)	AP	390	N	N	some

a)A: attacked or soluble; N: not attacked or insoluble

b)Strong reagents; weak reagents have little effect

c)Strong oxidising acids

d)Attacked by hot water

e)Heat distortion point below continuous-exposure temperature

f)Heat distortion temperature = 100 °F

g)maximum temperature for continuous exposure (in °F)

h)CP: condensation polymer; AP: addition polymer

The study of the effect of irradiation on organic substances often requires radiation sources with a high dose rate to do experiments on a reasonable timescale. The results of such high dose rate experiments are often extrapolated to repository conditions where the dose rate is about 1000-10000 times lower, a procedure that has often been criticised. However, there is some experimental evidence that the dose rate has no or at least little influence on the degradation processes and on the nature of degradation products formed (SISMAN et al. 1963, CHARLESBY & MOORE 1964, KÖRNER & DAGEN 1971, DAGEN 1980, ESCHRICH 1980, SWYLER et al. 1983). SCHNABEL (1978) writes: " **Though there are a few diverging results, the overwhelming majority of investigations arrived at the conclusion that true dose rate effects have not been evidenced so far during the irradiation of polymers when radiations of low LET like X-rays, γ-rays and fast electrons have been applied**". The total absorbed dose seems to determine the amount of degradation products that will be formed, irrespective whether this dose has been collected in a short time at high dose rate or over a longer timeperiod at low dose rate. However, since bondings have to be broken, a minimum amount of energy (radiation intensity) is required so that a minimum dose rate is required to initiate the degradation process.

The organic ion exchange resins investigated in this work are polystyrene based macromolecules (addition polymers) and are expected to be stable under alkaline conditions. Since they have been designed especially for their application in nuclear power stations, they also show a strong resistance against irradiative degradation processes, mainly because of their aromatic properties (REXER & WUCKEL 1965). The strong acidic ion exchange resins can tolerate a radiation dose between 1 and 10 MGy. The strong basic anion exchange resins have a slighty lower resistance against irradiation between 0.1 and 1 MGy absorbed dose. Irradiation of the resins will mainly cause a splitting off of the surface functional groups:

$$\text{Resin-}SO_3 \rightarrow \text{Resin} + SO_4^{2-} \qquad (3)$$

$$\text{Resin-}N(CH_3)_3 \rightarrow \text{Resin} + N(CH_3)_3 \qquad (4)$$

resulting in the formation of sulphate (in the case of strong acidic cation exchange resins) and methylamines (in the case of strong basic anion exchange resins) in solution. This splitting off reaction leads to an overall decrease in ion exchange capacity (SHIGEMATSU & OSHIO 1959, McCONNELL et al. 1993). Besides these water soluble products, low molecular weight gaseous products will also be formed.
For mixed bed resins (= mixture of cation and anion exchange resins) both sulphate and methylamines can be expected as radiolytic degradation products.

3. THE DEGRADATION OF STRONG ACIDIC ION EXCHANGE RESINS

The study of the interaction of the degradation products with radionuclides required the development of new techniques, especially since the ligands were present at low concentrations. The ion exchange method was further developed for these purposes. The theory behind it will be discussed in the following sections.

3.1 The ion exchange method to study metal-ligand interactions

3.1.1 The basic ion exchange method

The ion exchange method was originally designed to determine the stability constants of an ML complex by measuring the solid/liquid distribution coefficients of the metal M in absence (K_d^o) and presence (K_d) of different concentrations of the ligand L (SCHUBERT et al. 1950, SCHUBERT & LINDENBAUM 1952, SCHUBERT et al. 1958). The method ordinarily uses trace metal concentrations (where radioactive tracers are convenient), and a constant ionic strength medium. The advantage of this is the constancy of bulk cation concentration in both the solution and the resin phase and the consequent constancy of activity coefficients in both phases. Concentration may be used directly in the mass-action-law expression as a result. Another advantage is that the concentration of the metal bound to the ligand (ML) is

negligible compared with the total ligand concentration (L_T), thereby simplifying the calculation of the free ligand concentration (the free ligand concentration equals the total ligand concentration if reactions with hydrogen ions are negligible). When the following 1:1 complexation reaction in solution takes place (for simplicity, we neglect the signs for charge):

$$M + L \Leftrightarrow ML \tag{5}$$

the equation governing the ion exchange method can be written as:

$$\frac{K_d^o}{K_d} - 1 = K_{ML} \cdot [L] \tag{6}$$

with:

K_d^o = partition coefficient of M in the absence of ligand L
K_d = partition coefficient of M in the presence of ligand L
K_{ML} = stability constant of the ML-complex
[L] = free ligand concentration

The method can be applied only when the complex formed is neutral or negatively charged and does not adsorb on the ion exchange resin. From the measurement of both distribution coefficients, information on the stoichiometry of the reaction and the stability constant of the complex can be extracted (for more details see VAN LOON & KOPAJTIC 1990; ROSOTTI & ROSOTTI 1961).

3.1.2 The ion exchange method at different pH values

If the ligand is a weak acid or base, the complexation reaction is affected by the pH. When, in addition to (5), the following reaction takes place:

$$H + L \Leftrightarrow HL \tag{7}$$

with

$$K_{HL} = \frac{[HL]}{[H] \cdot [L]} \tag{8}$$

equation (6) can be written as :

$$\frac{K_d^o}{K_d} - 1 = K_{ML} \cdot \left(\frac{L_T}{1+K_{HL} \cdot [H]} \right) \qquad (9)$$

Graphs of equation (9) are shown in Fig.1. The concentration of the hypothetical ligand was fixed at $\log L_T = -5$ and a stability constant of the ML complex of $\log K_{ML} = 5$ was taken. The $\log K_{HL}$ of the ligand was varied between 4 and 7. The figure clearly shows the pH dependency of $K_d^o / K_d - 1$. As the distribution coefficient (K_d) decreases with increasing pH, the value of $K_d^o / K_d - 1$ increases with pH. When the pH equals the $\log K_{HL}$ of the ligand L, $K_d^o / K_d - 1$ reaches half of its maximum value which equals $K_{ML} \cdot L_T$ ($K_{ML} \cdot L_T = 1$ in this specific case). From experiments at different pH values, information on the **protonation constant** and the product $K_{ML} \cdot L_T$ can be derived. The individual value of K_{ML} or L_T cannot be derived from such experiments, unless one of the parameters is known.

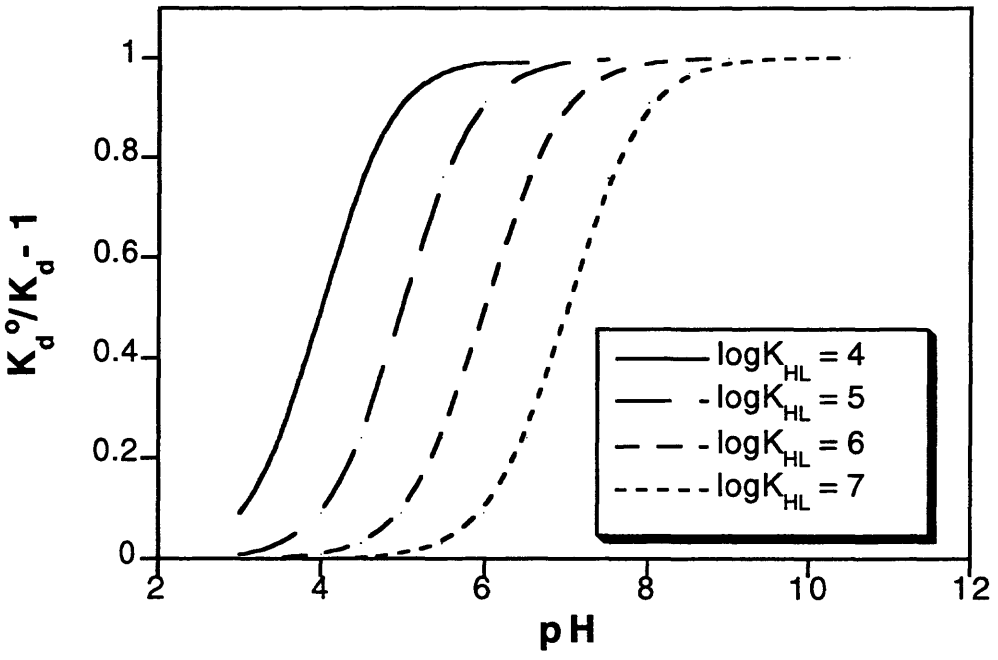

Figure 1: Values of $K_d^o / K_d - 1$ as a function of the pH for different values of $\log K_{HL}$ ($\log K_{ML} = 5$ and $\log L_T = -5$).

3.1.3 Titration of a ligand L with metal M in presence of an ion exchange resin

In the case of an unknown ligand, present at trace level concentrations, both the stability constant and the concentration of the ligand in solution can be determined by the ion exchange method. To achieve this, a solution containing the unknown ligand is titrated with a metal M in presence of the ion exchange resin. By monitoring the $K_d^o / K_d - 1$ value as a function of the total concentration of the metal M in solution (M_T), the end-point of the titration can be determined. Assume that only one ligand L (at a total concentration L_T) is present in solution and forms a complex ML with the metal M according to :

$$M + L \Leftrightarrow ML \tag{10}$$

The mass balance of M and L in solution is:

$$M_T = [ML] + [M] \tag{11}$$

$$L_T = [L] + [ML] \tag{12}$$

Equation (6) can be written as:

$$\frac{K_d^o}{K_d} - 1 = K_{ML} \cdot (L_T - M_T + [M]) \tag{13}$$

The relation between the total (M_T) and the free ([M]) metal concentration is given by:

$$M_T = \frac{[M] \cdot (1 + K_{ML} \cdot L_T) + K_{ML} \cdot [M]^2}{1 + K_{ML} \cdot [M]} \tag{14}$$

Rearranging equation (14) gives :

$$K_{ML} \cdot [M]^2 + (1 + K_{ML} \cdot (L_T - M_T)) \cdot [M] - M_T = 0 \tag{15}$$

The solution of this quadratic equation gives the free metal concentration for a given total ligand and metal concentration, provided that the stability constant of the complex formed is known. A plot of $K_d^o / K_d - 1$ as a function of the total metal concentration, M_T, for ligands forming complexes of different stability is given in Fig. 2. The concentration of the ligand was fixed at logL = -6. When information on both ligand concentration and stability constant is missing, the two parameters L_T and K_{ML} can be changed independently and the experimental points fit to equation (13). Only one set of the parameters L_T and K_{ML} gives an optimal fit to the experimental points.

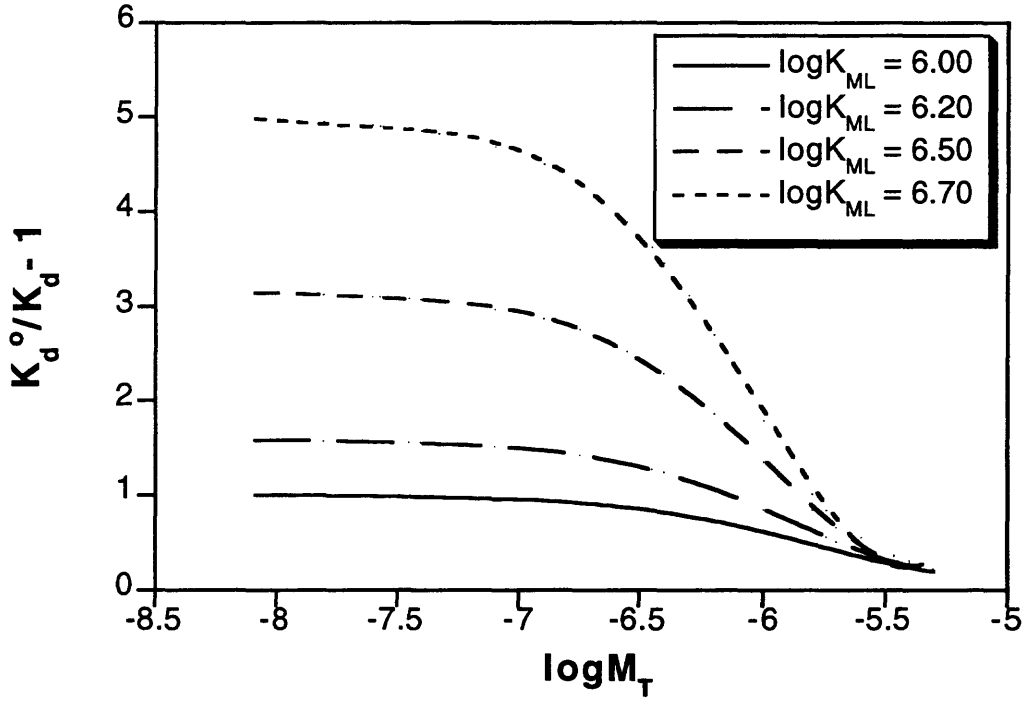

Figure 2: Values of $K_d^o / K_d - 1$ as a function of the total metal concentration in solution (M_T) for a total ligand concentration $\log L_T = -6$.

If two ligands are present and provided that they differ in concentration and form ML-complexes of different stability, both ligands can be characterised in terms of K_{ML1}, K_{ML2}, L_{T1} and L_{T2}.
Assuming the following reactions taking place in solution:

$$M + L_1 \Leftrightarrow ML_1 \qquad (16)$$

$$M + L_2 \Leftrightarrow ML_2 \tag{17}$$

with

$$K_{ML1} = \frac{[ML_1]}{[M] \cdot [L_1]} \tag{18}$$

and

$$K_{ML2} = \frac{[ML_2]}{[M] \cdot [L_2]} \tag{19}$$

The mass balance equations for the solution :

$$M_T = [M] + \sum_{i=1}^{2}[ML_i] \tag{20}$$

$$L_{T1} = [ML_1] + [L_1] \tag{21}$$

$$L_{T2} = [ML_2] + [L_2] \tag{22}$$

lead to the following equation :

$$M_T = \sum_{i=1}^{2} \frac{[M] \cdot (1+ K_{MLi} \cdot L_{Ti}) + K_{MLi} \cdot [M]^2}{1 + K_{MLi} \cdot [M]} - [M] \tag{23}$$

Rearranging equation (23) gives:

$$a[M]^3 + b[M]^2 + c[M] + d = 0 \tag{24}$$

with:

$a = K_{ML1} \cdot K_{ML2}$

$b = K_{ML1} \cdot (1+K_{ML2} \cdot L_{T2}) + K_{ML2} \cdot (1 + K_{ML1} \cdot L_{T1}) - K_{ML1} \cdot K_{ML2} \cdot M_T$

$c = 1 + K_{ML2} \cdot L_{T2} + K_{ML1} \cdot L_{T1} - (K_{ML1} + K_{ML2}) \cdot M_T$

$d = - M_T$

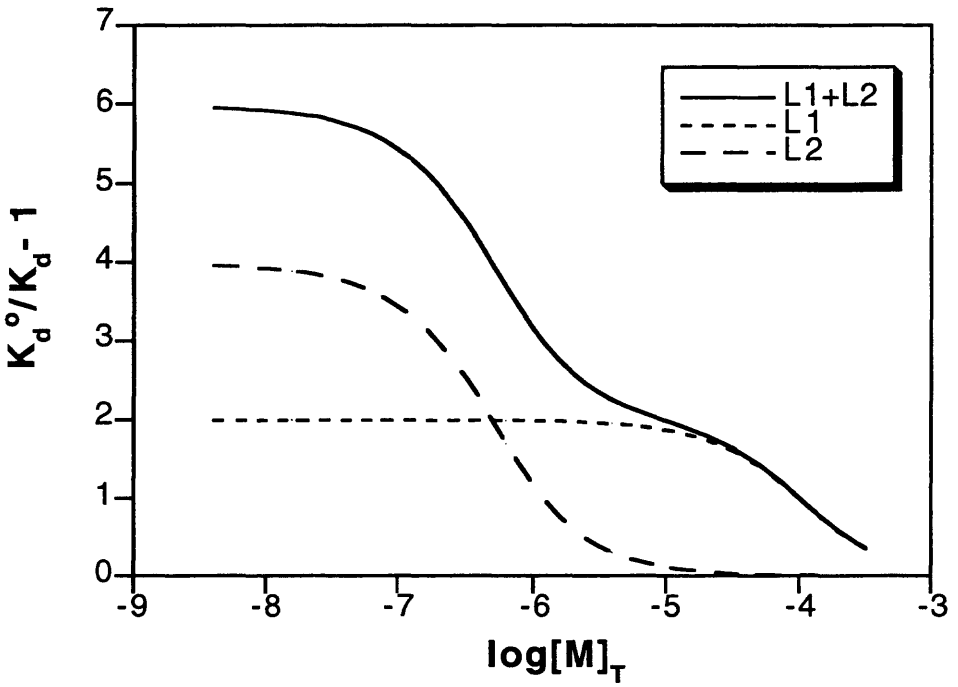

Figure 3: Values of $K_d^o / K_d - 1$ as a function of the total metal concentration (M_T) for a solution containing two ligands L_1 and L_2; ($\log L_{T1} = -4$, $\log K_{ML1} = 4.3$; $\log L_{T2} = -6.4$, $\log K_{ML2} = 7$).

The solution of this cubic equation gives the free metal concentration. The combination of equation (20), (21) and (23) results in the amount of metal complexed by ligand L_2 ($[ML_2]$):

$$[ML_2] = \frac{M_T - [M] - K_{ML1} \cdot [M] \cdot (L_{T1} - M_T + [M])}{1 + K_{ML1} \cdot [M]} \qquad (25)$$

Knowing the total amount of metal in solution (M_T), the free metal concentration ($[M]$) and the concentration bound to the second ligand ($[ML_2]$), the amount of metal bound to the first ligand ($[ML_1]$) can be calculated by applying equation (20).

The overall equation for $K_d^o / K_d - 1$ can now be written as :

$$\frac{K_d^o}{K_d} - 1 = K_{ML1} \cdot (L_{T1} - ML_1) + K_{ML2} \cdot (L_{T2} - ML_2) \qquad (26)$$

Fig. 3 illustrates $K_d^o / K_d - 1$ as a function of M_T. The total concentration of L_1 (L_{T1}) was 10^{-4} M and a stability constant of the ML_1 complex ($\log K_{ML1}$) of 4.3 was taken. For the second ligand, the total concentration of L_2 (L_{T2}) was fixed at $10^{-6.4}$ and the stability constant of the ML_2 complex ($\log K_{ML2}$) was 7.
The four parameters L_{T1}, K_{ML1}, L_{T2} and K_{ML2} can be changed independently so that the experimental results fit equation (26). Only one set of parameters gives an optimal fit to the experimental results.

3.2 Materials and methods

3.2.1 Irradiation of the ion exchange resins

Two strong acidic ion exchange resins - Lewatite S-100 (denoted hereafter as L) and Powdex PCH (denoted hereafter as P) - were converted to the sodium form by treating 100 g of the resin twice with 1000 cm^3 of 0.1 M NaOH, followed by four equilibration steps with 1000 cm^3 of 0.05 M NaOH. Finally, a mixture of 100 g resin and 1000 cm^3 of 0.05 M NaOH were obtained. The resin/water mixtures were divided into two equal parts. One part was placed in a stainless steel container and irradiated (denoted hereafter as B) in a ^{60}Co-cell to a total absorbed dose of 1.7 MGy. The dose rate in the ^{60}Co-cell was 8.5 kGy h^{-1}. After irradiation, the mixture was filtered through a 0.45 µm pore size membrane filter (Millipore type HA, 0.45 µm). The filter was prewashed with 500 cm^3 of 0.05 M NaOH to remove soluble organic carbon from the filter. The solutions were stored in glass vials at 4 °C.
The other part of the suspension (denoted hereafter as U) was put in a glass vial and left standing with regularly shaking for one hour at intervals of 6 hours. After one week, the suspensions were filtered in the same way as the irradiated samples. All solutions were analysed for pH, Na^+, inorganic carbon (IC), total dissolved organic carbon (DOC), SO_4^{2-} and oxalate.

3.2.2 pH-measurements

The pH of the solutions was measured by a Beckman Φ71 pH-meter with an Ingold combined glass electrode. The electrode was calibrated with Titrisol buffers (Merck) at pH 7 and 10.

3.2.3 Organic and inorganic carbon measurements

The total dissolved organic carbon (DOC) and the total inorganic carbon (IC) were analysed by a carbon analyzer (Dohrmann DC-180). For the DOC, UV-promoted persulphate oxidation was used. For the IC, the solutions were acidified and the CO_2 formed was removed by flushing the solutions with an oxygen stream. The amount of CO_2 formed was measured with an infrared detector. The apparatus was calibrated with standard solutions of potassium-biphthalate for the DOC-measurements and sodium-bicarbonate for the inorganic carbon measurements.

3.2.4 Sulphate, Na^+ and oxalate

SO_4^{2-} and oxalate were analysed by ion chromatography (Dionex 2010i) using an HPIC-AS4A column. The eluent used contained 1.8 mM Na_2CO_3 and 1.7 mM $NaHCO_3$. The components were detected by suppressed conductivity. Standards were made up from 1000 mg/l standard solutions (Merck).
The sodium in solution was measured by ICP-AES.

3.2.5 Cu-titrations

The irradiated solutions of the Powdex PCH resin (PB1) were diluted 8 times and the Lewatite S-100 (LB1) solutions were diluted 4 times. The ionic strength was adjusted to 0.1 M with 1 M $NaClO_4$. The dilutions were chosen so that an optimal concentration of the ligand had been reached. 25 cm^3 of the diluted solutions were placed in a 50 cm^3 titration vessel. The pH values of the solutions were adjusted to 3.5 with concentrated $HClO_4$ and the systems were

flushed with prewetted nitrogen to remove CO_2. Finally, the pH was adjusted to the desired value with NaOH. The solutions were then titrated with 0.005 M $Cu(NO_3)_2$ as described in VAN LOON & KOPAJTIC (1990). The same procedure was used for the non-irradiated solutions (PU1 and LU1). Unlike the irradiated solutions, these were not been diluted.

3.2.6 The ion exchange method with Ni^{2+}

10 g of a wet Dowex 50W X-4 cation exchange resin in the H^+-form were converted into the Na^+ form by washing the resin twice with 250 cm^3 0.1 M NaOH and equilibrating 3 times with 0.1 M $NaClO_4$. After equilibration, the resin was washed with demineralised water and dried at 50 °C. About 100 mg of the resin were transferred to 50 cm^3 centrifuge tubes. 20 cm^3 of a solution containing 0.1 M $NaClO_4$, 0.01 M buffer and oxalate in a concentration range between 0 and 20 ppm were added. The volume was then adjusted to 25 cm^3 with 5 cm^3 of a solution of 0.1 M $NaClO_4$ and 0.01 M buffer and spiked with ^{63}Ni (activity : 1000 Bq cm^{-3}). The final compositions of the solutions were 0.1 M $NaClO_4$, 0.01 M buffer and 0, 2, 4, 8 or 16 ppm of oxalate. The buffers used were acetate (pH=5), MES (pH=6), MOPS (pH=7), TRIS (pH=8) and taurine (pH=9). None of the buffers used forms complexes with Ni^{2+} (or only very weak complexes) and consequently do not interfere with the measurements (PERRIN & DEMPSEY 1974).
Different amounts of the resin water (10, 20 and 35 cm^3) were adjusted to pH = 3 with concentrated $HClO_4$ to remove any carbonates. The pH was then adjusted to the desired value and a buffer and $NaClO_4$ were added. The volume was finally made up to 50 cm^3. The final concentrations were 0.1 M Na^+ and 0.01 M buffer, giving an ionic strength of 0.1 M. Complexation experiments with ^{63}Ni were performed the same way as described for the solutions containing oxalate only. The resin/water mixtures were placed in an end-over-end shaker and equilibrated for 20 hours at room temperature. After equilibration, ^{63}Ni in solution was measured by liquid scintillation counting (Packard, Tricarb 2250 CA) using Instagel (Packard) as a scintillation cocktail. The partition coefficient (K_d) of ^{63}Ni was calculated from the difference in concentration (radioactivity) before and after equilibrium.
For the titration experiments with Ni^{2+}, 10 cm^3 of the resin water were adjusted to pH = 3 with concentrated $HClO_4$ to remove any carbonates. The pH was

then adjusted to pH = 7 and a buffer (MOPS), $NaClO_4$ and different amounts of $Ni(NO_3)_2$ were added. The solutions were made up to 50 cm^3. The final composition of the solutions was 0.1 M Na^+, 0.01 M MOPS and Ni^{2+} concentrations between 10^{-8} and 10^{-5} M. About 100 mg of resin (Dowex 50W X4) were transferred into 50 cm^3 centrifuge tubes and 20 cm^3 of the prepared solutions were added. The volume was then made up to 25 cm^3 by adding 5 cm^3 of a solution containing 0.01 M $NaClO_4$, 0.01 M MOPS and spiked with ^{63}Ni (activity : 1000 Bq cm^{-3}).

3.3 Results and discussion

Table 2 gives an overview of the chemical composition of the different resin solutions after and without irradiation. In the irradiated resin water, the concentration of Na^+, SO_4^{2-}, DOC, IC and oxalate are significantly higher than in the non-irradiated waters. The SO_4^{2-} in the water is caused by the splitting off of the sulfonic acid groups, followed by oxidation of the $\cdot SO_3$ formed to soluble SO_4^{2-} (see eq. 27). This splitting off reaction has been observed in all earlier work (MOHORCIC & KRAMER 1968, SEMUSHIN et al. 1979, BARLETTA et al. 1982, SWYLER et al. 1983, McCONNELL et al. 1993). Irradiations of dry cation exchangers produce mainly the SO_2-gas whereas ion exchange resins under water form mainly SO_4^{2-} (MOHORCIC & KRAMER 1968).

The sodium adsorbed on these surface SO_3-groups has been released with the SO_3 -groups, resulting in higher Na^+ concentrations. This is confirmed by the observed ratio between the increase of the Na^+ concentration and the SO_4^{2-} ($\Delta Na^+ / SO_4^{2-}$), which is close to one. The increase in oxalate concentration cannot be explained fully, but it might have been formed by $\cdot COO^-$ radicals generated by the oxidative degradation of the resins. Two such radicals can condense to form an oxalate molecule. Oxalate was also found to be an important degradation product in the irradiation of bitumen/water mixtures under high pH conditions (VAN LOON & KOPAJTIC 1991). The same mechanism for oxalate formation was proposed, although the $\cdot COO^-$ radicals, were postulated to be generated by the decarboxylation of fatty acids.

Table 2: Characteristics of the irradiated and non-irradiated resin waters.

Name	Dose (MGy)	pH	DOC (mM)	IC (mM)	ΣC (mM)	SO_4^{2-} (mM)	oxalate (mM)	Na^+ (mM)	ΔNa	$\Delta Na / SO_4^{2-}$	$\Sigma C / SO_4^{2-}$	C_{ox}/DOC
Lewatite S-100 (Cu- Titration)												
LB1	1.7	11.80	2.8	9.3	12.1	24.8	0.23	71	-	-	0.49	0.16
LU1	0	12.74	1.0	0.8	1.8	0	0	48	-	-	-	-
LB1-LU1			1.8	8.5	10.3	24.8	0.23	23	23	0.93	0.42	0.26
Powdex PCH (Cu-titration)												
PB1	2.17	10.21	8.7	13.3	22.0	25.5	0.46	76	-	-	0.86	0.11
PU1	0	12.81	0.3	1.7	2.0	0	0	48	-	-	-	-
PB1-PU1			8.4	11.6	20.0	25.5	0.46	28	28	1.10	0.78	0.11
Lewatite S-100 (Ni-experiments)												
LB2	1.7	11.73	2.9	9.8	12.7	21.6	0.31	70	-	-	0.59	0.21
LU2	0	12.75	1.3	1.5	2.8	0	0	48	-	-	-	-
LB2-LU2			1.6	8.3	9.9	21.6	0.31	22	22	1.02	0.46	0.38
Powdex PCH (Ni-experiments)												
PB2	1.7	11.85	4.2	10.9	15.1	17.0	0.26	68	-	-	0.89	0.12
PU2	0	12.60	0.4	3.2	3.6	0	0	49	-	-	-	-
PB2-PU2			3.8	7.7	11.5	17.0	0.26	19	19	1.12	0.68	0.14

PB = Powdex ,irradiated; PU = Powdex, non irradiated; LB = Lewatite, irradiated; LU = Lewatite, non irradiated

Oxalate contributes to only 10-15 % of the DOC for the Powdex resin and to 20-30 % in case of the Lewatite resin. The rather low DOC/SO_4^{2-} ratio indicates that the radiolytic degradation of these resins is mainly the splitting off of the SO_3-groups. The organic backbone of the resins seems hardly to be affected mainly because of its aromatic character (SISMAN et al. 1963, REXER & WUCKEL 1965). It is well known that aromatic compounds show a large resistance to irradiation because such molecules can dissipate the absorbed energy without destroying chemical bonds (MANION & BURTON 1952, BURTON & PATRICK 1954). This was also observed in other work on cation exchange resins (McCONNELL et al. 1993) where no detectable organic material could be leached from irradiated resins.

The CO_3^{2-} in solution was produced by the CO_2 generated from the organic matrix by irradiation. The formation of CO_3^{2-} and SO_4^{2-} is accompanied by H^+-generation, leading to a decrease in pH which has been observed for the irradiated solutions. The pH-drop is caused mainly by the oxidation of SO_3 to SO_4^{2-} for which the following (half-)reaction can be written:

$$\cdot SO_3^- + H_2O \rightarrow SO_4^{2-} + 2\,H^+ + e^- \qquad (27)$$

According to equaton (27) one mole of SO_4^{2-} and two moles of H^+ are generated. A rough calculation (based on the SO_4^{2-}-data) shows that during the irradiation between 40-50 mM protons have been generated. The initial amount of OH^- in solution is 50 mM and will be neutralised more or less completely by the generated protons.

Figures 4 and 5 show the titration curves of the resin waters (PB1 and LB1) with Cu^{2+}. The curves can be fitted by assuming the formation of a 1:1 complex:

$$Cu + L \Leftrightarrow CuL \qquad (28)$$

characterised by the stability constant :

$$K_{CuL} = \frac{[CuL]}{[Cu] \cdot [L]} \qquad (29)$$

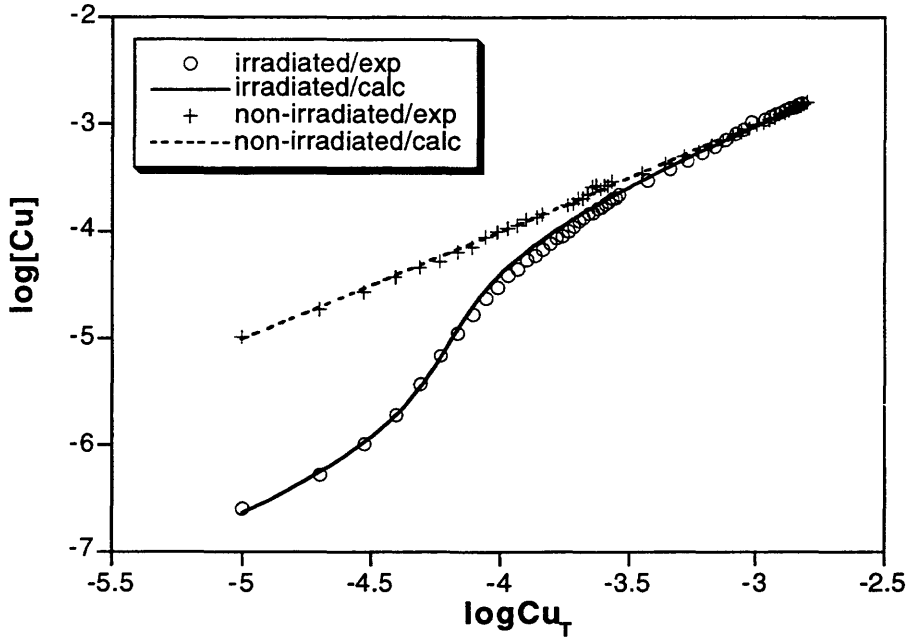

Figure 4: Titration of the Powdex PCH solutions (PB1 and PU1) with Cu^{2+} at pH = 6 and I = 0.1 M.

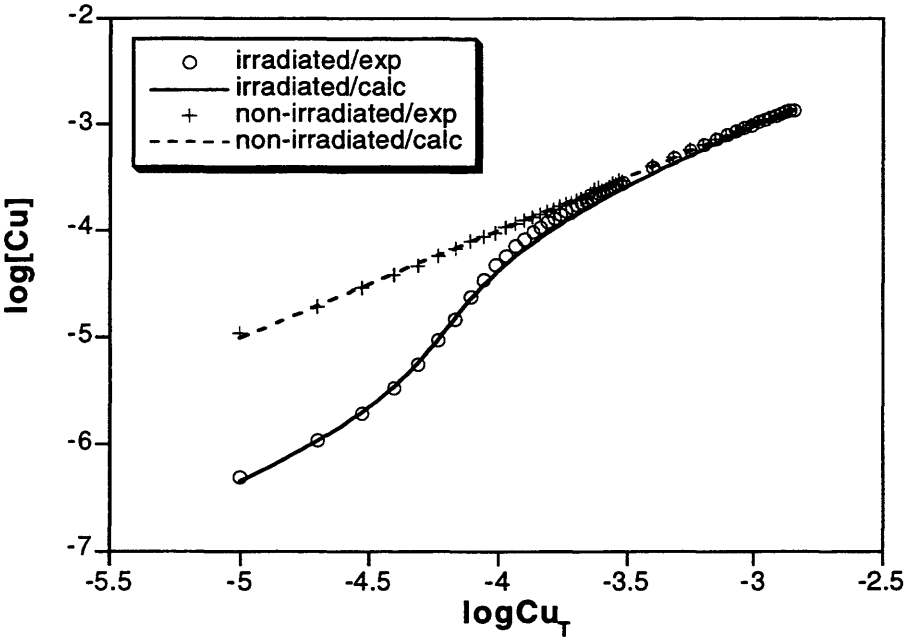

Figure 5: Titration of the Lewatite S-100 solutions (LB1 and LU1) with Cu^{2+} at pH = 6 and I = 0.1 M.

Combination of equation (29) with the mass balance equations :

$$Cu_T = [Cu] + [CuL] \quad (30)$$

$$L_T = [L] + [CuL] \quad (31)$$

results in :

$$Cu_T = \frac{[Cu] \cdot (1 + K_{CuL} \cdot L_T) + K_{CuL} \cdot [Cu]^2}{1 + K_{CuL} \cdot [Cu]} \quad (32)$$

with:

Cu_T	=	total concentration of Cu in solution
L_T	=	total concentration of ligand L in solution
[Cu]	=	concentration of the free, uncomplexed Cu in solution
[L]	=	concentration of the free ligand in solution
K_{CuL}	=	stability constant of the CuL complex

The stability constant and the ligand concentration derived from the titration with Cu^{2+} have been summarised in Table 3. The values of K_{CuL} are very similar to these obtained for the Cu-oxalate complex (VAN LOON & KOPAJTIC 1991).

Table 3: Overview of the logK and $logL_T$ values derived from the titrations of the resin-waters with Cu^{2+} at pH = 6 and I = 0.1 M. For comparison, results for bitumen and oxalate have been given.

Solution	$logK_{CuL}$	$logL_T$	dil	b)oxalate (titration)	b)oxalate (IC)
Powdex PCH (PB1)	5.80 ±0.08	-4.18	1:8	46.5	40.6
Lewatite S100 (LB1)	5.56 ±0.05	-4.20	1:4	22.2	19.8
a)Bitumen Mexphalt 90/30	5.83 ±0.17	-4.45		3.1	3.3
a)Bitumen Mexphalt 80/100	5.63 ±0.08	-4.10		7.0	7.6
a)Oxalate 5 ppm	5.82 ±0.17	-4.33		4.1	5.0

a) : taken from VAN LOON & KOPAJTIC 1991

b) : results in ppm

Also the concentrations of ligand derived from the titration curves are very similar to the concentrations of oxalate determined by ion chromatography. From the Cu-titration experiments, we can conclude that oxalate is the dominant complexing organic ligand generated by the irradiation of strong acidic ion exchange resins in presence of alkaline water containing oxygen.

Table 4 shows the results of the Ni-experiments for the solutions containing only the oxalate ligand. The predicted (pr) values have been calculated from:

$$\frac{K_d^o}{K_d} - 1 = K_{NiOx} \cdot [Ox] \qquad (33)$$

with $\log K_{NiOx} = 4.34$ at I = 0.1 M and [Ox] = 2, 4, 8, 16 ppm.

The predicted (pr) and observed (obs) values are in good agreement up to pH = 7. Beyond pH = 7, the two values deviate significantly from each other, i.e. a decrease in $K_d^o/K_d - 1$ can be observed. In the ideal case, the value of $K_d^o/K_d - 1$ should stay constant over the whole pH range. Only when a ligand Y is present that becomes important at high pH values in both the solutions containing the ligand of interest and in the blank solutions (K_d^o-determination), equation (33) can be written as :

$$\frac{K_d^o}{K_d} - 1 = \frac{K_{NiOx} \cdot [Ox]}{F} \qquad (34)$$

with $F = 1 + K_{NiY} \cdot [Y]$

The hydrolysis of Ni^{2+} can be neglected in the pH range studied, but it is possible that a small amount of CO_3^{2-} is present in the solutions and this can influence the $K_d^o/K_d - 1$ values beyond pH = 7. The factor (F) by which the $K_d^o/K_d - 1$ value was reduced at pH = 8 and 9 was calculated by dividing the theoretical (pr) value by the observed (obs) value. The values of F have been summarised in Table 4.

Table 4: $K_d^o / K_d - 1$ and F values for the different concentrations of oxalate at different pH values.

	2 ppm			4 ppm			6 ppm			8 ppm			
pH	pr	obs	F	pr	obs	F	pr	obs	F	pr	obs	F	**F**
5	0.50	0.49	1.02	0.99	0.95	1.04	1.99	1.85	1.07	3.98	3.85	1.03	**1.04**
6	0.50	0.52	0.96	0.99	1.00	0.99	1.99	1.99	1.00	3.98	4.26	0.93	**0.97**
7	0.50	0.45	1.11	0.99	0.94	1.05	1.99	1.82	1.09	3.98	3.84	1.04	**1.07**
8	0.50	0.27	1.85	0.99	0.50	1.98	1.99	1.23	1.62	3.98	2.14	1.86	**1.83**
9	0.50	0.20	2.50	0.99	0.32	3.09	1.99	0.69	2.88	3.98	1.46	2.72	**2.80**
5	0.50	0.25	2.00	0.99	0.83	1.19	1.99	1.78	1.12	3.98	3.65	1.09	**1.13**
6	0.50	0.51	0.98	0.99	0.96	1.03	1.99	1.99	1.00	3.98	4.15	0.96	**0.99**
7	0.50	0.49	1.02	0.99	0.98	1.01	1.99	2.26	0.88	3.98	4.30	0.93	**0.96**
8	0.50	0.41	1.28	0.99	0.75	1.32	1.99	1.36	1.46	3.98	2.39	1.66	**1.43**
9	0.50	0.30	1.67	0.99	0.50	1.98	1.99	-	-	3.98	1.92	2.07	**1.91**

These values of F have been used to correct the $K_d^o / K_d - 1$ values of the solutions containing the degradation products (under the assumption that the same ligand Y was present in these solutions). Figure 6 shows the results of the $K_d^o / K_d - 1$ measurements as a function of the pH for the solutions containing the degradation products (PB2, PU2, LB2 and LB2. The values obtained at pH 8 and 9 have been corrected by F. All the values have been multiplied by the dilution factor so that the reported $K_d^o / K_d - 1$ values represent the values for the undiluted solutions.

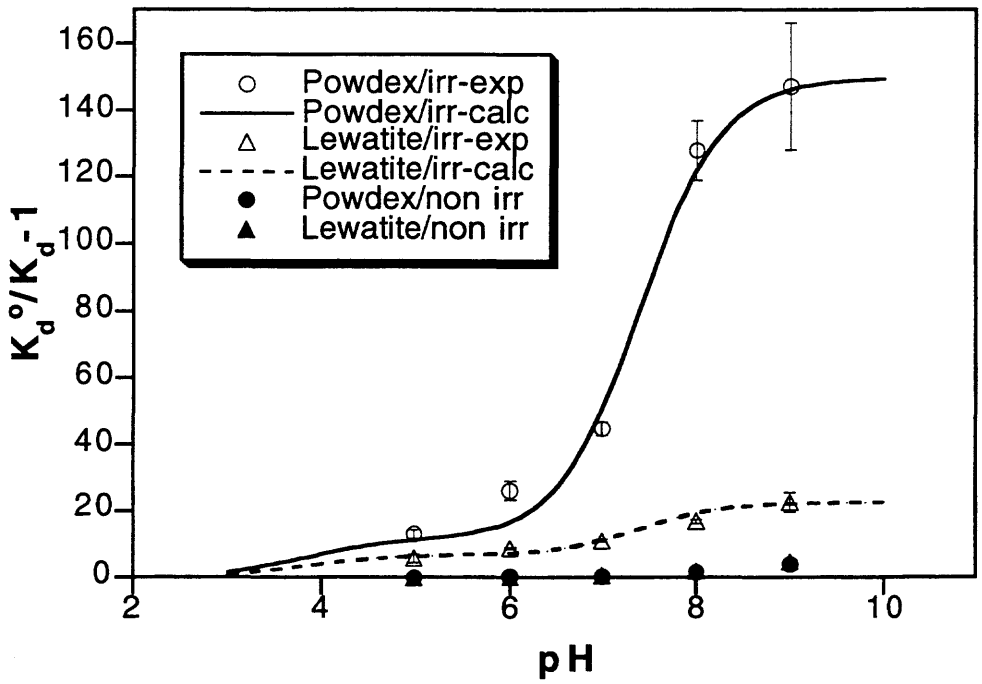

Figure 6: Values of $K_d^o / K_d - 1$ as a function of pH for an irradiated solution (Powdex = PB2 and Lewatite = LB2).

The values of $K_d^o / K_d - 1$ increase with the pH. From this observation we can conclude that beside oxalate another ligand (X) is present in these solutions. The lines in the graph have been calculated by :

$$\frac{K_d^o}{K_d} - 1 = K_{Niox} \cdot [ox] + K_{NiX} \cdot \frac{[X]_T}{1 + K_{HX} \cdot [H]} \qquad (35)$$

with:

$[X]_T$	=	total concentration of ligand X in solution
K_{HX}	=	protonation constant of ligand X
K_{NiX}	=	stability constant of the NiX complex
K_{Niox}	=	stability constant of the NiOx complex
[ox]	=	free oxalate concentration in solution

The parameters used for fitting the experimental results have been summarised in Table 5. For the calculation, a concentration of oxalate twice

that measured by ion chromatography for the solution PB2 had to be used. For the LB2 solution, the oxalate concentration as determined by ion chromatography could be used. A mean value for $\log K_H$ of 7.4 can be derived from these plots. Since it is expected that a chelate complex has been formed, this value is probably the first protonation constant of the unknown ligand X:

$$X^{2-} + H^+ \Leftrightarrow XH^- \qquad (36)$$

Table 5: Parameters used to fit the experimental results of the pH experiment. The concentrations of oxalate and X are given for the non-diluted solutions.

Parameter	Powdex PCH (PB2)	Lewatite S-100 (LB2)
log[ox]	-3.28	-3.51
$\log K_{Niox}$	4.34	4.34
$\log K_H$	7.40	7.40
$\log(K_{NiX} \cdot [X])$	2.14	1.20
$\log K_{NiX}$	7.20	7.10
$\log[X]_T$	-5.06	-5.90

Table 6: Parameters used to fit the experimental results of the titration experiments with Ni^{2+}. The concentrations of oxalate and X are given for the diluted solutions.

Parameter	Powdex PCH (PB2)	Lewatite S-100 (LB2)
log[ox]	-4.00	-4.10
$\log K_{Niox}$	4.34	4.34
log[X]	-6.40	-7.25
$\log K_{NiX}$	7.00	7.00

For the non irradiated solutions, there was no evidence for the presence of strong ligands. This is in agreement with the results of the Cu-titration experiments.
Figure 7 shows the results of the titration experiment with Ni^{2+}. The curves in the graph are calculated by equation :

$$\frac{K_d^o}{K_d} - 1 = K_{NiOx} \cdot (ox_T - [Niox]) + K_{NiX} \cdot (X_T - [NiX]) \qquad (37)$$

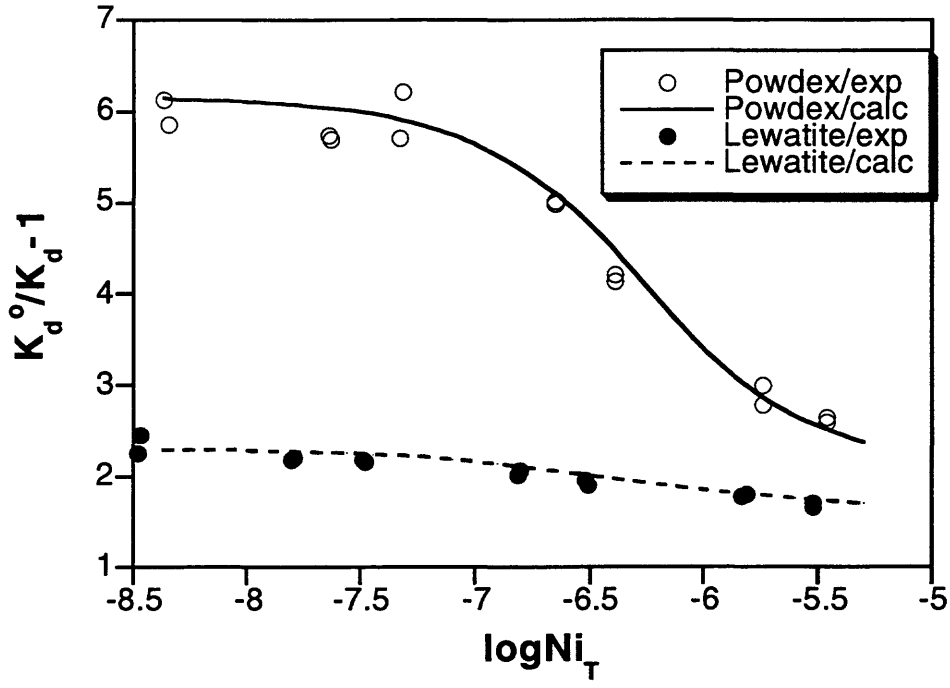

Figure 7: Values of $K_d^o / K_d - 1$ as a function of the total Ni-concentration in solution ($logNi_T$).

Again, an oxalate concentration twice that which has been measured by ion chromatography had to be used for solution PB2 in the calculation. Table 6 summarises the parameters used for fitting the experimental results. The stability constant of the NiX complex derived from this experiment is logK = 7. This value indicates that a chelate has been formed. Monodentate complexes have a much lower stability constant (logK < 2) (KOTRLY & SUCHA 1985). The concentration of the unknown ligand (log[X]) in the diluted solutions is

-6.40 for the PB2 solution and -7.25 for the LB2 solution. The total concentration ($\log X_T$) in the original undiluted solution equals -5.04 for the PB2 solution and -6 for the LB2 solution ([Ox]/[X]=309 for LB_2 and 28 for PB_2). The ligand X, of course, could not be detected in the titration experiments with Cu^{2+} under the experimental conditions used, i.e the concentration of ligand X (log[X]) was smaller than -6. After the first Cu-addition, the total Cu-concentration (logCu) was -5.3. Consequently, the ligand X was completely saturated with Cu from the beginning of the titration.

3.4 Conclusions

The ion exchange method is a helpful tool for studying metal-ligand interactions in situations where the ligand is present in trace concentrations and where no ion sensitive electrodes or other potentiometric techniques (e.g. pH-titrations) can be used. Information on the ligand concentration, interaction constant K_{ML} and protonation constant K_{HL} can be estimated by it.
Oxalate and an unknown ligand X are the main complexing degradation products of the radiolytic degradation of strong acidic cation exchange resins at high pH conditions.

The chemical (alkaline) degradation is very limited and does not lead to the formation of organic ligands. This can be explained by the high resistance of addition polymers towards alkaline conditions. Similar results were also reported by GREENFIELD et al. (1992).

3.5 The influence of degradation products on Ni-speciation

3.5.1 Introduction

The aim of the present modelling study is to assess the influence of degradation products of acidic ion exchange resins on the Ni-speciation in groundwaters and waters of high pH such as may be found in cement pore waters. As discussed above, oxalate and an unidentified ligand, termed X, turned out to be the most strongly complexing ligands detected among the

degradation products. Therefore, thermodynamic modelling will focus on these ligands.
Three basic problems have to be solved in this modelling study:

- In order to circumvent the pitfalls of "holes" in the thermodynamic data base, which are especially dangerous in the high pH range of cement pore waters, the type of dissolved species that may dominate are predicted by chemical reasoning. Missing stability constants are estimated using free energy relationships of thermodynamic data, i.e. correlations of stability constants of a certain ligand with different metal cations. In cases where little is known, e.g. about the formation of ternary Ni-ligand-hydroxo complexes, maximum values of their stabilities are assessed by chemical analogy. Subsequent sensitivity analyses show whether these species are important or not, and thus give hints for further experimental investigations.

- In order to cope with the large variability in the chemical composition of groundwaters and cement pore waters, the chemical system is reduced to the most important parameters influencing metal-organic complexation, i.e. concentration of Ca and Mg, pH and P_{CO_2} (partial pressure of CO_2)[1] Graphical representations of the results of speciation calculations in this reduced parameter space reveal their sensitivity to chemical composition much better than a series of computations carried out for a number of arbitrarily selected water compositions.

- The concentrations of oxalate and ligand X to be expected in pore waters of the near-field and far-field of radioactive waste repositories depend on various parameters, e.g. the amount of ion exchange resins present in

---

[1] The rationale behind the choice of Ca and Mg as the most important cations competing with radionuclide complexes is the following. Alkaline metal cations form very weak complexes and thus Na and K do not influence the speciation to a significant level even if they are present in large concentrations. The complexation strength of Mg is very similar to Ca, whereas Sr complexes are always weaker then Ca complexes (HUMMEL 1992). In a first approximation, the sum of the Ca and Mg concentration is used in our calculations applying common Ca,Mg stability constants. Considering its weak complexes and generally low concentrations, Sr is neglected. In the high pH region of cement pore waters. Mg and carbonate concentrations are vanishingly small. Thus the high pH model is reduced to a simple Ca-pH system.

different waste types, the degradation kinetics of the resins, corrosion and degradation of different compartments of the repository, to name just a few. These ligand concentrations cannot be used as fixed parameters in speciation calculations if some more generally applicable results are the aim of the modelling exercise. Therefore the "backdoor approach" (HUMMEL 1992) is used in this study, in a special version adapted to our problem, beginning with the question: "What concentrations must the ligand have in order to significantly influence the speciation of a given radionuclide?"

3.5.2 The thermodynamic data base

Stability constants describing the hydrolysis of Ni and Ca are taken from the comprehensive monograph "The Hydrolysis of Cations" by BAES & MESMER (1986); no attempt was made to derive "better" constants from the available experimental data. Ca starts to hydrolyse above pH 12 and the only hydrolysis product formed is $CaOH^+$, whose stability constant is sufficiently well known for the present modelling study. The hydrolysis of Ni is more complex than that of Ca. As stated by BAES & MESMER (1986, p.246): "*The only mononuclear hydrolysis product of Ni(II) whose stability is known well, is $NiOH^+$. The less certain values for $Ni(OH)_{2(aq)}$ and $Ni(OH)_3^-$ from solubility measurements have been used to estimate the stability of $Ni(OH)_4^{2-}$. Small amounts of the polynuclear species $Ni_4(OH)_4^{4+}$ form rapidly at high Ni(II) concentrations (over 0.1 M) before precipitation of $Ni(OH)_2$ occurs.*" In our modelling study we are interested in low Ni concentrations, so only mononuclear species only are considered in the speciation model. The ± values included in Table 7 for Ca and Ni hydrolysis data reflect the uncertainty in stability constants assigned by BAES & MESMER (1986).

The Ca carbonate system was extensively studied by PLUMMER & BUSENBERG (1982). They made approximately 350 new measurements of the solubilities of calcite, aragonite and vaterite in CO_2-H_2O solutions between 0 and 90 °C and carefully reviewed the older literature about this subject. They conclude that their solubility products are internally consistent with an aqueous model that includes the $CaHCO_3^+$ and $CaCO_{3(aq)}$ ion pairs. The stability constants for these ion pairs including the uncertainties assigned by PLUMMER & BUSENBERG (1982) are also listed in Table 7.

In contrast to the very well know Ca-carbonate equilibria, no reliable study has been published exploring the Ni-carbonate system. Actually, a search for experimental investigations of transition metal carbonate complexation reveals a remarkable, almost complete lack of data. Until quite recently, in the transition metal series Mn(II), Fe(II), Co(II), Ni(II), and Cu(II), only the Cu(II) carbonate system had been studied. All other data, if included in thermodynamic data bases at all, were estimated by various extrapolation procedures. This lack of data prompted a study of the Fe(II) carbonate system (BRUNO et al. 1992), because, as stated by the authors: "*It appears somewhat surprising that for Fe(II), a major metal in natural systems, no experimental data are available to date and that the importance of Fe(II)-carbonate complexes remains controversial.* " Left with just two data points in the Mn to Cu transition metal series, Fe(II) from BRUNO et al. (1992), and Cu(II) from BYRNE & MILLER (1985), we have to rely on data of organic ligands and chemical systematics.

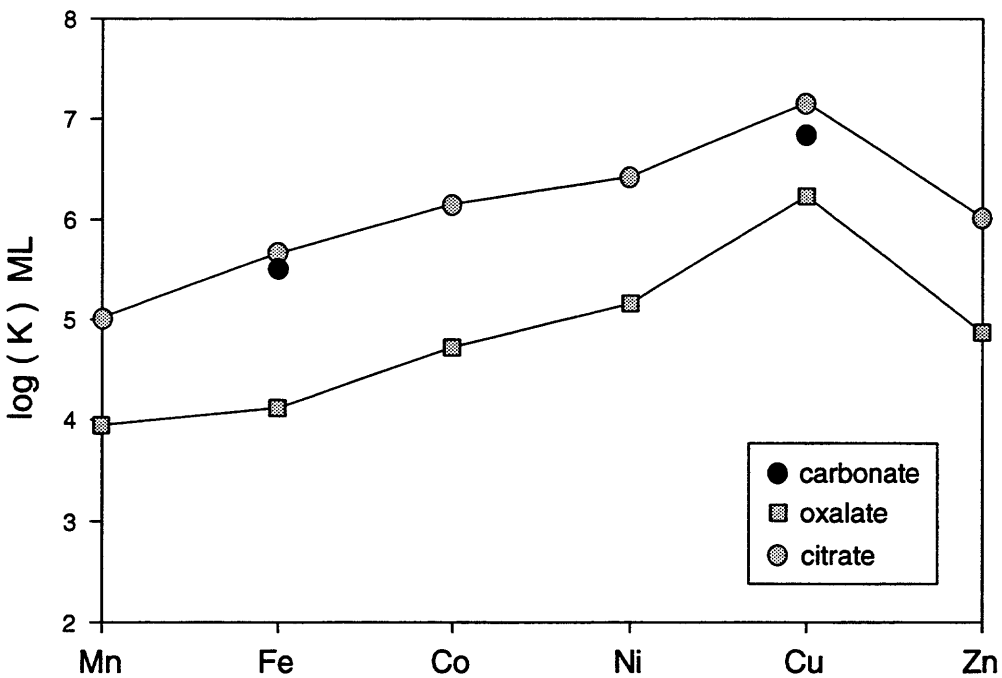

Figure 8: The Irving-Williams series of transition metal complexation (IRVING & WILLIAMS 1953). Oxalate and citrate data are taken from SMITH and MARTELL (1989) and MARTELL and SMITH (1977). The copper carbonate constant comes from BYRNE & MILLER (1985), the ferrous iron carbonate constant is taken from BRUNO et al. (1992).

Fig.8 shows the Irving-Williams series of organic transition metal complexes for two organic ligands (IRVING & WILLIAMS 1953). The oxalate curve is practically identical with the original curve published by these authors. Citrate data have been added in Fig.8 for illustrative purposes. There is no obvious reason why carbonate, acting like oxalate as a bidentate but somewhat stronger ligand, should not follow the Irving-Williams series. The stability constants of Fe(II)-carbonate (log K_1 = 5.5) and Cu(II)-carbonate (log K_1 = 6.8) are therefore taken as the lower and upper limits, respectively, of the unknown Ni-carbonate constant. The stability of the Ni carbonate 1:1 complex thus is estimated as log $K_1 = 6 \pm 0.5$.

By analogy to other metal cations, Ni is expected to form also rather stable 1:2 and probably even 1:3 complexes in addition to 1:1 carbonate complexes. To estimate the strength of these complexes, the analogy to oxalate complexes is used again, in order to support the systematic variation found in the few experimental data on the stability of metal-carbonate complexes.

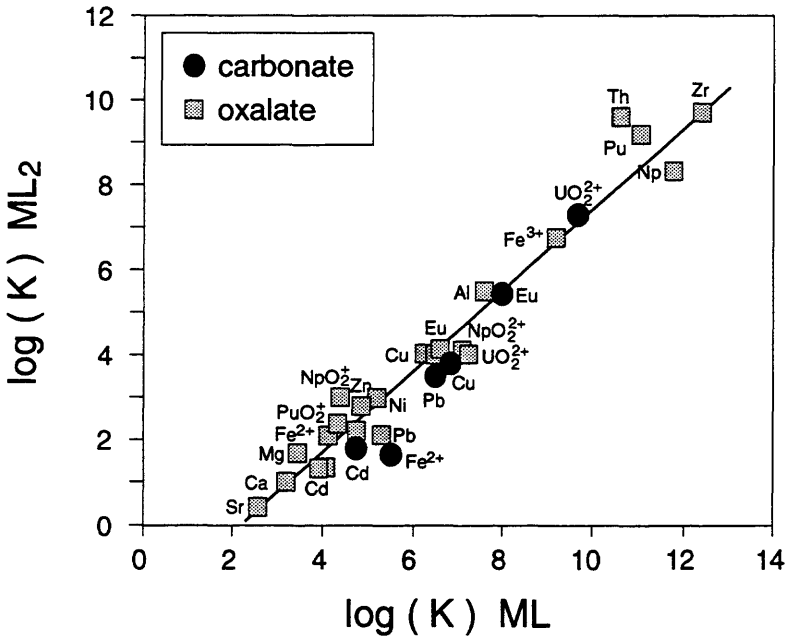

Figure 9: Correlation of the stepwise formation constants of metal oxalate 1:1 and 1:2 complexes. Data are taken from SMITH & MARTELL (1989) and MARTELL & SMITH (1982, 1977). The solid line is obtained by regression analysis: $\log K_{Mox2} = (-2.1 \pm 0.6) + (0.95 \pm 0.08) \cdot \log K_{Mox}$. The carbonate data, closely following the oxalate relation, are taken form the following sources: Cd: RAI et al. (1991), Fe(II): BRUNO et al. (1992), Pb: BILINSKI & SCHINDLER (1982), Cu: BYRNE & MILLER (1985), Eu: LEE & BYRNE (1993), U(VI): GRENTHE et al. (1992).

Table 7: Thermodynamic Database*).

Species	logK	Reference	Reaction
$Ni(OH)^+$	-9.86 ± 0.03	B & M	$Ni^{2+} + H_2O \Leftrightarrow Ni(OH)^+ + H^+$
$Ni(OH)_{2(aq)}$	-19 ± 1	B & M	$Ni^{2+} + 2\,H_2O \Leftrightarrow Ni(OH)_{2(aq)} + 2\,H^+$
$Ni(OH)_3^-$	-11 ± 0.5	B & M	$Ni(OH)_{2(aq)} + H_2O \Leftrightarrow Ni(OH)_3^- + H^+$
$Ni(OH)_4^{2-}$	< -14	B & M	$Ni(OH)_3^- + H_2O \Leftrightarrow Ni(OH)_4^{2-} + H^+$
$NiCO_{3(aq)}$	6 ± 0.5	estimated	$Ni^{2+} + CO_3^{2-} \Leftrightarrow NiCO_{3(aq)}$
$Ni(CO_3)_2^{2-}$	3 ± 1	estimated	$NiCO_{3(aq)} + CO_3^{2-} \Leftrightarrow Ni(CO_3)_2^{2-}$
$Ni(CO_3)_3^{4-}$	1.5 ± 1	estimated	$Ni(CO_3)_2^{2-} + CO_3^{2-} \Leftrightarrow Ni(CO_3)_3^{4-}$
$Niox_{(aq)}$	5.2	M & S[1]	$Ni^{2+} + ox^{2-} \Leftrightarrow Niox_{(aq)}$
$Niox_2^{2-}$	3	M & S[1]	$Niox_{(aq)} + ox^{2-} \Leftrightarrow Niox_2^{2-}$
$Niox_3^{4-}$	1.5 ± 0.5	estimated	$Niox_2^{2-} + ox^{2-} \Leftrightarrow Niox_3^{4-}$
$Ni(OH)ox^-$	≤ -10	estimated	$Niox_{(aq)} + H_2O \Leftrightarrow Ni(OH)ox^- + H^+$
$Ni(OH)_2ox^{2-}$	≤ -11	estimated	$Ni(OH)ox^- + H_2O \Leftrightarrow Ni(OH)_2ox^{2-} + H^+$
$NiX_{(aq)}$	7.84	this work	$Ni^{2+} + X^{2-} \Leftrightarrow NiX_{(aq)}$
NiX_2^{2-}	≤ 5	estimated	$NiX_{(aq)} + X^{2-} \Leftrightarrow NiX_2^{2-}$
NiX_3^{4-}	≤ 3	estimated	$NiX_2^{2-} + X^{2-} \Leftrightarrow NiX_3^{4-}$
$Ni(OH)X^-$	≤ -10	estimated	$NiX_{(aq)} + H_2O \Leftrightarrow Ni(OH)X^- + H^+$
$Ni(OH)_2X^{2-}$	≤ -11	estimated	$Ni(OH)X^- + H_2O \Leftrightarrow Ni(OH)_2X^{2-} + H^+$
$CaOH^+$	-12.85 ± 0.1	B & M	$Ca^{2+} + H_2O \Leftrightarrow Ca(OH)^+ + H^+$
$CaHCO_3^+$	1.11 ± 0.07	P & B	$Ca^{2+} + HCO_3^- \Leftrightarrow CaHCO_3^+$
$CaCO_{3(aq)}$	3.22 ± 0.14	P & B	$Ca^{2+} + CO_3^{2-} \Leftrightarrow CaCO_{3(aq)}$
$Caox_{(aq)}$	3.2	S & M	$Ca^{2+} + ox^{2-} \Leftrightarrow Caox_{(aq)}$
$Caox_2^{2-}$	1	M & S[2]	$Caox_{(aq)} + ox^{2-} \Leftrightarrow Caox_2^{2-}$
$Caox \cdot H_2O_{(s)}$	-8.78	S & M	$Caox \cdot H_2O_{(s)} \Leftrightarrow Ca^{2+} + ox^{2-} + H_2O$
$Caox \cdot 3H_2O_{(s)}$	-8.32	S & M	$Caox \cdot 3H_2O_{(s)} \Leftrightarrow Ca^{2+} + ox^{2-} + 3\,H_2O$
$CaX_{(aq)}$	5 ±1	estimated	$Ca^{2+} + X^{2-} \Leftrightarrow CaX_{(aq)}$
CaX_2^{2-}	≤ 3	estimated	$CaX_{(aq)} + X^{2-} \Leftrightarrow CaX_2^{2-}$
Hox^-	4.266±0.001	S & M	$H^+ + ox^{2-} \Leftrightarrow Hox^-$
HX^-	7.82	this work	$H^+ + X^{2-} \Leftrightarrow HX^-$

For a detailed discussion of data selection and estimation see text.

*)The references used for selecting these data in Table 7 are: B & M: BAES & MESMER (1986); S & M: SMITH & MARTELL (1989); M & S^1: MARTELL & SMITH (1982); M & S^2: MARTELL & SMITH (1977); P & B : PLUMMER & BUSENBERG (1982).

The stability constants for consecutive metal oxalate 1:1 and 1:2 complexes closely follow a linear relationship over ten orders of magnitude, as Fig.9 shows. The few metal carbonate data seem to follow a very similar linear relation, and we therefore feel encouraged to estimate the stability constant of Ni-carbonate 1:2 complexes as log $K_2 = 3 \pm 1$.

Data for metal-oxalate 1:3 complexes are scarce, but the few data still follow a linear relationship (Fig. 12b). Usually investigations in carbonate systems do not extend to very high carbonate concentrations and thus, virtually no data are available for metal-carbonate 1:3 complexes. The only exception is $UO_2(CO_3)_3^{4-}$ (GRENTHE et al. 1992) whose measured consecutive stability constant comes rather close to the oxalate relation. Note, that the formally analogous complex $UO_2ox_3^{4-}$ does not fit into the overall oxalate relation (Fig.12b) due to steric reasons. Whereas three carbonate ligands fit in the equatorial plane of UO_2^{2+}, the bulkier oxalate molecules cannot be arranged in such a way that all three oxalates concomitantly can coordinate as bidentate ligands. If we courageously assume, based on just one data point ($UO_2(CO_3)_3^{4-}$), that the oxalate relation still can be applied to metal-carbonate 1:3 complexes in the same way as to 1:2 complexes, a value of $\log K_3 = 1.5 \pm 1$ is estimated from $\log K_2$ and the linear relation in Fig.12b.

The first protonation constant of oxalate is taken from SMITH & MARTELL (1989) who evaluated a large number of experimental data and derived a value of log $K = 4.266 \pm 0.001$. This represents the best known thermodynamic constant in the framework of this modelling study, but unfortunately also the least important one. It shows that in all common groundwaters (pH > 5), and high pH waters, oxalate is completely deprotonated, and therefore the exact value of the first oxalate protonation constant has no influence on the modelling results at all. The constant is included in the present data base for completeness only.

The values for Ca-oxalate complexation constants are derived from the data collected by SMITH & MARTELL (1989) and MARTELL & SMITH (1977). These authors report data on the Ca-oxalate 1:1 complex from various authors measured at different temperatures and different ionic strengths. Data

measured at 37 °C and varying ionic strength up to 0.5 M all result in $\log K_1$ = 3.3 when extrapolated to zero ionic strength using the Davies equation. At 25 °C and I=0 a constant of log K_1 = 3.2 is selected by SMITH & MARTELL (1989), whereas at 18 °C and I=0 a value of log K_1 = 3.0 is reported. Allowing for a slight variation of stability constants with temperature, these data reveal a consistent picture and thus the value given for 25 °C is included into the present thermodynamic model.

MARTELL & SMITH (1977) report only one investigation, where sufficiently high oxalate concentration allowed the derivation of complexation constants, not only for Ca-oxalate 1:1 complexes, but also for 1:2 complexes ($\log K_1$ = 1.66 and $\log\beta_2$ = 2.69). The experiments were done at 25 °C and high ionic strength (1 M). Extrapolation of the constants to zero ionic strength using the Davies equation most probably results in erroneous values. Interaction coefficients for the more appropriate SIT equation (GRENTHE et al. 1992) at present are not available for Ca oxalate equilibria. There is, however, a way out of this unfortunate situation. The stepwise stability constant $\log K_2$ of the reaction:

$$Caox_{(aq)} + ox^{2-} \Leftrightarrow Caox_2^{2-} \qquad (38)$$

equals 1.0.

Extrapolating $\log K_2$ to zero ionic strength ($\log K_2^0$) involves the summation of activity coefficients $\log\gamma_i$ for individual species i:

$$\log K_2^0 = \log K_2 + \log\gamma_{Ca(ox)_2^{2-}} - \log\gamma_{Caox} - \log\gamma_{ox^{2-}} \qquad (39)$$

Applying the Davies equation:

$$\log\gamma_i = -z_i^2 \cdot D_{Davies} \qquad (40)$$

where z_i is the charge of species i and D_{Davies} the expanded Debye-Hückel term of the Davies equation (at 25 °C):

$$D_{Davies} = 0.5 \cdot \left(\frac{\sqrt{I}}{1+\sqrt{I}} - 0.3 \cdot I \right) \qquad (41)$$

reduces equation (39) to:

$$\log K_2^0 = \log K_2 + \Delta z^2 \cdot D_{Davies} \quad (42)$$

The net change of charge of reaction (38), Δz^2, is zero and thus the Davies equation predicts no change in $\log K_2$ with varying ionic strength. This prediction is only valid for low ionic strength ($I < 0.1$ M). At higher ionic strength ($I > 0.1$ M) it is more appropriate to apply the SIT equation (GRENTHE et al. 1992):

$$\log \gamma_i = -z_i^2 \cdot D_{SIT} + \sum_j \varepsilon_{(i,j)} \cdot m_j \quad (43)$$

where $\varepsilon_{(i,j)}$ are the specific ion interaction coefficients, m_j the concentration of ion j and D_{SIT} the Debye-Hückel term of the SIT equation (at 25 °C):

$$D_{SIT} = 0.5091 \cdot \left(\frac{\sqrt{I}}{1+1.5 \cdot \sqrt{I}} \right) \quad (44)$$

In the case of experimental data measured in solutions of strong 1:1 electrolytes such as $NaClO_4$, equation (39) reduces to:

$$\log K_2^0 = \log K_2 + \Delta z^2 \cdot D_{SIT} + \Delta \varepsilon \cdot I \quad (45)$$

As in the case of the Davies equation, the Debeye-Hückel term of equation (39) again vanishes when Δz^2 is zero. The net change of the specific ion interaction coefficients, $\Delta \varepsilon$, remains the only possible contribution to a change of $\log K_2$ with varying ionic strength.

The individual interaction coefficients for oxalate-species are unknown but the order of magnitude of $\Delta \varepsilon$ can be estimated. The interaction coefficient of uncharged species such as Caox is assumed to be zero (GRENTHE et al. 1992). If we further consider that the ion specific interaction parameters of SIT depend in the first place on charge and only in the second place vary with the size of the complexes, we expect the interaction parameters of ox^{2-} and $Niox_2^{2-}$ to be rather similar. In summary, the variation of $\log K_2$ with ionic strength from zero to 1 M is expected to be less than 0.1, and thus a value of

$\log K_2$ = 1.0 is included in our present model. As can be seen in Fig. 9, the $\log K_1$ - $\log K_2$ values for Ca oxalate selected here fit excellently into the overall oxalate relationship derived from a large set of stability data.
Inserting $\log K_2$ = 1.0 into the oxalate relation of Fig.12b results in $\log K_3 < 0$. The (hypothetical) formation of Ca oxalate 1:3 complexes therefore can safely be ignored in our modelling study.
The stability constants for Ni-oxalate complexation are derived from MARTELL & SMITH (1982). For 1:1 complexes they report a value measured at 25 °C, and extrapolated to zero ionic strength of $\log K_1$ = 5.16. As the stability of Ni-oxalate complexes is one of the key parameters in this modelling study, an independent investigation was carried out by VAN LOON & KOPAJTIC (1991) using the Schubert ion exchange method. They found a value of $\log K_1$ = 4.27 ± 0.05 at 20 °C and I=0.11 M, extrapolated to zero ionic strength using the Davies equation: $\log K_1$ = 5.13 ± 0.05. Considering the experimental uncertainty, these two independent results justify the use of a rounded off value of $\log K_1$ = 5.2.
Looking for studies at higher oxalate concentrations we are faced with the same situation as in the case of Ca-oxalates. The only values reported by MARTELL & SMITH (1982) stem from experiments done at 25 °C and high ionic strength ($\log K_1$ = 3.7 and $\log \beta_2$ = 6.6 at I=1 M). Consequently, the same arguments apply as in the Ca case, and a value of $\log K_2$ = 3 at I=0 is derived from these data. Again, the $\log K_1$-$\log K_2$ values for Ni-oxalate selected here excellently fit into the overall oxalate relationship derived from a large set of stability data, as can be seen in Fig.9, which gives some additional confidence in the present data selection.
No experimental data are reported for Ni-oxalate 1:3 complexes. Free energy relationships, however, of oxalate complexes (Fig.12b), in accord with the observation that Ni(II) prefers a maximum coordination number of 6, suggest the existence of the equilibrium:

$$Niox_2^{2-} + ox^{2-} \Leftrightarrow Niox_3^{4-} \qquad (46)$$

Inserting $\log K_2$ = 3 into the linear relationship shown in Fig.12b, results in an estimate of the stepwise stability constant $\log K_3$ = 1.5 ± 0.5.
In the high pH range of cement pore waters (pH>12), the Ni-oxalate complexes probably hydrolyse and form ternary Ni-hydroxo-oxalate

complexes which may dominate the Ni-speciation. To our present knowledge, no study of oxalate complexation in alkaline solutions has yet been published. We already used the carbonate-oxalate analogy to estimate stability constants of Ni-carbonate complexes. Now we use this analogy the other way to derive at least some qualitative information concerning oxalate complexation in alkaline solutions. Grenthe and co-workers published two studies of Zn-(FERRI et al. 1987a) and Pb-(FERRI et al. 1987b) carbonate complexation in alkaline solutions (pH > 10) using rather high carbonate concentrations (1 M Na_2CO_3). In the case of Zn, the experimental data are best described by $Zn(CO_3)_2^{2-}$, $Zn(OH)_4^{2-}$ and $ZnCO_3(OH)_2^{2-}$ as major species in alkaline solutions. The authors conclude: "*The stoichiometric compositions of the zinc complexes indicate that zinc(II) has tetrahedral coordination geometry in these complexes.*" The experimental data of the Pb carbonate system are interpreted in terms of $Pb(CO_3)_2^{2-}$, $Pb(OH)_3^-$ and $PbCO_3OH^-$. The authors state: "*The stoichiometry of these species strongly indicates a coordination geometry with the Pb(II) at the apex of square or trigonal pyramids. This is in fact the coordination geometry found in several solid Pb(II) compounds.*" This pyramidal coordination is caused by a stereochemically "active" ion-pair. In both cases, the species predominating at 1 M CO_3^{2-} with increasing pH are $M(CO_3)_2^{2-}$, the ternary hydroxo-carbonate complex, and finally the pure hydroxo complex. The predominance range of the mixed complex extends over about one pH unit, above pH 11 for Zn and beyond pH 12 for Pb.

Nickel generally prefers octahedral coordination of ligands, with one remarkable exception: the limiting complex with hydroxide is found to be $Ni(OH)_4^{2-}$. Even larger changes in maximum coordination numbers between carbonate and hydroxide are found in the case of Th. ÖSTHOLS et al. (1994) interpret experimental data in terms of $Th(OH)_{4(aq)}$, $ThCO_3(OH)_3^-$, and $Th(CO_3)_5^{6-}$. This means a change from maximum coordination number 10 (carbonate) to 4 (hydroxide), with a mixed complex of coordination number 5. As yet there is no sound theory explaining the sometimes very low coordination numbers of hydroxo complexes. The following therefore clearly belongs to the category of artful armwaving rather than sound estimation technique. We do not expect the formation of mixed hydroxo-carbonate complexes with maximum coordination number 6, such as $NiCO_3(OH)_4^{4-}$ or $Ni(CO_3)_2(OH)_2^{4-}$. Considering the small negative charges of mixed complexes of Zn, Pb and Th and taking into account the difference in maximum coordination numbers of Ni- and Th-hydroxo and -carbonato complexes,

complexes like $Ni(OH)ox^-$ and $Ni(OH)_2ox^{2-}$ probably are formed. Hydrolysis of metal-ligand complexes is always somewhat weaker than hydrolysis of the (hydrated) cation itself. Therefore, based on the first hydrolysis constant of Ni ($logK \approx -10$) an upper limit of $logK < -10$ is estimated for the equilibrium:

$$Niox_{(aq)} + H_2O \Leftrightarrow Ni(OH)ox^- + H^+ \quad (47)$$

and $logK < -11$ for

$$Ni(OH)ox^- + H_2O \Leftrightarrow Ni(OH)_2ox^{2-} + H^+ \quad (48)$$

These estimated values are also included in Table 7, but they should be used with utmost care!

Ligand X is at present characterised by two experimentally determined stability constants, namely the complexation constant $logK_{NiX} \approx 7$ and the protonation constant $logK_{HX} \approx 7.4$, both measured at an ionic strength of 0.1 M. In addition, considering the chemical composition of the resin waters (e.g. Table 2) it is concluded that ligand X is most probably a pure oxo-ligand. The molecular structure and hence, the charge of ligand X is not yet known. An attempt was made to assess X's charge and ligand class by plotting stability constants of 1:1 Ni-organic complexes (ML) of common oxo-ligands against their first protonation constants (HL). As can be seen in Fig.10, the ligand classes cluster in different areas of the ML-HL plot: The protonation constants of carboxylic acids range from 3 to 7 with non-overlapping clusters for mono-, di- and tricarboxylic acids. Carbonyl ligands and hydroxo-carbonyl ligands like acetylacetone and tropolone cluster in the region $6 < HL < 10$ and $5 < ML < 7$. Phenol-type ligands like salicylic acid, catechol or tiron are at the "high end" of the stability constants plot with $HL > 10$ and $ML > 7$. NiX stability is close to salicylic acid stability, but the high protonation constants of phenols rule out ligand X being a phenol type ligand. The protonation constant of ligand X lies in the range of carbonyl type ligands with charge -1 and is higher than the first protonation constant of citrate with charge -3. Extrapolating stability constants measured at 0.1 M to zero ionic strength gives different results depending on the assumed ligand charge. The rectangle labelled X in Fig.10 shows the variability caused by using charge -1 (left) or -3 (right). As long as speciation calculations are carried out at ionic strength 0.1 M these effects vanish of course for the measured stability constants. For estimated constants the uncertainty due to an arbitrary choice of the ligand charge is negligible

compared to the uncertainties of the estimation procedures. Thus, an operational ligand charge of -2 was chosen for all subsequent calculations. Note, that giving the stability constants of NiX and HX in Table 7 with two decimal places does not indicate any "precision" but simply restores the measured values for speciation calculations at ionic strength 0.1M. In summary, no clear-cut conclusions from Fig.10 can be drawn as to the charge and the nature of ligand X.

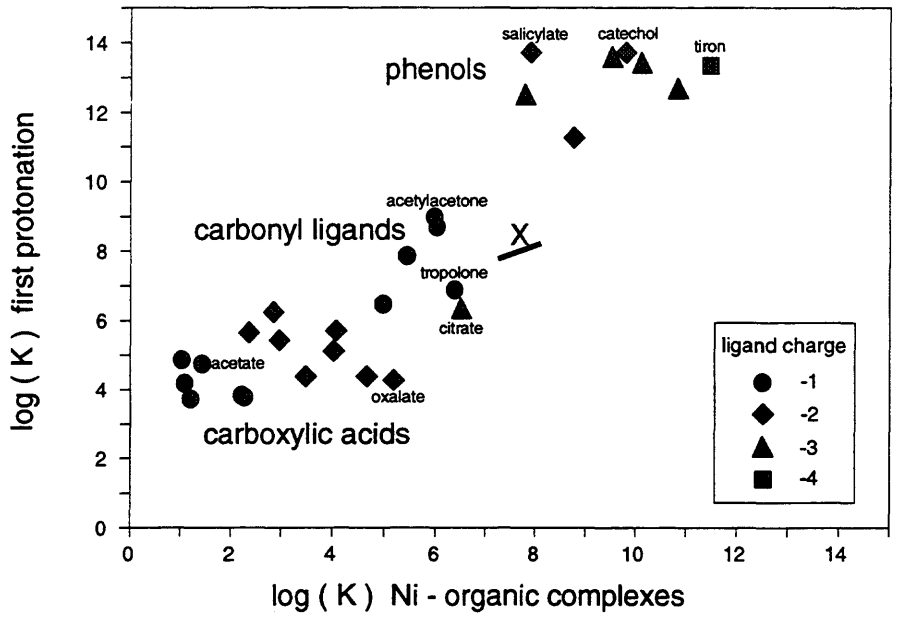

Figure 10: The first protonation constants of organic ligands plotted against the stability constants of their 1:1 Ni-organic complexes. Common oxo-ligands are selected comprising the classes of phenols, carboxylic acids and carbonyl ligands. The black rectangle represents the experimental data of ligand X.

The next question concerns the Ca and Mg competition due to the formation of CaX and MgX complexes. Fig.11 reveals a strong linear correlation between Ni and Ca 1:1 complexes with oxo-ligands. The solid line is obtained by regression analysis:

$$\log(K_{CaL}) = (0.56 \pm 0.44) + (0.56 \pm 0.07) \cdot \log(K_{NiL}) \qquad (49)$$

A similar linear correlation exists for Ni and Mg complexes (not shown):

$$\log(K_{MgL}) = (0.09 \pm 0.36) + (0.70 \pm 0.05) \cdot \log(K_{NiL}) \qquad (50)$$

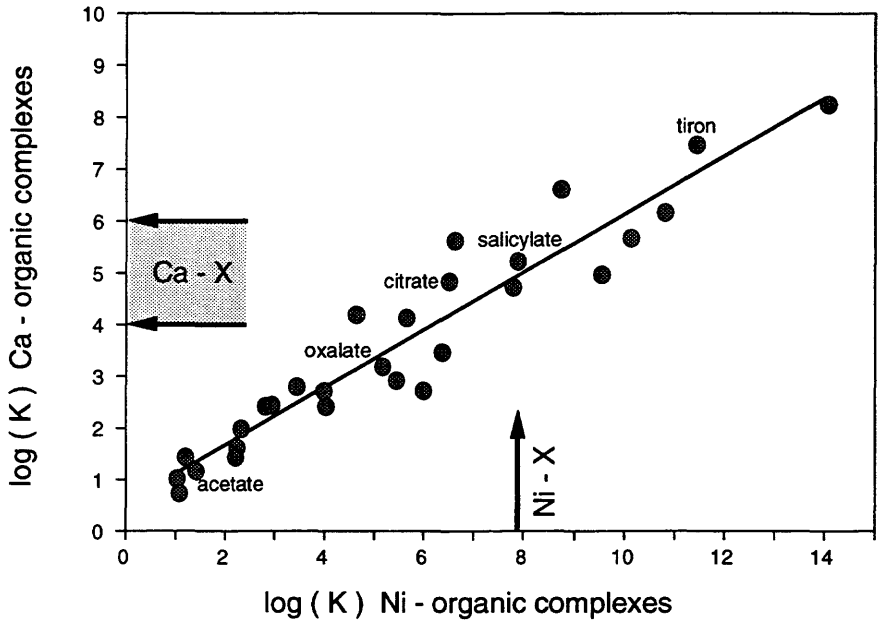

Figure 11: Stability constants of Ni and Ca 1:1 complexes with common organic oxo-ligands. The regression line, calculated by equation (49), is used to estimate the stability constant of CaX. The gray area shows the uncertainty of the estimated value.

Inserting the stability constant log K_{NiX} = 7.84 in eqs.(49) and (50) gives: $\log K_{CaX}$ = 5.0 ± 1.2 and $\log K_{MgX}$ = 5.6 ± 1.0 (all uncertainties marked by ± here refer to a 95% confidence level). As the results for CaX and MgX are rather similar considering their associated uncertainty ranges, the competition of Ca and Mg with Ni-complexation can be reduced to one parameter using the sum of Ca and Mg concentrations and a common stability constant logK = 5 ± 1 in subsequent speciation calculations.

By analogy with oxalate, complexes like NiX_2^{2-} and CaX_2^{2-}, and probably NiX_3^{4-}, may predominate within some ligand concentration ranges. The consecutive formation constants of ML_x complexes in general are correlated with ML_{x-1} data for the same ligand, but the actual values for ML_x constants depend in a complex manner on the nature of the ligand, i.e. on ligand charge, number of functional groups and ligand size. The nature of ligand X is as yet unknown and thus, correlations found, e.g. for oxalate or citrate, cannot be used directly to estimate the stability of MX_y complexes. Instead, an attempt

was made to assess at least upper limits for MX_y stability constants, in order to test if such complexes could have any significant influence on speciation calculations. Fig. 10 shows that ligand X plots in the neighbourhood of the clusters of carbonyl ligands and carboxylic acids. Therefore, data for representative ligands of these classes are plotted in Fig.12. As can be seen in Figs.12a and b, the values of the carbonyl ligand acetylacetone (acac) are strongly correlated and close to the oxalate data. This is not surprising as both molecules act as small bidentate ligands with charge -1 (acac) or -2 (ox). If ligand X thus is a very small molecule containing only two carbonyl (and/or carboxyl) groups, as a "worst case scenario" the stability of MX_2 and MX_3 complexes should plot in the acac-ox data range. If ligand X is bulkier than acac or ox, MX_3 complexes will not form, and MX_2 complexes may follow the citrate correlation or may also not form at all. In summary, upper limits of stability constants are estimated for the following equilibria: $\log K < 5$ for $NiX_{(aq)} + X^{2-} = NiX_2^{2-}$, $\log K < 3$ for $NiX_2^{2-} + X^{2-} = NiX_3^{4-}$ and $\log K < 3$ for $CaX_{(aq)} + X^{2-} = CaX_2^{2-}$.

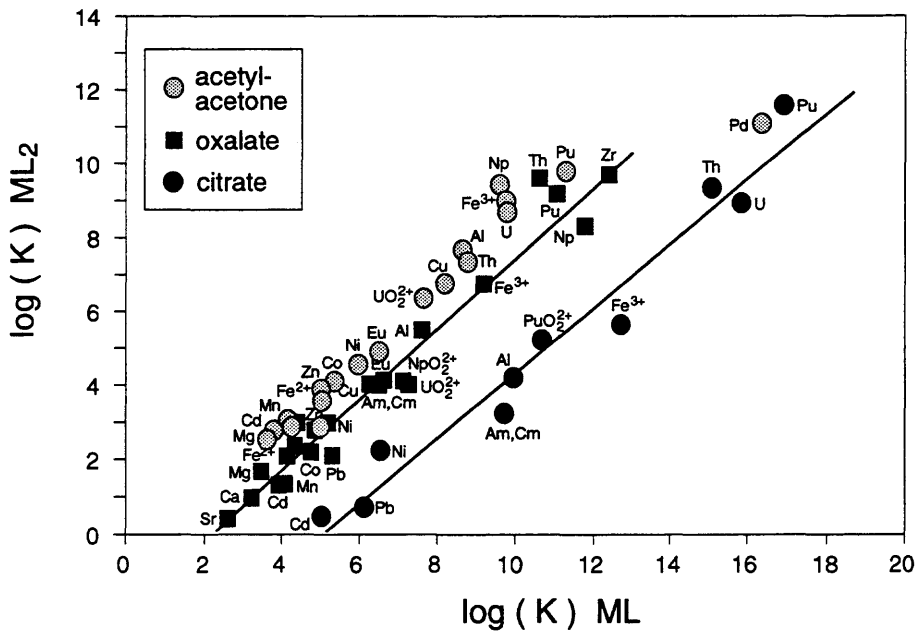

Figure 12a: Correlation of stepwise formation constants of 1:1 and 1:2 metal-organic complexes. Data are taken from SMITH & MARTELL (1989) and MARTELL & SMITH (1982, 1977). The solid lines are obtained by regression analysis.

Oxalate: $\log K_{Mox2} = (-2.1 \pm 0.6) + (0.95 \pm 0.08) \cdot \log K_{Mox}$

Citrate: $\log K_{Mcit2} = (-4.5 \pm 1.5) + (0.88 \pm 0.13) \cdot \log K_{Mcit}$.

Furthermore, in the high pH range of cement pore waters, mixed Ni-hydroxo-X complexes may dominate the speciation in the same way as ternary Ni-hydroxo-oxalate complexes. Upper limits of stability constants thus are estimated by analogy with oxalate.

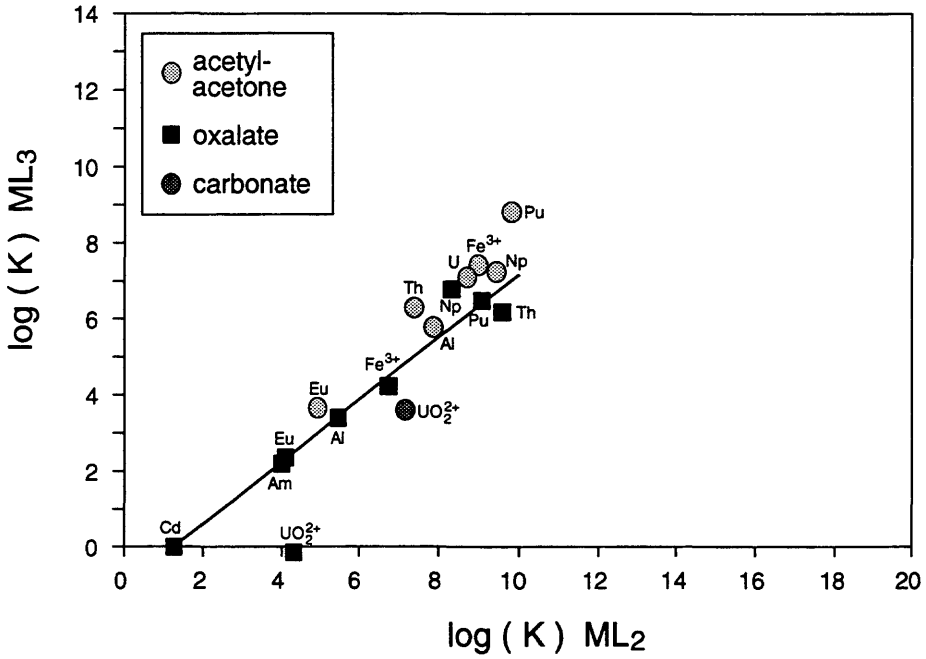

Figure 12b: Correlation of stepwise formation constants of 1:2 and 1:3 metal-ligand complexes. Data for organics are taken from SMITH & MARTELL (1989) and MARTELL & SMITH (1982, 1977). Data for U(VI) carbonate are taken from GRENTHE et al. (1992). The solid line is obtained by regression analysis for oxalate: $\log K_{Mox3} = (-1.0 \pm 1.0) + (0.82 \pm 0.16) \cdot \log K_{Mox2}$.

3.5.3 Oxalate

Speciation calculations were done in the simplified chemical system [Ca + Mg] -pH-P_{CO_2}-[Ni]-[oxalate] using the programme "BACKDOOR"[2] currently under

[2] The programme is designed for the quick exploration of the geochemical and thermodynamic space with respect to the impact of any given ligand on any given metal cation. "BACKDOOR" will be described in detail in a later publication that will also discuss the use of advanced computer graphics as tools for this "Odyssey in parameter space".

development. The parameter range for groundwaters is defined as follows: $6 \leq pH \leq 9$, 10^{-4} M $\leq$ [Ca + Mg] $\leq 10^{-2}$ M, $P_{CO_2} = 10^{-2}$ bar (and down to 10^{-5} bar), $[Ni]_{total} < 10^{-5}$ M, ionic strength I = 0.1 M. For cement pore waters the following ranges were chosen: $11 \leq pH \leq 13$, 10^{-3} M $\leq$ [Ca] $\leq 10^{-1}$ M, $P_{CO_2} = 10^{-12}$ bar, $[Ni]_{total} < 10^{-5}$ M, ionic strength I = 0.22 M. The thermodynamic constants, given in Table 7 at I=0, are extrapolated to the chosen ionic strength using the Davies equation.

The level of significant influence was (arbitrarily) chosen to be a constant fraction of [Ni-organic complexes] / $[Ni]_{total}$ = 0.5, which means that 50% of Ni in solution is complexed by the organic ligand.

"BACKDOOR" results for oxalate in groundwater are shown in Fig.13a as a 3D plot.

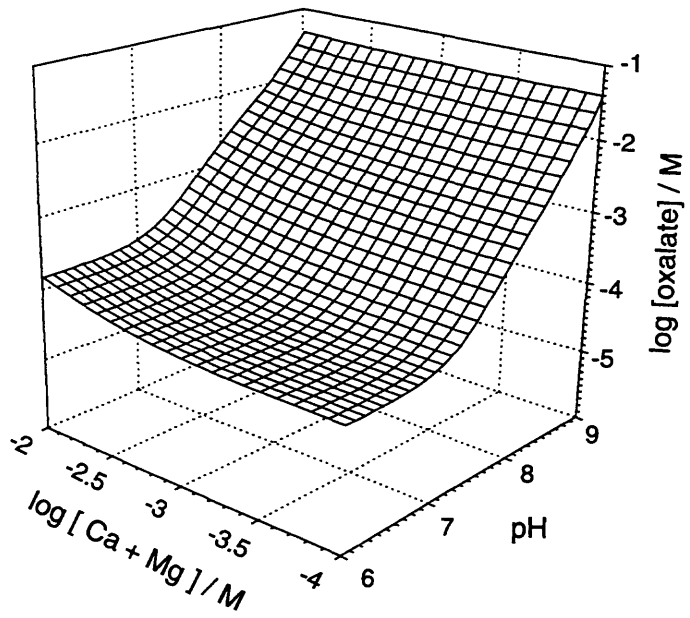

Figure 13a: The influence of oxalate on the complexation of Ni in groundwaters at $P_{CO_2} = 10^{-2}$ bar. For any given pH and Ca + Mg concentration, the surface shows the amount of oxalate needed to reach 50% Ni-oxalate complexation.

The oxalate surface is calculated as a function of pH and $\log[Ca + Mg]_{total}$. The picture may be interpreted as follows: For any given pH and calcium + magnesium concentration, the amount of oxalate needed to reach 50% Ni-

oxalate complexation is shown by the surface. As can be seen in Fig.13a, the results are almost independent on the calcium + magnesium concentration, but there is a significant pH dependence for pH > 7.5. Increasing the pH in this region increases competitive effects due to the formation of Ni-carbonato complexes and thus, more oxalate is needed to complex 50% of $[Ni]_{total}$.

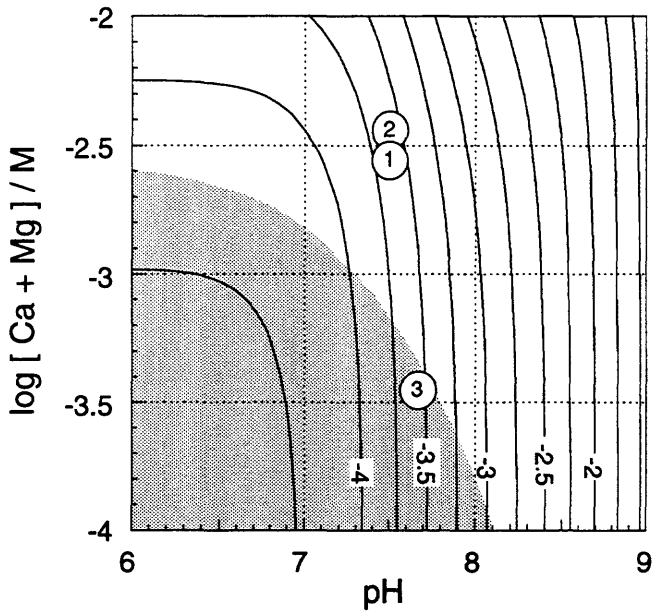

Figure 13b: The influence of oxalate on the complexation of Ni in groundwaters at $P_{CO_2} = 10^{-2}$ bar. The amount of oxalate needed to complex 50% Ni can be read directly from the contour lines. For comparison, some groundwater data are included: (1) Wellenberg marl pore water (BAEYENS & BRADBURY 1994), (2) Oberbauenstock marl pore water (BAEYENS & BRADBURY 1991), (3) Crystalline reference water (PEARSON & SCHOLTIS 1993). The gray area shows the range where oxalate is able to influence the Ni-speciation if equilibria with Ca-oxalate solids are considered. Outside this gray area the oxalate concentrations indicated by the contour lines cannot be reached due to Ca-oxalate precipitation.

Fig.13b shows the same results as Fig.13a but as a contour plot. Whereas the surface plot of Fig.13a gives a vivid impression of the importance of the organic ligand, the contour plot of Fig.13b is better suited to derive quantitative

information. The amount of oxalate needed to complex 50% Ni for any given pH and calcium + magnesium concentration can be directly read from the contour lines. For comparison, pH and [Ca + Mg] values of some reference groundwaters at $P_{CO_2} \approx 10^{-2}$ bar are included in Fig.13b. As can be seen from the contour plot, in all cases about $10^{-3.5}$ M oxalate is needed in order to complex 50% Ni.

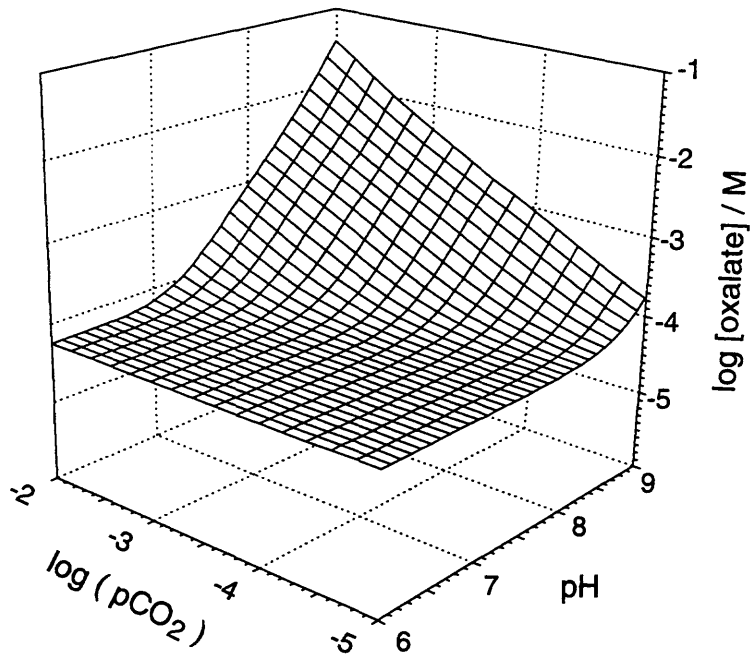

Figure 14a: The influence of oxalate on the complexation of Ni in groundwater at [Ca + Mg] = 10^{-3} M. The 50% organic complexation surface is shown.

The influence of carbonate competition on Ni-oxalate complexation is clearly revealed in Fig.14: The concomitant effects of increasing pH and increasing P_{CO_2} require higher oxalate concentrations due to the formation of Ni-carbonato complexes. For low P_{CO_2} and low pH values where Ni-carbonato complexes are minor species or are not formed at all, the oxalate concentration needed to complex 50% Ni reaches a plateau of about 10^{-4} M (Fig.14b). Data for marl pore waters, at a level of [Ca + Mg] $\approx 10^{-3}$ M, are included in Fig.14b for illustration. The pH of these pore waters is only known within one order of magnitude, which leads to some variation in modelled pore water chemistry under the assumption that the marl pore waters are in equilibrium with calcite and dolomite (BAEYENS & BRADBURY 1994). As can

be seen comparing (1) and (2) in Figs.13b and 14b, increasing the pH decreases P_{CO_2}, and also decreases the Ca and Mg concentration.The net effect of these correlated variations due to the uncertainty in pH is a constant Ca and carbonate competition.This is the secret behind the observation that the amount of oxalate needed to complex 50% Ni remains constant in spite of the variations in pH, P_{CO_2} and Ca and Mg concentration.

In high pH waters, some influence of pH and calcium concentration on the results is seen but at a rather high oxalate concentration (Fig.15). As can be seen in Fig.15b, almost 0.1 M oxalate is needed to complex 50% Ni in fresh cement pore waters. This value slowly decreases with advancing cement degradation but never drops below 10^{-3} M, even in very late degradation stages.

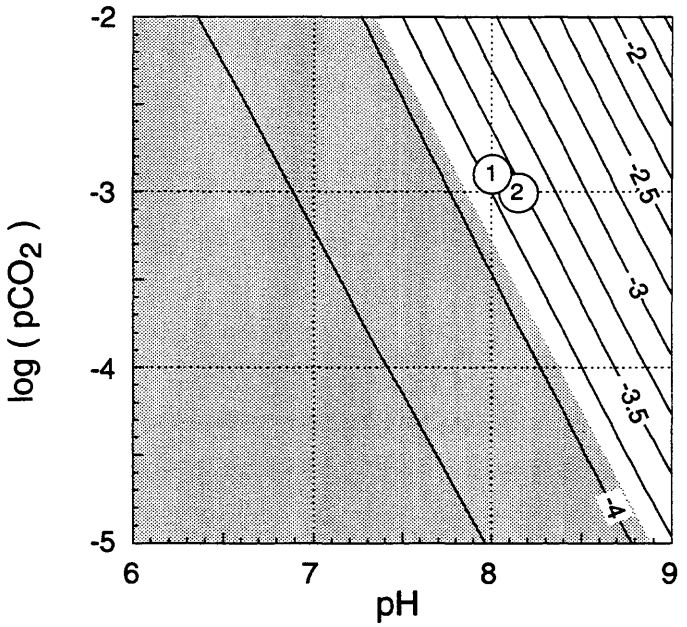

Figure 14b: The same results as Fig.14a but shown as contour plot. (1) Wellenberg marl pore water (BAEYENS & BRADBURY 1994), (2) Oberbauenstock marl pore water (BAEYENS & BRADBURY 1991). The gray area shows the range where oxalate is able to influence the Ni-speciation if equilibria with Ca-oxalate solids are considered. Outside this gray area the oxalate concentrations indicated by the contour lines cannot be reached due to Ca-oxalate precipitation.

Some questions about the influence of oxalate on Ni-speciation remain to be answered:

- What is the influence of uncertainty in estimated stability constants on the results?

- Are results obtained with the simplified chemical system representative for groundwaters and cement pore waters?

- Is there any upper concentration limit of oxalate to be expected in the waters considered here?

In the parameter space of groundwaters (Figs.13 and 14) the uncertainties in speciation calculations arise from the estimated properties of Ni-carbonate species and $Niox_3^{4-}$. The competition of carbonato complexes is visible in figs. 13 and 14 as parameter regions where more than 10^{-4} M oxalate is needed to have 50 % of the Ni complexes by oxalate, i.e. above pH 7.5 in Fig. 13. Here, the uncertainty of the estimated $NiCO_{3(aq)}$ of ± 0.5 log units causes an uncertainty of the oxalate surface of the same order of magnitude. In the range of $10^{-2.5}$ M oxalate, around pH 8.5 in Fig.13, the major species are $Ni(CO_3)_2^{2-}$ and $Niox_2^{2-}$. Above $10^{-2.5}$ M oxalate, the 1:3 carbonate and oxalate species predominate. Due to the partly correlated uncertainties of these estimated consecutive stability constants, the overall uncertainty of the oxalate surface is expected to increase from ± 0.5 log units at $10^{-3.5}$ M to ± 1 at 10^{-2} M oxalate. In other words, the uncertainty is large at high oxalate concentrations and decreases with decreasing concentration.
In the parameter space of high pH waters, the species $Ni(OH)_2ox^{2-}$ predominates the organic speciation, if the maximum values of all estimated constants of Table 7 are used in the computations (Fig.15). If the value for $Ni(OH)_2ox^{2-}$ stability is decreased by one order of magnitude, $NiOHox^-$ and $Niox_3^{4-}$ predominate with increasing pH, and the oxalate surface shifts to higher values by up to 0.5 log units. The results for high pH waters (Fig.15) represent a worst case scenario; neglecting $Niox_3^{4-}$ and/or using smaller values for $Ni(OH)ox^-$ and $Ni(OH)_2ox^{2-}$ than the upper limits given in Table 7 increases further the already high oxalate concentrations. In summary, for the present purposes it is not necessary to put any effort in an experimental determination of stability constants for these complexes.

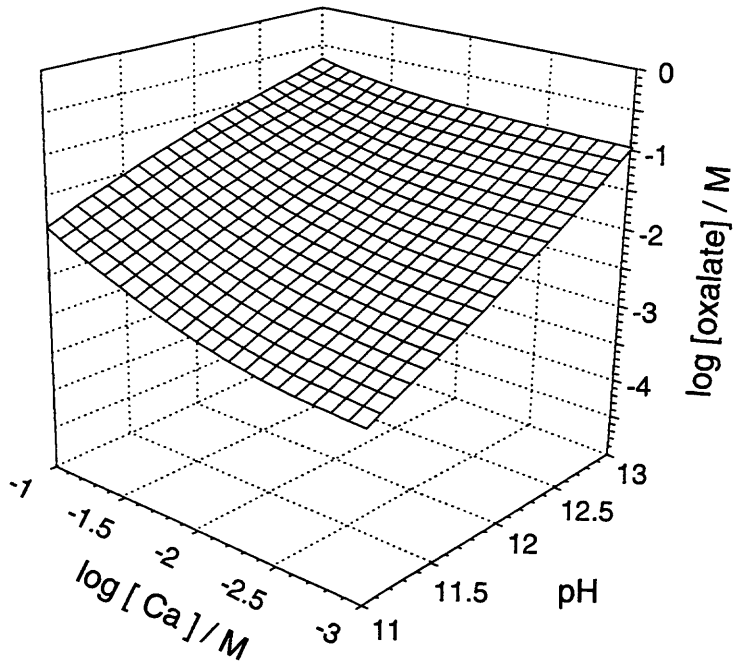

Figure 15a: The influence of oxalate on the complexation of Ni in high pH waters. The maximum values in Table 7 are used for the speciation calculations. The 50% organic complexation surface is shown.

Answering the second question, as to the justification using a simplified chemical system, the Oberbauenstock marl pore water, (2) in Fig.14b, was chosen as a test example. The water at P_{CO_2} = 10^{-3} bar is characterised by pH 8.2 and high concentrations of sodium (0.11 M), chloride (0.06 M) and sulphate (0.025 M). Speciation calculations were done using the programme MINEQL/PSI. For the simplified chemical system [Ca + Mg]-pH-P_{CO_2}-[Ni]-[oxalate] the results are identical to the BACKDOOR calculations (Fig.14b), i.e. 50% Ni oxalate complexes at $\log[ox]_{total}$ = -3.5. For the full chemical system the oxalate concentration increases to $\log[ox]_{total}$ = -3.4. The concomitant action of all competing reactions like the formation of Ni-sulphate, -chloride and - fluoride complexes as well as Ca-sulphate and Na-oxalate complexes has no significant influence on the overall result. It is therefore concluded that the simplified chemical system used here is sufficient to assess the influence of oxalate on Ni-speciations. This conclusion may not be valid for all possible water compositions, but in any case of doubt only a single test speciation calculation using the full chemical composition is necessary.

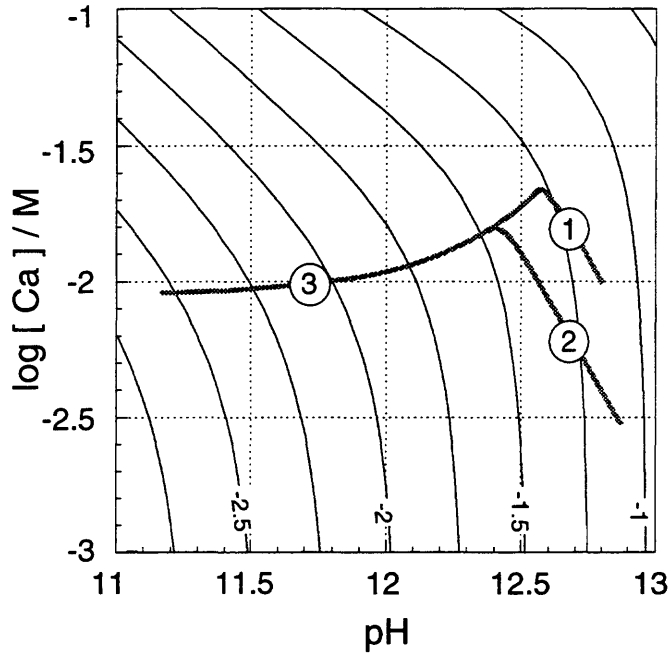

Figure 15b: The same results as Fig.15a but shown as contour plot. For comparison, pH and calcium concentrations of pore waters of cement degrading in a marl-type groundwater (BERNER 1990) are added as gray-shaded areas: (1) Sulphate resistant Portland cement in early degradation stages, (2) cement mixed with German Trass in early degradation stages and (3) both cements in later degradation stages. Physically all conditions above the gray lines cannot exist in cement pore waters.

Calcium oxalate solids are found as naturally occurring minerals whewellite ($Caox \cdot H_2O$) and weddelite ($Caox \cdot 3H_2O$). If the slightly more soluble weddelite is included in the speciation calculations, upper limits of aqueous oxalate concentrations can be calculated. For the marl pore waters at $P_{CO_2} = 10^{-3}$ bar, (1) and (2) in Fig.14b, the predicted maximum aqueous oxalate concentration is 10^{-4} M based on the solubility of Ca-oxalate. In other words, maximal 14% of the dissolved Ni is complexed as Ni-oxalate. For a fresh cement pore water, (1) in Fig.15b, the maximum aqueous oxalate concentration is 10^{-5} M; no Ni-oxalate complexes are formed at this low oxalate concentration. Thus, if precipitation of Ca-oxalate is considered, significant influence of oxalate is limited to certain [Ca]-pH ranges. The gray areas in Figs.13b and 14b show the accessible parameter space if solid Ca-oxalate is considered, i.e. the range where oxalate is able to influence the Ni-speciation. At the borderline of

the gray area a maximum of 50% Ni-oxalate complexes is expected, e.g. for the crystalline reference water, (3) in Fig.13b. Outside this area the oxalate concentrations necessary for a significant influence (i.e. 50 % Ni-complexation) cannot be reached due to the precipitation of Ca-oxalate. Within the parameter range of cement pore waters (Fig.15b) precipitation of Ca-oxalate completely prevents any influence of oxalate on Ni.

3.5.4 Ligand X

The thermodynamic behaviour of ligand X is characterised by two measured stability constants for NiX and HX. The stabilities of all other probably important complexes are estimated (see Table 7) and most of these estimated values can only be given as upper limits defining a worst case scenario. The stability range of CaX is well established by a linear free energy relationship (Fig.11) but the actual values of NiX_2^{2-}, NiX_3^{4-} and CaX_2^{2-} strongly depend on the as yet unknown nature of ligand X.

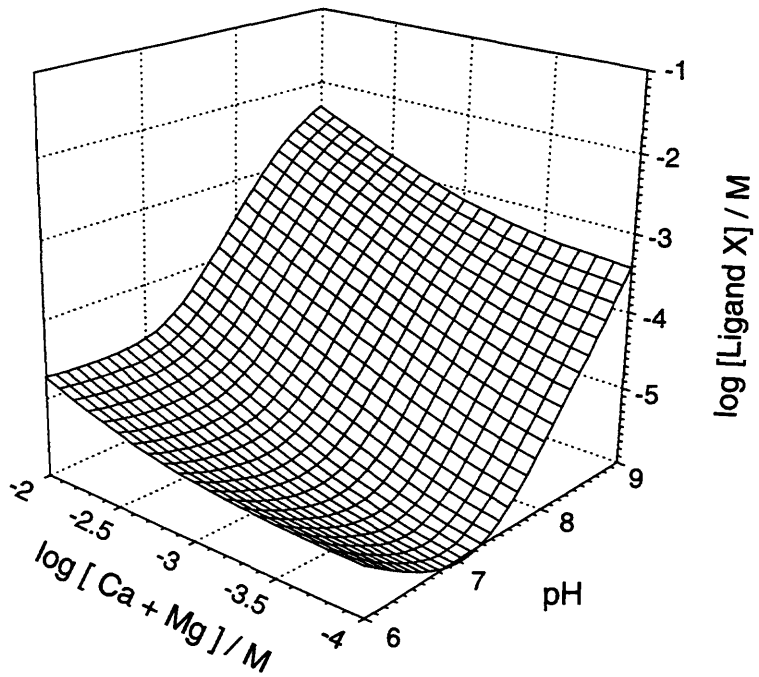

Figure 16a: The influence of ligand X on the complexation of Ni in groundwaters at $P_{CO_2} = 10^{-2}$ bar. The maximum values in Table 7 are used for the speciation calculations. The 50% Ni-organic complexation surface is shown.

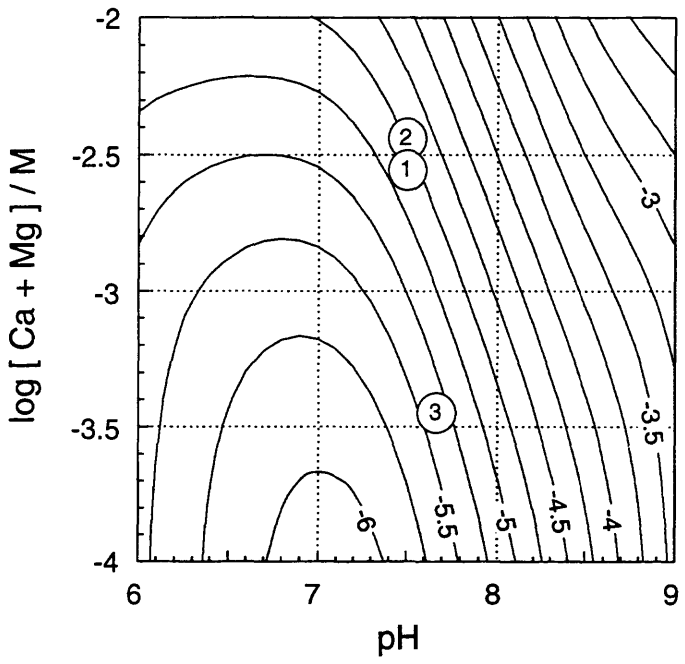

Figure 16b: The same results as Fig.16a but shown as contour plot. For comparison, some groundwater data are included: (1) Wellenberg marl pore water (BAEYENS & BRADBURY 1994), (2) Oberbauenstock marl pore water (BAEYENS & BRADBURY 1991), (3) Crystalline reference water (PEARSON & SCHOLTIS 1993).

Furthermore, the existence of $Ni(OH)_2X^{2-}$ and $Ni(OH)X^-$ species is considered somewhat speculative, relying completely on the analogy with oxalate.

A base case was therefore defined comprising the measured complexes NiX and HX and all estimated complexes at their maximum values (Table 7). The impact of using other than these maximum values on the Ni speciation is then compared with the results of the base case. The same parameter range for "BACKDOOR" calculations is used as for oxalate, except that the results for groundwaters are valid only for $[Ni]_{total} < 10^{-7}$ M.

The influence of ligand X on the Ni-speciation in groundwaters (Fig.16a) follows the same general pattern as oxalate (Fig.13a), i.e. minimal X concentrations in the neutral pH range and increasing X concentrations with increasing pH above 7.5 due to the competition of Ni-carbonato complexes. The differences between oxalate and ligand X may be described in quantitative rather than qualitative terms: In general, the concentrations of ligand X needed to complex 50% Ni are one to two orders of magnitude lower

than the oxalate concentrations, reflecting the considerably higher stability of Ni-X complexes. In addition, a more pronounced dependency on [Ca + Mg] concentration can be seen in Fig.16b than in Fig.13b. The slight increase in X concentration needed to complex 50% Ni with decreasing pH in the acidic region is caused by the onset of the protonation of ligand X below pH 7.

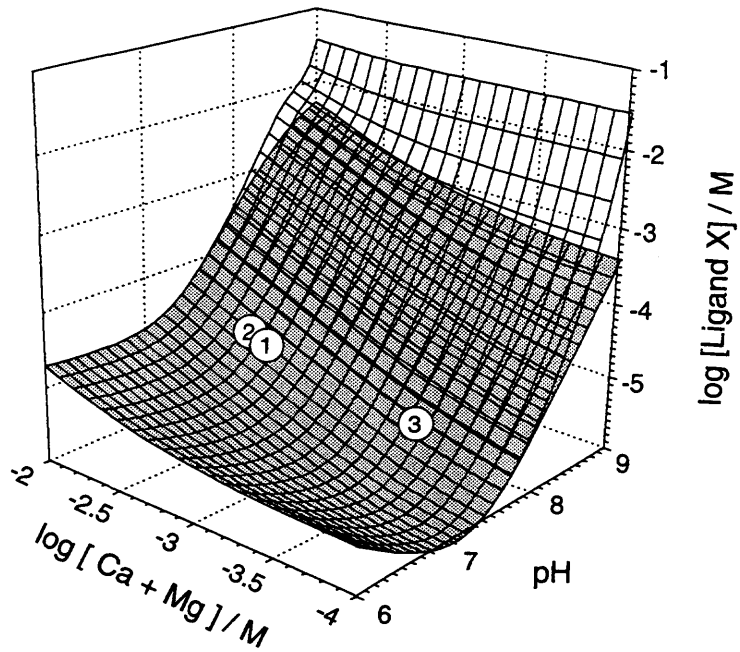

Figure 17: The influence of estimated stability constants for ligand X on the complexation of Ni in groundwaters at P_{CO_2} = 10^{-2} bar. The 50% Ni-organic complexation surfaces are shown. Gray surface: The maximum values in Table 7 are used for the speciation calculations (same as Fig.16a). This represents the worst case. White surface: NiX_2^{2-}, NiX_3^{4-} and CaX_2^{2-} are ignored in the speciation model. For comparison, some groundwater data are included: (1) Wellenberg marl pore water (BAEYENS & BRADBURY 1994), (2) Oberbauenstock marl pore water (BAEYENS & BRADBURY 1991), (3) Crystalline reference water (PEARSON & SCHOLTIS 1993).

In the base case, Fig.16 and gray surface of Fig.17, the maximum values for NiX_2^{2-}, NiX_3^{4-} and CaX_2^{2-} (Table 7) are included in the speciation calculations. This represents a worst case scenario, valid only if ligand X is a molecule as small as oxalate or acetylacetone. If ligand X is bulkier, e.g. like citrate, the stability constants of these complexes may be orders of magnitude below the selected maximum values.

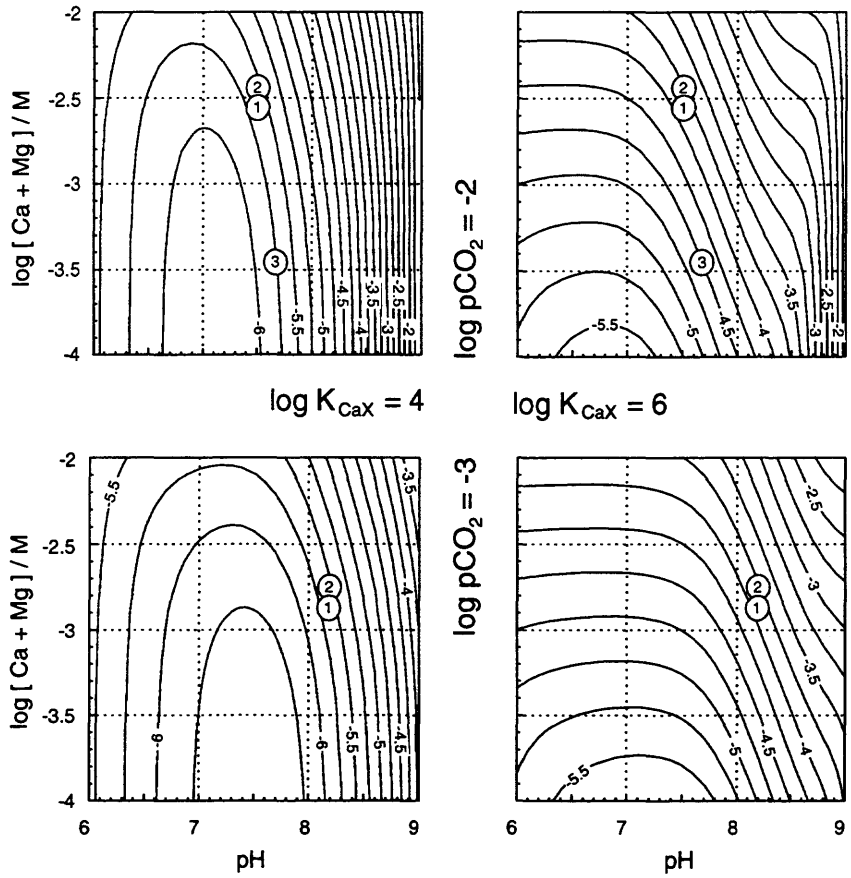

Figure 18: The influence of estimated stability constants for ligand X on the complexation of Ni in groundwaters. 50% contour lines are shown. Speciation calculations were done neglecting NiX_2^{2-}, NiX_3^{4-} and CaX_2^{2-} complexes, but varying the CaX stability constant at different values of P_{CO_2}. For comparison, some groundwater data are included: (1) Wellenberg marl pore water (BAEYENS & BRADBURY 1994), (2) Oberbauenstock marl pore water (BAEYENS & BRADBURY 1991), (3) Crystalline reference water (PEARSON & SCHOLTIS 1993).

If in the extreme case, NiX_2^{2-}, NiX_3^{4-} and CaX_2^{2-} are completely ignored, the white surface of Fig.17 results. A noticeable difference to the base case is seen only for pH > 8. The differences become significant beyond pH 8.5, where the already high X concentrations increase by more than one order of magnitude compared with results of the worst case scenario. In the case of our reference groundwaters, however, the possibly existing NiX_2^{2-}, NiX_3^{4-} and CaX_2^{2-} complexes do not influence the results at all. We safely can ignore them in these cases.

Having settled the problem of the estimated data for NiX_2^{2-}, NiX_3^{4-} and CaX_2^{2-} complexes, another question remains to be discussed, namely how the uncertainty in the estimated CaX stability constant influences the results, especially for the reference groundwaters? Therefore, additional "BACKDOOR" calculations were done neglecting NiX_2^{2-}, NiX_3^{4-} and CaX_2^{2-} complexes, but varying the CaX stability constant at different values of P_{CO_2}.

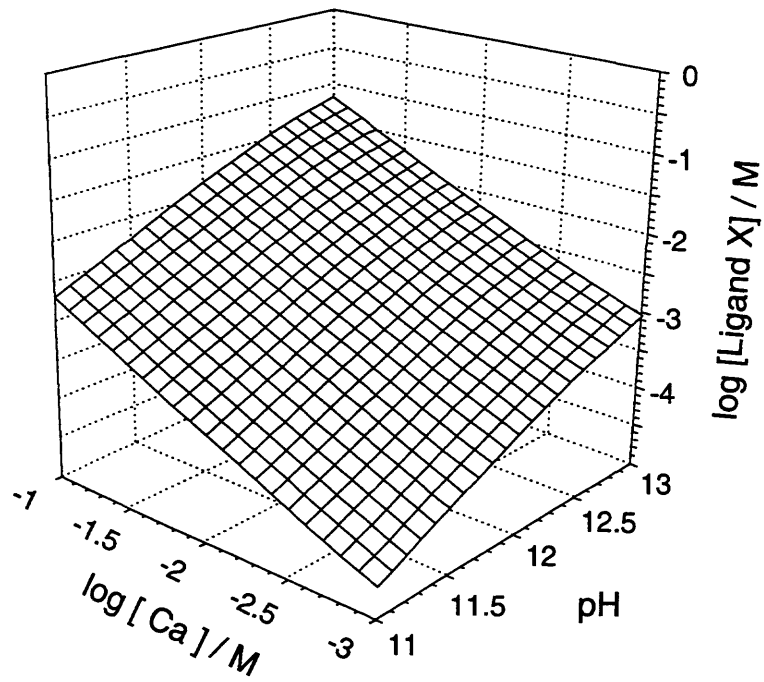

Figure 19a: The influence of ligand X on the complexation of Ni in high pH waters. The maximum values in Table 7 are used for the speciation calculations. The 50% Ni-organic complexation surface is shown.

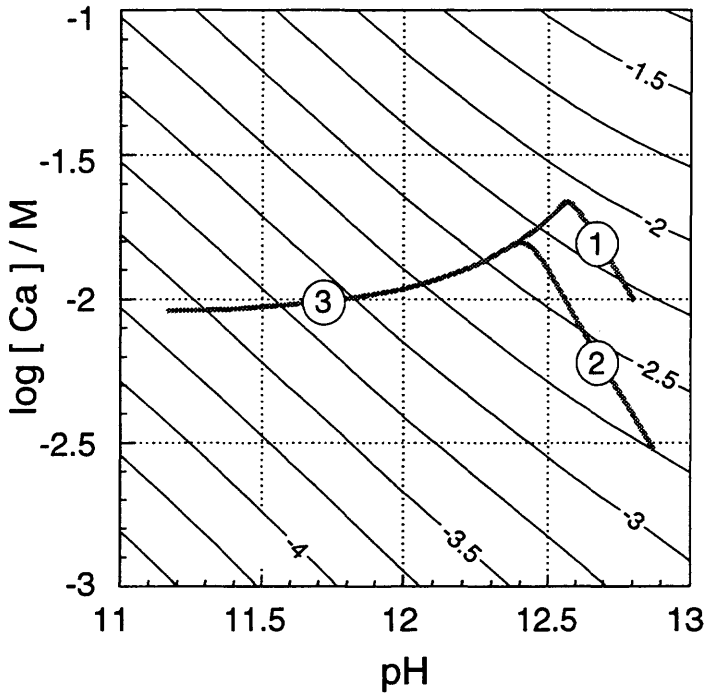

Figure 19b: The same results as Fig.19a but shown as contour plot. For comparison, pH and calcium concentrations of pore waters of cement degrading in a marl-type groundwater (BERNER 1990) are added as gray-shaded areas: (1) Sulphate resistant Portland cement in early degradation stages, (2) cement mixed with German Trass in early degradation stages and (3) both cements in later degradation stages. Physically all conditions above the gray lines cannot exist in cement pore waters.

As can be seen in Fig.18, an uncertainty of two orders of magnitude in CaX stability (5 ± 1, see Table 7) causes an uncertainty in calculated X concentration needed to complex 50% of Ni between one order of magnitude at low calcium concentrations (10^{-4} M) up to two orders of magnitude at high calcium concentrations (10^{-2} M).

The concentration of ligand X, necessary for 50% Ni-complexation, thus ranges for the crystalline reference water, (3) in Fig.18, between $10^{-4.5}$ M and $10^{-5.7}$ M, and for the marl pore waters, (1) and (2) in Fig.18, between $10^{-3.8}$ M and $10^{-5.7}$ M. Note, that in the case of minimal Ca competition, the same X concentrations are needed for the marl waters and the crystalline waters, whereas at maximum Ca competition, the X concentrations differ by about one order of magnitude, due to the higher Ca and Mg concentrations of the marl

waters. In contrast to this overall Ca competition effect, the correlated variations in pH, P_{CO_2} and Ca and Mg concentration of marl groundwaters, (1) and (2) in Fig.18, have no influence on the competitive effects; the same X concentration is needed for significant influence at $P_{CO_2} = 10^{-2}$ bar and 10^{-3} bar; the same effect as already discussed for oxalate.

The influence of ligand X on the Ni-speciation in high pH waters (Fig.19a) shows a similar pattern as oxalate (Fig.15a). Basically two differences between oxalate and X behaviour at high pH are detected by comparing Figs.15 and 19: The X surface generally is shifted by one order of magnitude towards lower concentrations, reflecting the stronger Ni-complexation by ligand X. In addition, the competitive effects of Ca are more pronounced in the case of ligand X due to the stronger Ca-complexation by ligand X. Therefore, the X surface (Fig.19a) is more inclined than the oxalate surface (Fig.15a). The Ca competition imposes some uncertainty on the results, pretty much the same way as already discussed for groundwaters. Ligand X concentrations between 10^{-3} M and 10^{-2} M are needed to complex 50% Ni in fresh cement pore water (pH > 12.5). The X concentrations slightly increase, due to strong Ca competition, for the model cement pore waters shown in Fig.19b during the early degradation stages, and then slowly drop below 10^{-3} M in the very late degradation stages.

In the parameter space of cement pore waters, the species $Ni(OH)_2X^{2-}$ predominates the organic speciation, if the maximum values of all estimated constants of Table 7 are used in the computations (Fig.19a and gray surface of Fig.20). This represents a worst case scenario. If, as already discussed for groundwaters, NiX_2^{2-}, NiX_3^{4-} and CaX_2^{2-} are completely ignored, and in addition the consecutive stability constants of $NiOHX^-$ and $Ni(OH)_2X^{2-}$ are diminished by one order of magnitude each, the white surface of Fig.20 results. The ligand X surface generally is shifted by more than one order of magnitude towards higher values; it compares now with the "worst case oxalate surface" of Fig.15a. In summary, any deviation from the maximum values of estimated stability constants leads to an increase of predicted concentrations of ligand X needed to complex 50% Ni.

A last check remains to be done, namely if the results obtained so far, using a simplified chemical system, are representative for groundwaters and cement pore waters. The marl pore water given by BAEYENS & BRADBURY (1991) was used as a test example, representing groundwaters with high

concentrations of sodium, chloride and sulphate. A cement pore water at pH 12.6, representing early degradation stages of cement, was taken from BERNER (1990). Speciation calculations, done with the programme MINEQL/PSI for the simplified chemical system and the full water compositions, reveal negligible differences: 0.1 log units in X concentration for the marl pore water and 0.04 log units for the cement pore water.

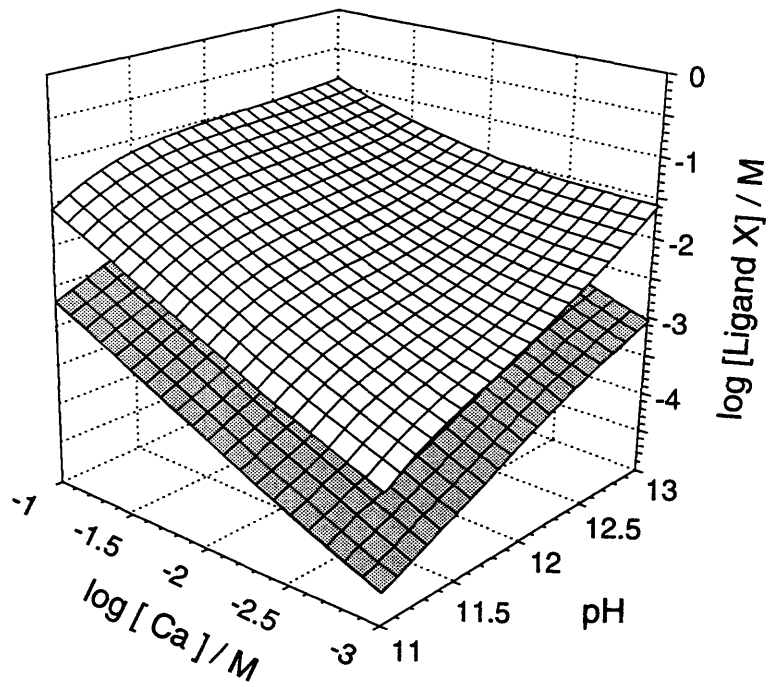

Figure 20: The influence of estimated stability constants for ligand X on the complexation of Ni in high pH waters. The 50% Ni-organic complexation surfaces are shown. Gray surface: The maximum values in Table 7 are used for the speciation calculations (same as Fig.19a). This represents the worst case. White surface: NiX_2^{2-}, NiX_3^{4-} and CaX_2^{2-} are ignored in the speciation model, and in addition the consecutive stability constants of $NiOHX^-$ and $Ni(OH)_2X^{2-}$ are diminished by one order of magnitude each.

4 THE DEGRADATION OF STRONG BASIC ANION EXCHANGE RESINS AND MIXED BED ION EXCHANGE RESINS

4.1 Materials and methods

4.1.1 Irradiation of anion exchange resins

Two strong anion exchange resins (Lewatite M-500 and Powdex PAO) were converted to the OH^- form by washing 100 g of the resin four times with 1500 cm^3 of 0.05 M NaOH. After the last treatment, 0.05 M NaOH was added to make the solid to liquid ratio 0.1 (100 g of dry resin in 1000 cm^3 0.05 M NaOH). The suspension was divided into two equal parts.
One part was put into a stainless steel container for irradiation in a ^{60}Co-cell. The container was designed in such a way that volatile degradation products (such as amines) could be collected (Figure 21). The basic volatile degradation products were purged from the reaction mixture with N_2 and scrubbed by a H_2SO_4-solution:

$$R\text{-}NH_2 + H^+ \Leftrightarrow R\text{-}NH_3^+ \qquad (51)$$

The protonated amines are not volatile and stay in solution. The temperature of the reaction mixture was kept at 25 °C by a special cooling system. After a total absorbed dose of 1.7 MGy, the mixture was filtered through a 0.45 µm filter (Millipore, type HA, 0.45 µm). The filter was prewashed with 500 cm^3 of 0.05 M NaOH to remove soluble organic carbon. After filtering, the solution was stored in glass vials at 4 °C.
The other part of the supension was put in a polyethylene bottle and left standing without irradiation for about 10 days (equal to the time of irradiation). After this time, the solution was filtered and stored in the same way as the irradiated samples. All solutions were analysed for pH, total dissolved organic carbon (DOC), oxalate and amines.

4.1.2 Irradiation of mixed bed ion exchange resins

A mixed bed ion exchange resin (Amberlite MB1, composed of an Amberlite IR-120 cation exchange resin and an Amberlite IRA-420 anion exchange resin in a 1:1 ratio) was equilibrated with 0.05 M NaOH. This equilibration step converted the cation exchange resin to the Na-form and the anion exchange resin to the OH-form. The solid/liquid ratio was 0.1 (100 g dry resin in 1000 cm^3 solution). After equilibration, the suspension was divided into two equal parts. One part was put in a stainless steel container and irradiated in a ^{60}Co-cell. The other part was put in a polyethylene bottle and left standing without irradiation for 10 days (equal to the time of irradiation). After treatment, the solution was recovered from the suspensions by filtering as described in 4.1.1. All solutions were analysed for pH, total dissolved organic carbon (DOC), sodium, oxalate, sulphate and amines.

4.1.3 Analytical procedures

The same analytical techniques were used as described in 3.2.2 (pH-measurements), 3.2.3. (organic carbon), 3.2.4 (sodium, oxalate and sulphate). The concentration of NH_4^+ and amines (methylamine, dimethylamine and trimethylamine respectively) were measured by ion chromatography (Dionex 2010i) using a HPIC-CS3 column. The eluent contained 25 mM HCl and 0.25 mM diaminopropionic acid hydrochloride (DAP·HCl). The amines eluting from the column were detected by suppressed conductivity. The apparatus was calibrated with standards made up from concentrated amine solutions (Merck, analytical grade).

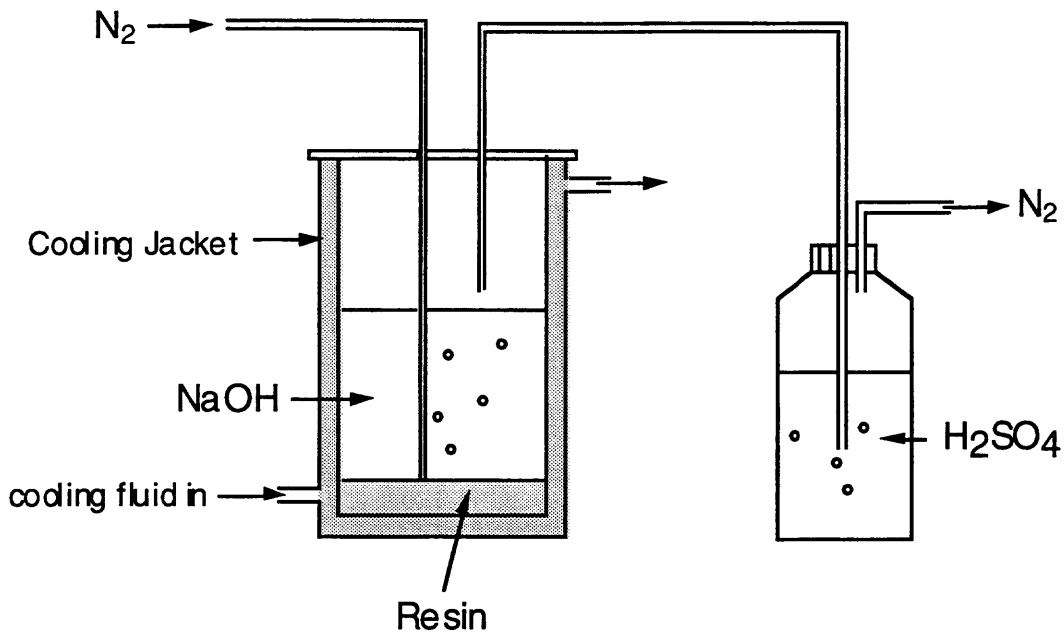

Figure 21: Schematic view of the degradation cell used for the radiolytic degradation of anion and mixed bed ion exchange resins.

4.1.4 Adsorption studies

To check whether degradation products (or organics in general) form complexes with metals, the effect of the degradation products (or organics) on the adsorption of a metal can be studied. This takes advantage of the fact that the adsorption of a metal M on a solid phase S will be decreased when a ligand L, forming a non-sorbing ML complex with the metal M, is present.
Assume that the metal M sorbs reversibly and linearly on a site S on a solid phase by the following reaction:

$$M + S \Leftrightarrow MS \qquad (52)$$

The extend of sorption can be expressed by a sorption coefficient K_d^o as follows:

$$K_d^o = \frac{MS}{M} \quad (cm^3/g) \qquad (53)$$

where MS is the amount of metal sorbed on the solid phase S in mol/g and M is the amount of metal in the equilibrium solution expressed as mol/cm^3. When a ligand L is present in solution, forming a 1:1 complex with M according to:

$$M + L \Leftrightarrow ML \tag{54}$$

with:

$$K_{ML} = \frac{[ML]}{[M] \cdot [L]} \tag{55}$$

the adsorption of the metal M will be decreased. Assuming that the ligand itself and the complex formed do not sorb on the solid, the sorption coefficient (K_d) can be written as:

$$K_d = \frac{MS}{M + ML} \tag{56}$$

$$K_d = \frac{MS}{M \cdot (1+K_{ML} \cdot [L])} \tag{57}$$

Combining equation (57) with equation (53) results in:

$$K_d = \frac{K_d^o}{1+K_{ML} \cdot [L]} \tag{58}$$

The effect of the ligand L on the adsorption can be expressed as a sorption reduction factor (F_{red}):

$$F_{red} = \frac{K_d^o}{K_d} = 1 + K \cdot [L] \tag{59}$$

As can be seen from equation (59), the sorption reduction factor (F_{red}) is independent of the solid phase used in sorption studies and depends only on the free ligand concentration [L] in solution and on the stability constant K_{ML} of the complex formed. **Consequently, it doesn't matter what kind of solid phase is used in this kind of sorption studies, as long as the sorption is linear, reversible and the complex formed and the ligand do not sorb on the solid phase.**

The effect of the degradation products on the adsorption of Eu on calcite at pH 12.6 was studied. Calcite was used as the solid phase in our experiments because the sorption of Eu on this solid phase can be measured relatively well. Eu was used as an analogue for trivalent actinides. 1M NaOH and $NaClO_4$ were added to different aliquots of the degradation mixture and the volumes were made up to 100 cm^3. The final composition of the solutions was 0.05 M NaOH and 0.05 M $NaClO_4$. The carbon concentration could be calculated from the dilution. 30 cm^3 of these diluted solutions were placed in 50 cm^3 centrifuge tubes. 2 cm^3 of a $CaCO_3$ suspension (1mg/cm^3 in 0.05 M NaOH + 0.05 M $NaClO_4$) and 3 cm^3 of a ^{152}Eu-solution (0.05 M NaOH + 0.05 M $NaClO_4$, spiked with ^{152}Eu) were added. The suspensions were shaken end over end for 15 hours (this time was enough to reach sorption equilibrium) and centrifuged at 20,000 rpm for 30 minutes. 2 cm^3 aliquots of the supernatant were sampled and assayed for ^{152}Eu in a NaI γ–counter (Packard, Minaxi γ–counter). The adsorption of ^{152}Eu (K_d and K_d^o) was calculated from the difference in radioactivity before and after sorption equilibrium. By doing so, the sorption of Eu on the vessel walls was not taken into account and consequently, the calculated sorption coefficients were overestimated. Experiments showed that as much as 50 to 70 % of the ^{152}Eu inventory could be found back on the vessel walls. The sorption coefficients were therefore been overestimated by up to 0.3 to 0.5 log-units.

4.2 Results and discussion

4.2.1 Degradation products of anion exchange resins

Table 8 shows the most important degradation products observed during the radiolytic degradation of anion exchange resins. As was expected, the most important radiolytic degradation products observed are amines such as ammonia, methylamine, dimethylamine and trimethylamine. Similar results have been reported by HALL & STREAT (1963). The trimethylamine group is split off from the backbone (denoted hereafter as R) by the irradiation:

$$R\text{-}CH_2\text{-}N(CH_3)_3^+OH^- \rightarrow R\text{-}CH_2OH + N(CH_3)_3 \qquad (60)$$

Table 8: Characteristics of the irradiated and non-irradiated (anion and mixed bed) resin waters.

Name	Dose (MGy)	pH	DOC (mM)	SO_4^{2-} (mM)	oxalate (mM)	Na^+ (mM)	NH_3 (mM)	methyl amine (mM)	dimethyl amine (mM)	trimethyl amine (mM)
					Powdex PAO					
P-PAO-B	1.7	12.45	139	0.29	n.d.	48	21	5.6	11.1	11.4
P-PAO-U	0	12.70	3.2	0.12	n.d.	50	n.d.	n.d.	n.d.	n.d.
1)P-H_2SO_4		n.m.	64.0	n.m.	n.m.	n.m.	5.3	0.93	0.42	0.26
					Lewatite M-500					
L-M500-B	1.7	12.66	268	0.08	n.d.	53	18	9.8	19.0	14.0
L-M500-U	0	12.67	0.78	0.08	n.d.	53	n.d.	n.d.	n.d.	n.d.
1)L-H_2SO_4		n.m.	58.8	n.m.	n.m.	n.m.	1.9	0.51	2.4	17.0
					Amberlite MB1					
A-MB1-B	1.7	12.92	20.5	2)0.12	n.d.	89	1.1	0.23	0.13	0.04
A-MB1-U	0	12.66	0.26	n.d.	n.d.	49	0.19	n.d.	0.03	0.07
1)A-H_2SO_4		n.m.	7.4	n.m.	n.m.	n.m.	6.3	0.30	0.62	3.53

n.d. = not detectable; n.m. = not measured

P-PAO-B = Powdex ,irradiated; P-PAO-U = Powdex, not irradiated; L-M500-B = Lewatite, irradiated; L-M500-U = Lewatite, not irradiated;

A-MB1-B = Amberlite, irradiated; A-MB1-U = Amberlite, not irradiated

1) = H_2SO_4 phase used to collect the volatile degradation products (amines) formed during irradiation

2) the total sulphur in solution is 37.5 mM (measured by ICP-AES)

Secondary amines can be formed as follows:

$$R\text{-}CH_2N(CH_3)_3^+OH^- \rightarrow R\text{-}CH_2N(CH_3)_2 + CH_3OH \quad (61)$$

$$R\text{-}CH_2N(CH_3)_2 + H_2O \rightarrow R\text{-}CH_2OH + (CH_3)_2NH \quad (62)$$

Trimethylamine and dimethylamine in solution is further degraded to ammonia and methylamine (HALL & STREAT 1963):

$$N(CH_3)_3 \rightarrow CH_3N=CH_2 + CH_4 \quad (63)$$

$$CH_3N=CH_2 + H_2O \rightarrow CH_3NH_2 + CH_2O \quad (64)$$

$$(CH_3)_2NH \rightarrow CH_2=NH + CH_4 \quad (65)$$

$$CH_2=NH + H_2O \rightarrow NH_3 + CH_2O \quad (66)$$

Removal of hydrogen can also result in the destruction of aliphatic amines to produce ammonia and formaldehyde (HALL & STREAT 1963):

$$(CH_3)_2NH - 2H \rightarrow CH_2=NCH_3 \quad (67)$$

$$CH_2=NCH_3 + H_2O \rightarrow CH_3NH_2 + CH_2O \quad (68)$$

$$CH_3NH_2 - 2H \rightarrow CH_2=NH \quad (69)$$

$$CH_2=NH + H_2O \rightarrow NH_3 + CH_2O \quad (70)$$

The formaldehyde formed in reaction (64), (66), (68) and (70) can react further with the aliphatic amines:

$$CH_3NH_2 + CH_2O \rightarrow CH_3NHCH_2OH \quad (71)$$

The deamination of such quaternary ammonium anion exchange resins can occur by direct action of radiation on the resin or by attack of radiolysis products of water in contact or associated with the resin. The relative

contribution of these processes to the overall deamination depends on the water content of the resin, i.e. the more water present, the higher the contribution of the latter process (AHMED et al. 1966).

The DOC content of the irradiated water is high (139 mM for Powdex PAO and 268 mM for Lewatite M-500) compared to the non-irradiated systems (3.2 mM for Powdex PAO and 0.78 mM for Lewatite M-500). Although the high concentration of organic carbon is supposed to be explained mainly by the deamination process, the measured concentration (C_{meas}) is always higher than that calculated from the amine concentration in solution by:

$$[C]_{cal} = [(CH_3)_3N]\cdot 3 + [(CH_3)_2NH]\cdot 2 + [CH_3NH_2] \qquad (72)$$

where square brackets denote the concentration of the amines in mM. $[C]_{cal}$ is also given in mM. Calculated and measured DOC values are summarised in Table 9.

Table 9: Measured and calculated total organic carbon content in irradiated Powdex PAO and Lewatite M-500 resin solutions.

Resin	$[C]_{meas}$ (mM)	$^1[C]_{calc}$ (mM)
P-PAOB	139	62 (45 %)
P-H_2SO_4	64	51 (80 %)
L-MB500-B	268	90 (34 %)
L-H_2SO_4	59	56 (95 %)
A-MB1-B	20.5	0.61 (3 %)
A-H_2SO_4	7.4	12.1 (164 %)

1) = calculated by equation (72)

(%) = fraction of the measured carbon

For the scrubber solutions (H_2SO_4-solution) the calculated and measured carbon concentrations are comparable, meaning that they can be explained mainly by the presence of amines. For the other solutions, the agreement between calculated and measured DOC content is much poorer. From this

observation, it can be concluded only that organic compounds other than amines are present in solution. Equation (72) underestimates the organic carbon in solution because it does not take into account the C-containing degradation products of trimethylamine such as CH_4 and CH_2O given in reaction (63-70) and CH_3NHCH_2OH given in reaction (71). In the absence of a radiation field, no amines could be detected. Also the DOC content of the solutions was very low compared with that of the irradiated solutions.

4.2.2. Degradation products of mixed bed resins

The composition of the water from the mixed bed resin (Amberlite MB1) is also included in Table 8. Normally, one would expect that the degradation products of a mixed bed resin would just be a mixture of degradation products of the cation and anion exchange resins of which it is composed. As can be seen from Table 8, only small amounts of sulphate (the main degradation product of cation exchange resins) and amines (the main degradation products of anion exchange resins) are present in solution. The carbon calculated from the amines present in solution is only 3 % from the measured carbon. Also the sulphate (0.12mM) is only a small fraction (0.1 %) of the total sulphur present in solution (37.5 mM). This means that other degradation products were formed during the irradiation of the mixed bed resin. From the increase of both the Na^+ and the pH in the irradiated solution, it can be concluded that surface $-SO_3$ and $-N(CH_3)_3$ groups have been split off from the backbone. The intermediate species produced are mainly radicals which react with each other. The low concentration of both sulphate and amines might be explained by recombination of the radicals produced from both type of resins, resulting in a kind of sulpho-amine product. Analytical evidence for such compounds, however, is not available. BAUMANN (1966) also observed a lower sulphate yield for the irradiation of mixed bed ion exchange resins compared to the individual resin. The lower sulphate yield, however, was explained by a partial readsorption of the sulphate by the anion exchange component of the mixed bed resin.

4.2.3 Adsorption of Eu on calcite

Figure 22 shows the effect of the degradation products of the different anion and mixed bed ion exchange resins on the adsorption of Eu on calcite at pH 12.6 at an ionic strength of 0.1 M. The dotted area on the figure represent the uncertainty in the determination of K_d^o (= partition coefficient of Eu in the absence of degradation products). The degradation products do not have a significant effect on the adsorption of Eu and calcite. A small effect was observed for the Powdex PAO anion exchange resin that had not been irradiated. These results show that the amines in solution (ammonia, methylamine, dimethylamine and trimethylamine) do not form complexes with Eu^{3+} under the experimental conditions. It can also be concluded that, beside amines, no other ligands (that could not be identified) are present in the degradation solutions. These conclusions are representative for hard[3] cations like lanthanides and, especially in the context of out work, the trivalent actinides. Soft[3] cations like Pd, Ag and Ni, however, have different complexation behaviour and thus, the sorption study on Eu does not rule out the presence of other compounds which may form complexes only with these soft cations (for more details see section 4.3).

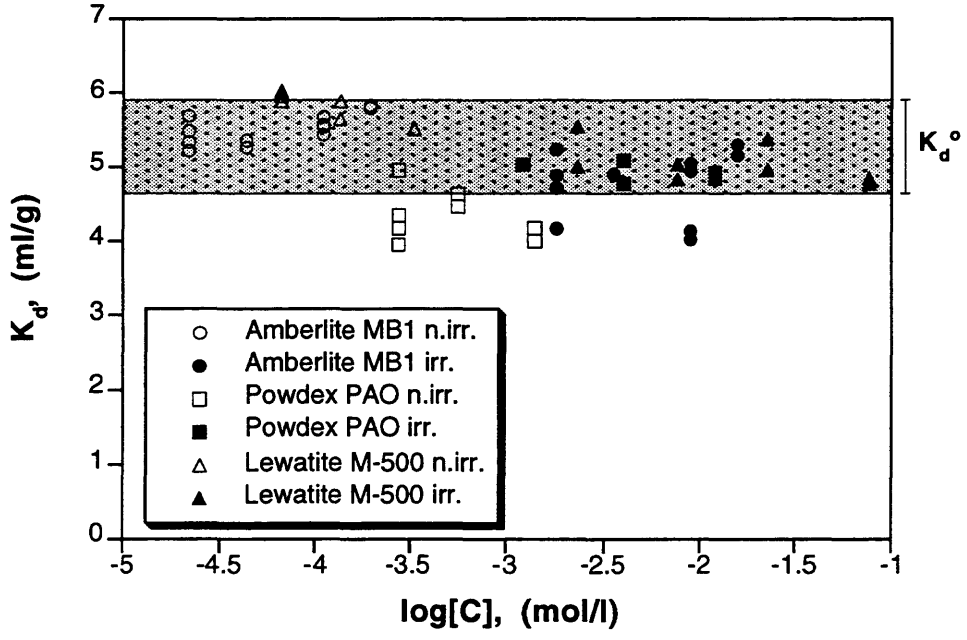

Figure 22: Effect of radiolytic and chemical degradation products of anion and mixed bed resins on the adsorption of Eu on calcite at pH 12.6 and I = 0.1 M.

4.3 Speciation of radionuclides in the presence of degradation products

4.3.1 General overview

The only degradation products forming complexes with radionuclides in the case of strong basic anion exchange resins and mixed bed ion exchange resins are ammonia, mono-, di- and trimethylamine. Therefore, we focus on the complexing properties of these ligands.

It has been known since the pioneering work of Jannik Bjerrum on "Metal Ammine Formation in Aqueous Solutions" (BJERRUM 1941) that ammonia forms strong complexes with "soft" cations such as Ni, Cu, Ag, Hg and Pd. On the other hand, its affinity to "hard" cations such as Ca, Mg and actinides is relatively weak[3]. As can be seen in Fig. 23, the stability of metal-ammonia 1:1 complexes spans ten orders of magnitude. At the lower end, Ca and Mg representing "hard" cations range at logK $\approx$ 0. At the upper end, Pd forms the strongest known metal-ammonia complexes. The other "soft" cations range in between these extreme cases.

Experimental data about complex formation of mono-, di- and trimethylamine are rather scarce in the literature. The data shown in Fig. 23 appear to be reliable. The experimental conditions and methods vary for different metal cations, and no attempt was made to extrapolate the experimental results to a common basis. For a specific cation, however, only data measured by the same author for ammonia and the other amines at comparable experimental conditions were selected. The data reveal a rather consistent picture: Ammonia and methylamine show nearly the same affinity towards complex formation. The stability of the complexes is essentially governed by the properties of the functional group. As discussed by ILCHEVA & BJERRUM (1976), the greater steric bulk of methylamine has a slight influence only on the uptake of the last amine molecules. With the exception of methylmercury, the stability constant of methylamine complexes is slightly lower than the

---

[3] Cations and ligands can be classified as "hard" and "soft" acids and bases (LANGMUIR 1979). Soft infers that the species' electron cloud is deformable or polarisable and may enter into electronically unique states in complexation. Hard cations are comparatively rigid and non-deformable and tend to form largely electrostatic bonds with ligands.

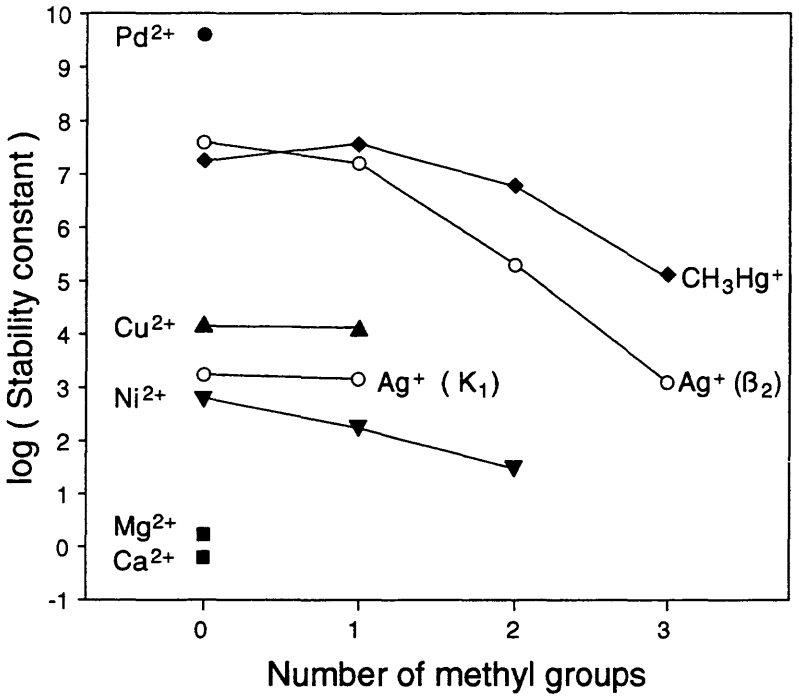

Figure 23: Selected stability constants of metal-amine complexes as a function of the number of methyl groups (0: ammonia, 1: methylamine, 2: dimethylamine, 3: trimethylamine). The stability constants refer to the formation of 1:1 complexes (K_1) if not otherwise stated, β_2 is the cumulative formation constant of a 1:2 complex. The data are taken from the following sources: Ca, Mg: BJERRUM (1941), 23 °C, 2 M NH_4NO_3. Ni: RORABACHER & MELENDEZ-CEPEDA (1971), 25 °C, 1 M $HClO_4$. Ag (K_1, ammonia): BJERRUM (1941), 30 °C, 0.5 M NH_4NO_3. Ag (K_1, methylamine): BJERRUM (1950), 25 °C, 0.5 M $CH_3NH_3NO_3$. Ag (β_2): BRITTON & WILLIAMS (1935), 15 °C, Ag_2O solubility in amine solutions at variable concentrations. Cu (ammonia): BJERRUM (1941), 30 °C, 2 M NH_4NO_3. Cu (methylamine): ILCHEVA & BJERRUM (1976), 25 °C, 2 M $CH_3NH_3NO_3$. CH_3Hg: RABENSTEIN et al. (1974), 25 °C, 0.5 M amine solutions. Pd: RASMUSSEN & JØRGENSEN (1968), 25 °C, 1 M $NaClO_4$.

constant for ammonia complexes. The stabilities of the bulkier amine complexes, however, decrease significantly with increasing number of methylgroups. As a general rule, the stability constants show the following relation:

ammonia ≈ methylamine > dimethylamine > trimethylamine

Therefore, in the remaining sections we focus our discussion on the complexation of ammonia as the most powerful ligand within this series. The complexation with methylamine is expected to be the same order of magnitude as ammonia, at a maximum. The influence of di- and trimethylamine complexation on metal speciation is always significantly weaker than the inluence of ammonia. Pd and Ni are chosen in the following as representative "soft" cations because of their importance in safety assessment (BAEYENS & McKINLEY 1989).

4.3.2 Speciation calculations for nickel and palladium

To get a first impression of the influence of ammonia on the speciation of Ni and Pd, some scoping calculations were done using the programme "BACKDOOR" (see chapter 3.5.3). The simplified chemical system [Ca]-pH-[Ni,Pd]-[ammonia] was investigated by assuming a total metal concentration in solution of 10^{-6} M. The thermodynamic data used in these calculations were taken from Table7 (Ni- and Ca-hydroxo complexes) and from the original papers. Data for Ca- and Ni-ammonia complexes come from BJERRUM (1941). The data of this pioneering work passed the test of time, little variation is found comparing Bjerrum's data obtained half a century ago with the results of later publications. Data for Pd-ammonia complexation were taken from the reliable work of RASMUSSEN & JØRGENSEN (1968). The effect of ionic strength on equilibria involving ammonia is very small as there is no change in overall charge due to complexation with an uncharged ligand, but the effect is not zero. In general, the stability constants tend to decrease slightly with decreasing ionic strength. Thus, to be on the safe side, the original (maximum) values obtained at high ionic strength (up to 2 M) are used in our calculations. The consecutive stability constants log K_x for the equilibria:

$$M(NH_3)_{x-1} + NH_3 \Leftrightarrow M(NH_3)_x \qquad (73)$$

are: Ca: -0.2, -0.6; Ni: 2.80, 2.24, 1.73, 1.19, 0.75, 0.03; Pd: 9.6, 8.9, 7.5, 6.8. The hydrolysis of Pd, which has to be considered in this context, is still an area of uncertainty, as is discussed in detail in the next section. For our scoping

calculations we used the only experimental Pd hydrolysis data available, that of NABIVANETS & KALABINA (1970).

The results of the BACKDOOR calculations are presented in Fig.24 as surfaces showing the conditions under which 50% of the total metal present is complexed with ammonia. For Ni, very high ammonia concentrations, up to the molar range , are needed in order to complex at least 50% of the metal cation at pH 13. The Pd surface is rather similar, but is shifted about two orders of magnitude towards lower ammonia concentrations. Considering the large difference in affinity of both metal cations to ammonia, this result is not surprising. In addition, the Ca competition is insignificant due to the very low affinity of Ca to ammonia. This is a marked contrast to the results of oxalate and ligand X and further simplifies the chemical system to pH-[Ni,Pd]-[ammonia].

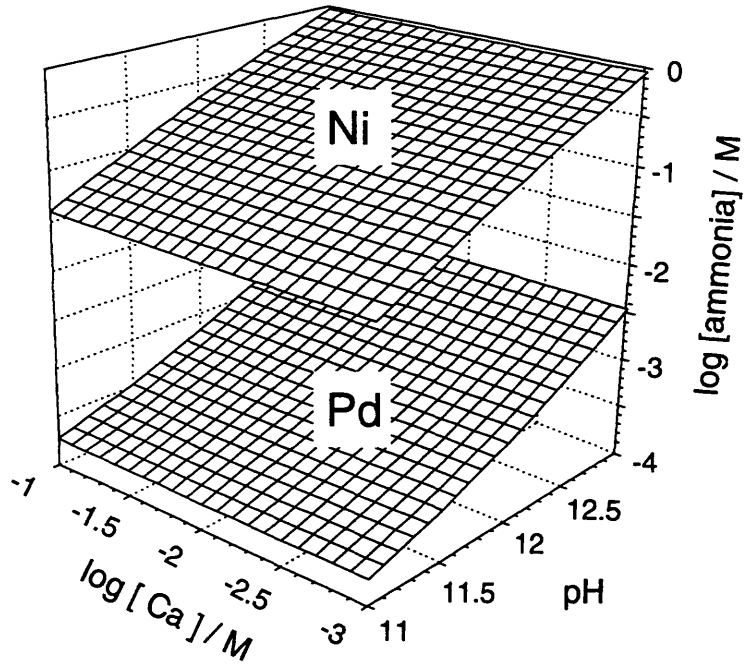

Figure 24: The influence of ammonia on the complexation of Ni and Pd in high pH waters. The 50% metal-ammonia complexation surfaces are shown.

The concentrations of ammonia needed to significantly influence the speciation of Ni are so high that no effect in safety assessment is expected, even if the hydrolysis constants of Ni are somewhat uncertain and the existence of possible mixed Ni-hydroxo-ammonia complexes cannot be ruled

out. Shifting the Ni-ammonia surface in Fig. 24 down by two or three orders of magnitude in order to cope with these uncertainties, still may keep ammonia out of the "region of significance" from a safety assessment point of view. The situation is different for Pd. Cascading very pessimistic assumptions about the uncertainties in Pd hydrolysis and the existence of mixed complexes easily could shift the Pd-ammonia surface into the micromolar region or even below that level. Therefore, it was necessary to have a closer look at the system Pd(II)-H_2O-NH_3.

4.4.3 Detailed inspection of the system Pd(II)-H_2O-NH_3

Pd-ammonia complexation was studied very carefully by RASMUSSEN & JØRGENSEN (1968) by means of pH titrations and absorption spectra. They found a stepwise complexation of Pd by ammonia with a limiting complex containing four ammonia ligands, $Pd(NH_3)_4^{2+}$. Their stability constants are among the few reliable data for Pd complexation (WANNER 1984, p.4).
The situation is worse for Pd hydrolysis. According to WANNER (1984, p.152-154), no reliable investigations have yet been published on the hydrolysis of $Pd(H_2O)_4^{2+}$ solutions. Only two papers about the subject have been identified. IZATT et al. (1967) studied the hydrolysis of Pd by pH titration and by spectrophotometry. The pH titrations were done in the region pH = 0.5 to 2.3 and total Pd concentrations of $1mM \leq [Pd]_{total} \leq 6mM$. WANNER (1984) remarks that under these experimental conditions the uncertainty in $[H^+]$ measurements is of the order of magnitude of that of $[Pd]_{total}$. In addition, an equilibration time of five hours in the pH titration experiments indicates that some polymerisation may have occurred, although the authors interpreted their results using mono-nuclear species only (Pd^{2+}, $PdOH^+$ and $Pd(OH)_{2(aq)}$). The spectrophotometric data also presented problems. The molar extinction coefficients for the $PdOH^+$ and $Pd(OH)_{2(aq)}$ species were affected by experimental errors of 30% and 85%, respectively. And, as IZATT et al. (1968) wrote, "*It was found that only certain choices of data points resulted in positive β_n values. Those β_n values which were positive showed good agreement.*" In other words, the authors calculated positive values of "stability constants" only if they combined a certain subset of spectroscopic data ignoring all the rest. This does not actually increase our confidence in their work and we agree with WANNER (1984), that the stability constants published by IZATT et al. (1968)

cannot be considered as reliable data. Furthermore, besides all these uncertainties and pitfalls in their investigation, a study in the pH region 0.5 to 2.3 cannot give any qualitative hints on the species predominating in the alkaline pH range (pH > 10).

NABIVANETS & KALABINA (1970) studied the complexation of Pd^{2+} with hydroxide within the region $-0.7 \leq pH \leq 13.5$ by solubility, comparative dialysis, and ion-exchange methods. The solubility of palladium hydroxide, tentatively assumed to be "$Pd(OH)_2$", was investigated in the pH range $1.1 \leq pH \leq 13.5$. The authors summarised their results qualitatively: "*In the pH range 3 - 11 the solubility remains constant at $4 \cdot 10^{-6}$ M, indicating that in this pH range, molecular forms of palladium (i.e. neutral complexes) are present in equilibrium with the solid phase. The solubility increases in more acidic and more alkaline solutions; this is characteristic for amphotheric hydroxides.*" In addition, they investigated the effects of hydrolytic polymerisation by comparative dialysis with Co as reference ion. They conclude that "*in solutions with pH > 12, the dialysis coefficient is close to unity (≈ 0.9), indicating that there is no polymerisation*". In the acidic region (pH < 2), however, significantly less palladium diffused through the membrane than expected from the solubility measurements. These differences were interpreted as due to significant amounts of hydrolytic polymers of palladium in solution. The authors therefore studied the influence of the concentration of palladium on its polymerisation at a constant $HClO_4$ concentration of 0.1 M (pH = 1). The results obtained were used to calculate an average polymerisation factor. WANNER (1984) criticises the authors for not investigating the polymerisation at other pH values than 1, and for simply interpreting their average polymerisation factor in terms of formation of hexamers, a model which works at pH 1 only within a limited range of Pd concentrations. Nevertheless, the authors used their postulated hexamer model in order to interpret solubility measurements between pH 1.5 and 2 and to calculate a stability constant for the formation of $Pd(OH)_{2(aq)}$. The consecutive stability constants for the 1:3 and 1:4 Pd-hydroxo complexes were estimated by NABIVANETS & KALABINA (1970) from the slope of the solubility curve at pH > 12. Because of all these uncertainties and unresolved problems, we agree with WANNER (1984), that further investigations are necessary to obtain reliable data describing the hydrolysis of $Pd(H_2O)_4^{2+}$. For the present study, however, we use the data of NABIVANETS & KALABINA (1970) as a starting point in our investigation of

the system Pd(II)-H_2O-NH_3, because their solubility measurements up to pH 13.5 give at least a semi-quantitative picture of the hydrolysis behaviour of Pd even if the stability constants derived may be wrong by more than one order of magnitude.

Using the data of RASMUSSEN & JØRGENSEN (1968), and of NABIVANETS & KALABINA (1970), a predominance diagram of the system Pd(II)-H_2O-NH_3 was calculated (Fig.25). In contrast to standard predominance plots, in Fig. 25 the predominance areas of species are limited by 50% lines. It is therefore an "absolute majority" plot. If a species has a "relative majority" within a certain region, but never reaches 50% of the total dissolved Pd, it does not appear in this plot. This is the case for $Pd(OH)^+$, which does not show up in Fig. 25. Instead, an "empty" space extends between the predominance areas of Pd^{2+} and $Pd(OH)_{2(aq)}$. In addition, the parameter space which has been experimentally investigated is shown as grey areas in Fig. 25.

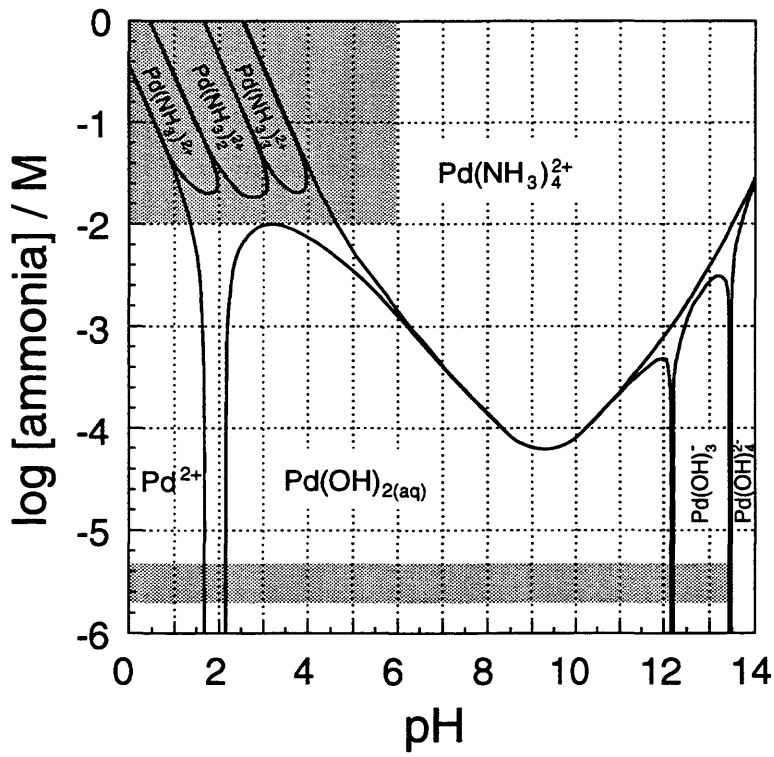

Figure 25: Predominance diagram of the system Pd(II)-H_2O-NH_3. The predominance areas of species are limited by 50% lines. The experimentally investigated parameter space is shown as grey areas (upper left corner: RASMUSSEN & JØRGENSEN (1968), grey stripe at arbitrary low ammonia content: hydrolysis study of NABIVANETS & KALABINA (1970)).

The parameter space of the investigation of RASMUSSEN & JØRGENSEN (1968) appears in the upper left corner. The parameter space of the hydrolysis study of NABIVANETS & KALABINA (1970) formally cannot be shown in this plot, but was included for illustrative purposes as a grey stripe at (arbitrary) low ammonia content.

As already mentioned, the existence of the series of $Pd(NH_3)_x^{2+}$ species (x = 1...4) and the irrespective stability constants are well established. But we do not know if $Pd(NH_3)_4^{2+}$ really predominates from pH 4 up to pH 14 as Fig. 25 suggests. The large predominance field of this species in Fig.25 is just an extrapolation; no quantitative experimental data are available beyond pH 6. On the contrary, qualitative chemical evidence exists, that Pd-ammonia complexes undergo hydrolysis and form rather stable ternary complexes at high pH values.

As described in some detail in Gmelin's Handbook (GMELIN 1942, pp.376-377), a palladium-ammonia-dihydroxo compound, $Pd(NH_3)_2(OH)_2$, named "Palladamin" by MÜLLER (1853), has been known since the middle of the last century. Different chemical pathways are mentioned in GMELIN (1942) to synthesize "Palladamin" which finally is obtained as small orange colored octahedral crystals. Palladamin is stable in a CO_2-free atmosphere up to 100 °C. Its solution as well as the crystalline solid take up CO_2 rapidly forming $Pd(NH_3)_2CO_3$. It is remarkable in this context that to our present knowledge, the formation of pure palladium carbonate compounds has never been observed, either in nature or in the laboratory. The formation of mixed complexes with "hard" anions like carbonate or oxalate, however, seems to be preferred, as long as at least two Pd bonds are occupied by ammonia or amine ligands. The long list of mixed compounds of this type described in GMELIN (1942) corroborates this general observation.

Further qualitative evidence and at least some rough estimates for Pd - ammonia hydrolysis constants can be derived from the work of WANNER (1984). His PhD thesis is a very detailed and reliable study of the formation and hydrolysis of Pd(II)-complexes with pyridine, bipyridyl and phenanthroline, which are mono- and bi-dentate aromatic amine ligands. The hydrolysis of these Pd-amine complexes results in the formation of mono-nuclear $PdL(OH)_{2(aq)}$ complexes, at around pH 8 (L = bipyridyl or phenanthroline). In the case of ternary $PdLpy_x^{2+}$ complexes (py = pyridine, x = 1,2) experimental hydrolysis data can be explained by the formation of $PdLpy(OH)^+$ (a quarternary complex !) and finally $PdL(OH)_{2(aq)}$. For a detailed discussion of

intermediate poly-nuclear hydrolysis products of these complexes see WANNER (1984). As we are dealing in our modelling study with trace concentrations of Pd only, these poly-nuclear complexes are not of importance here, but we may use the mono-nuclear hydrolysis products as analogues for Pd-ammonia hydrolysis products. Table 10 shows that the affinity of these aromatic amine ligands and of NH_3 for Pd is not very different and consequently can be used as chemical analogues. Thus, the reaction of $PdLpy^{2+}$ with OH^- to form $PdLpy(OH)^+$ ($\log K_1 \approx 8.5$) is taken as model for the intermediate hydrolysis product $Pd(NH_3)_3OH^+$. Likewise, the reaction of PdL^{2+} with 2 OH^- to form $PdL(OH)_{2(aq)}$ ($\log\beta_2 \approx 16$) is taken as model for the final hydrolysis product $Pd(NH_3)_2(OH)_{2(aq)}$.

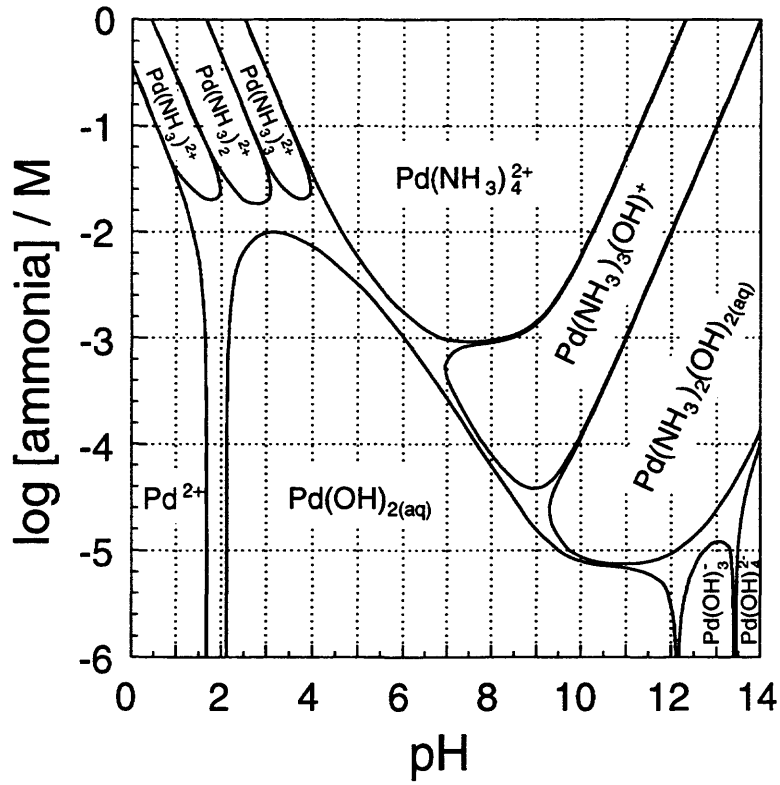

Figure 26: Predominance diagram of the system Pd(II)-H_2O-NH_3 including mixed ammonia-hydroxo complexes into the model. The formation constants of the mixed complexes are estimated by analogy using hydrolysis data of WANNER (1984).

Table 10: The stability of palladium(II) complexes with (poly)amine ligands.

Ligand[1]	#[2]	$\log K_1$	$\log K_2$	$\log K_3$	$\log K_4$	$\log\beta_{(max)}$	Conditions[3]	Ref[4]
NH3	1	9.6	8.9	7.5	6.8	32.8	I = 1.0M, 25 °C	[a]
py	1	8.4	7.7	6.6	5.9	28.6	I = 1.0M, 25 °C	[b]
bipy	2	9.8	8.9			28.7	I = 0.1M, 25 °C	[b]
phen	2	20.7	10.4			31.1	I = 0.1M, 25 °C	[b]
gly	2	15.25	12.25			27.5	I = 1.0M, 20 °C	[c]
IDA	3	17.5	9.3			26.8	I = 1.0M, 20 °C	[c]
NTA	4	17.1	6.6			23.7	I = 1.0M, 20 °C	[c]
EDTA	6	24.5				24.5	I = 1.0M, 20 °C	[c]
TETA	6	25.8				25.8	I = 1.0M, 20 °C	[c]
PETA	6	26.4				26.4	I = 1.0 M, 20 °C	[c]
HDTA	6	26.3				26.3	I = 1.0M, 20 °C	[c]
TMTA	6	28.8				28.5	I = 1.0M, 20 °C	[c]
DTPA	8	29.7				29.7	I = 1.0M, 20 °C	[c]
en	2	>20	18.4			>38.4	I = 1.0M, 25 °C	[a]
trien	4	39.4				39.4	I = 0.1M, 25 °C	[d]

1) py: pyridine, bipy: 2,2'-bipyridyl, phen: 1,10-phenanthroline, gly: glycinate
IDA: iminodiacetate, NTA: nitrilotriacetate,
EDTA: ethylenediaminetetraacetate, TETA: tetramethylenedinitrilotetraacetate
PETA: pentamethylenedinitrilotetraacetate, HDTA: hexamethylenedinitrilotetraacetate
TMTA: trimethylenedinitrilotetraacetate, DTPA: diethylenetriaminepentaacetate
en: ethylenediamine, trien: triethylenetetramine

2) #: number of functional groups per molecule able to coordinate with a metal cation.

3) The stability constants are valid for the given ionic strength and temperature.

4) References :

[a] RASMUSSEN & JØRGENSEN (1968)
[b] WANNER (1984)
[c] ANDEREGG & MALIK (1976)
[d] ANDEREGG & YAN

Including the two species $Pd(NH_3)_3OH^+$ and $Pd(NH_3)_2(OH)_{2(aq)}$ in our model calculations changes the predominance diagram in the alkaline region (Fig.26). The two main differences of this new model are that the area of $Pd(NH_3)_4^{2+}$ predominance is smaller and that the predominance of Pd-amine complexes extends to lower concentrations of ammonia in the alkaline pH region (pH > 8). The latter effect has particular consequences on the minimum concentration of ammonia needed to significantly influence Pd speciation in high pH waters. The 50% line in the region pH > 12 is shifted by about two orders of magnitude towards lower ammonia concentrations by introducing mixed Pd-ammonia-hydroxo complexes in our speciation model (Fig.27). The stability constants for these mixed complexes, of course, are first estimates only, taken by analogy from Wanner's thesis (WANNER 1984).

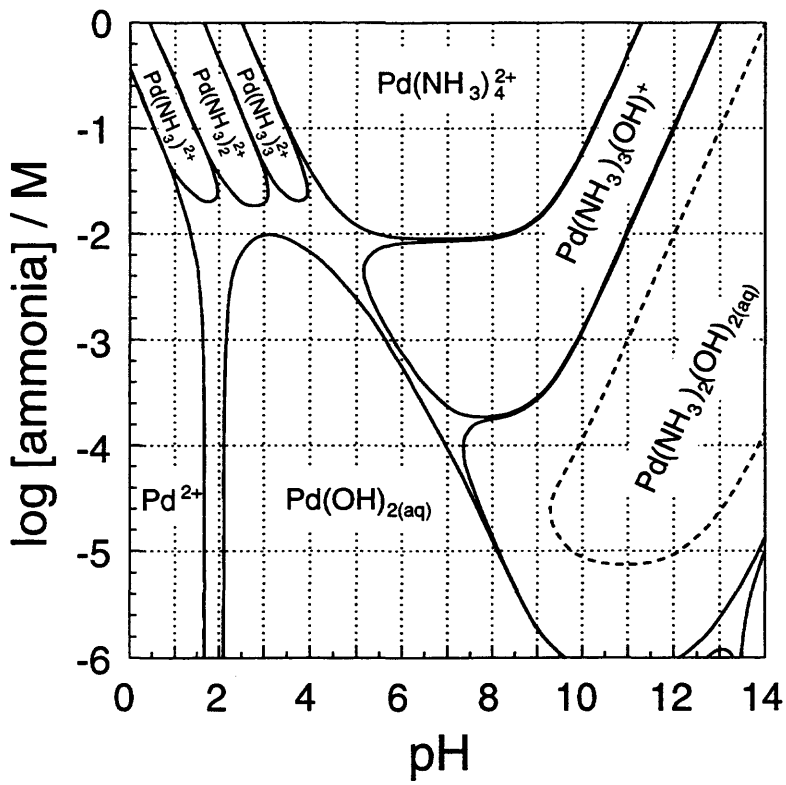

Figure 27: Predominance diagram of the system Pd(II)-H_2O-NH_3. The consecutive formation constants of the mixed complexes are increased by one order of magnitude.The dotted line shows the original predominance area taken from Fig. 26 for comparison.

The question now becomes whether we can estimate any upper limits for these stability constants, and provide, in consequence, the lower limit of significant ammonia concentrations. If we tentatively increase the stability constants for both consecutive hydrolysis equilibria by one order of magnitude ($\log K_1 \approx 9.5$, $\log\beta_2 \approx 18$), another predominance diagram can be computed (Fig.27). The 50% line of minimum ammonia concentration decreased, as expected, by another order of magnitude. The predominance area of mixed Pd-ammonia-hydroxo complexes now extends to the acidic region (pH 5) and to rather high ammonia concentrations (10 mM ammonia).

This latter observation allows us to derive upper limits for the stability constants of mixed complexes. In their comprehensive study of Pd-ammonia complexation, RASMUSSEN & JØRGENSEN (1968) carefully explored the parameter space from millimolar to molar concentrations of ammonia up to pH 6 at various total concentrations of Pd. They found no effects due to hydroxo or mixed hydroxo complexes. For example, they reported absorption spectra of the complex $Pd(NH_3)_4^{2+}$ at millimolar and 2 M ammonia concentration at pH 6. No difference is seen between the spectra recorded at 2 M and at a few millimoles of ammonia. If the stability constants of mixed Pd-ammonia-hydroxo complexes would be as high as assumed in computing Fig.27, RASMUSSEN & JØRGENSEN (1968) certainly would have detected their influence on titration experiments and absorption spectra. We therefore conclude that the stability constants used in computing Fig.26 ($\log K_1 \approx 8.5$, $\log\beta_2 \approx 16$) represent about the maximum values to be expected for the formation of $Pd(NH_3)_3OH^+$ and $Pd(NH_3)_2(OH)_{2(aq)}$ (It makes no sense to adjust these estimated values by less than an order of magnitude; it would imply into a numerical precision which cannot be reached by such rough estimates).

Having settled the question of ammonia species, the problem of unreliable data on palladium hydrolysis remains to be discussed. When no thermodynamic data are available or the reliability of published data are in doubt, stability constants can be estimated using some sort of theoretical prediction technique. The tables published by BROWN & WANNER (1987) contain such predicted stability constants. These estimates are based on the "Unified Theory of Metal Ion Complexation" developed by BROWN & SYLVA (1987). The Brown and Sylva theory is based on strict chemical systematics

and introduces the novel concept of "electronicity", which can be thought of as the "freeness" of the valence electrons. The free parameters in this theory are especially well calibrated for mono-hydroxo complexes. Using the predicted constants of BROWN & WANNER (1987) for Pd(II)-hydroxo complexation, a further predominance diagram was computed (Fig.28). The picture dramatically changed compared with the other predominance plots (Figs.25 - 27). The mixed complexes are gone and $Pd(OH)_4^{2-}$ dominates the parameter space up to 30 mM ammonia concentration.

Here, the first contradiction to experimental results appears. As already mentioned, RASMUSSEN & JØRGENSEN (1968) found the same absorption spectra of $Pd(NH_3)_4^{2+}$ at 2 M and millimolar concentration of ammonia. According to Fig.28, in the millimolar range $Pd(OH)_4^{2-}$ would predominate, whereas the spectroscopic results prove the predominance of $Pd(NH_3)_4^{2+}$.

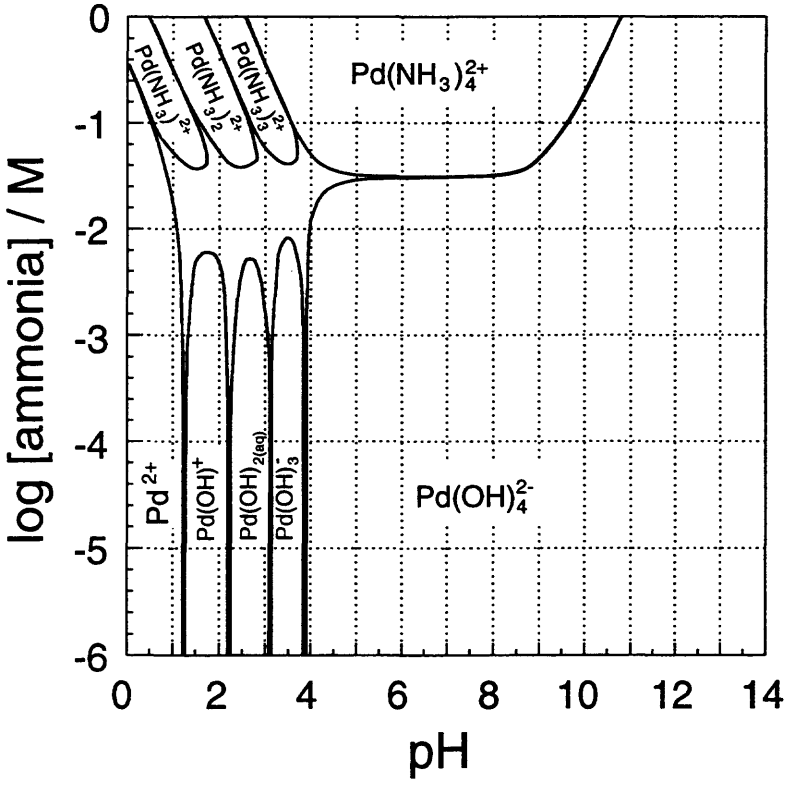

Figure 28: Predominance diagram of the system Pd(II)-H_2O-NH_3. Predicted hydrolysis constants of BROWN & WANNER (1987) are used instead of NABIVANETS & KALABINA (1970) data as in Figs. 25 to 27.

A second, even more serious contradiction concerns the solubility of palladium oxide hydrates. Freshly precipitated palladium oxide hydrate is

soluble in acids like acetic acid as well as in alkali hydroxide solutions; it is insoluble in water. Heating or drying causes the precipitate to loose bound water and makes the product insoluble even in strong acids or bases (GMELIN 1942, p.263-264). Palladium does not form hydroxides with definite water contents, but rather precipitates as palladium oxide hydrates, $PdO \cdot xH_2O$, with varying water concentrations. No crystal structure data are known for these hydrates, in contrast to the well defined PdO. These observations are qualitatively in accord with solubility and hydrolysis data (Fig.29). The solid line for "$Pd(OH)_2$" in Fig. 29 is calculated using the data of NABIVANETS & KALABINA (1970) ignoring poly-nuclear complexes. The solubility product of PdO is not measured directly but calculated from thermochemical data.

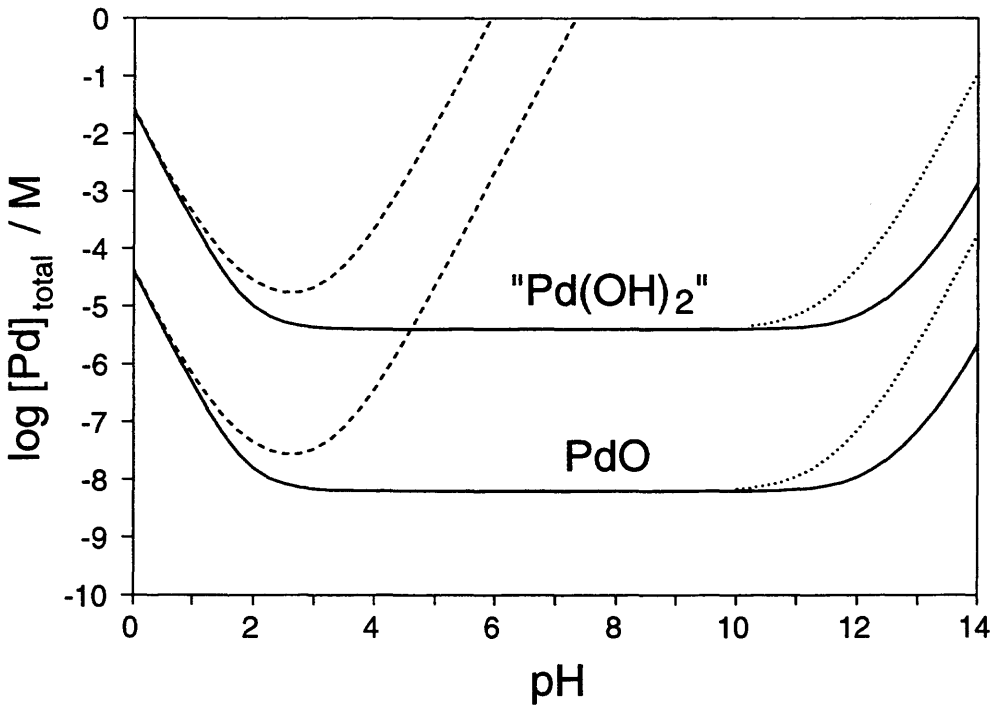

Figure 29: Solubility of "$Pd(OH)_2$", palladium oxide hydrate, and PdO. Solid lines: Data of NABIVANETS & KALABINA (1970) are used ignoring poly-nuclear hydrolysis products; the solubility product of PdO is calculated from thermochemical data. Dashed lines: Hydrolysis constants of BROWN & WANNER (1987) are used instead of NABIVANETS & KALABINA (1970) data. Dotted lines: The consecutive formation constants of $Pd(OH)_3^-$ and $Pd(OH)_4^{2-}$ from NABIVANETS & KALABINA (1970) increased by one order of magnitude each.

The solubility curves for "$Pd(OH)_2$" and PdO reflect the qualitatively observed amphotheric behaviour and the effect of "ageing", i.e. dehydration of the oxide hydrates to the final product, water-free PdO. In contrast to chemical evidence, the predicted hydrolysis constants of BROWN & WANNER (1987) postulate an entirely different solubility behaviour of palladium oxide hydrates (dashed lines in Fig.29).

Using the same solubility products as for computation of the base case (solid lines), even PdO is predicted to be totally soluble in water and slightly alkaline solutions. We could argue that the solubility products may be wrong by several orders of magnitude, but even if we decrease them by ten orders of magnitude, the pronounced asymmetry of predicted solubility behaviour remains. If we adjust the solubility products in such a way that the solids are soluble only in alkaline solutions but not in plain water, we end up with Pd precipitates absolutely insoluble even in strongest acids which contradicts well established chemical knowledge. We conclude that the strict chemical systematics in the Brown and Sylva theory fails in the case of Pd and that the predicted hydrolysis constants for $Pd(OH)_3^-$ and $Pd(OH)_4^{2-}$ are wrong by several orders of magnitude. These predicted constants must not be used in speciation calculations, as they lead to grossly erroneous results as shown in Fig. 28.

Thus for Pd hydrolysis we are left with the experimental data of NABIVANETS & KALABINA (1970). As discussed above, they are not reliable data so we have to bound the uncertainty of the published constants considering additional information. In the range of high pH waters, the stability of $Pd(OH)_3^-$ and $Pd(OH)_4^{2-}$ is of special interest. The data of NABIVANETS & KALABINA (1970) suggest that $Pd(OH)_4^{2-}$ dominates at pH > 13.5 (Figs. 25 and 26). Recently, ZAITSEV et al. (1991) reported the preparation and crystal structure determination of alkaline-earth tetra-hydroxopalladates(II). The crystal structure of $Ba[Pd(OH)_4]\cdot H_2O$ was solved, showing that the Pd-complex has square-planar coordination. The observed intermolecular hydrogen bonds in this structure and the presence of OH deformation bands in the 600 to 1000 cm^{-1} region of IR spectra indicate the formation of metal-hydroxide coordinate bonds, i.e. the formation of $Pd(OH)_4^{2-}$. These crystalline compounds are obtained from solution when the sodium hydroxide concentration ranges from 4 to 8 M NaOH. We conclude therefrom that the stability constant derived by NABIVANETS & KALABINA (1970) for $Pd(OH)_4^{2-}$ is close to its lower limit; an

even lower constant is incompatible with the observed formation of alkaline-earth tetra-hydroxopalladates(II) in 4 M NaOH solutions.
The hydrolysis constants, on the other hand, could be underestimated due to the largely unresolved problems of modelling the formation of poly-nuclear complexes. The values of the consecutive formation constants of $Pd(OH)_3^-$ and $Pd(OH)_4^{2-}$, however, cannot be underestimated by several orders of magnitude, because this would result in pronounced asymmetric solubility behaviour of Pd precipitates, as discussed above. A tentative increase of both constants by one order of magnitude each increases the solubility of Pd in the range of high pH waters by two orders of magnitude (dotted line in Fig.29).

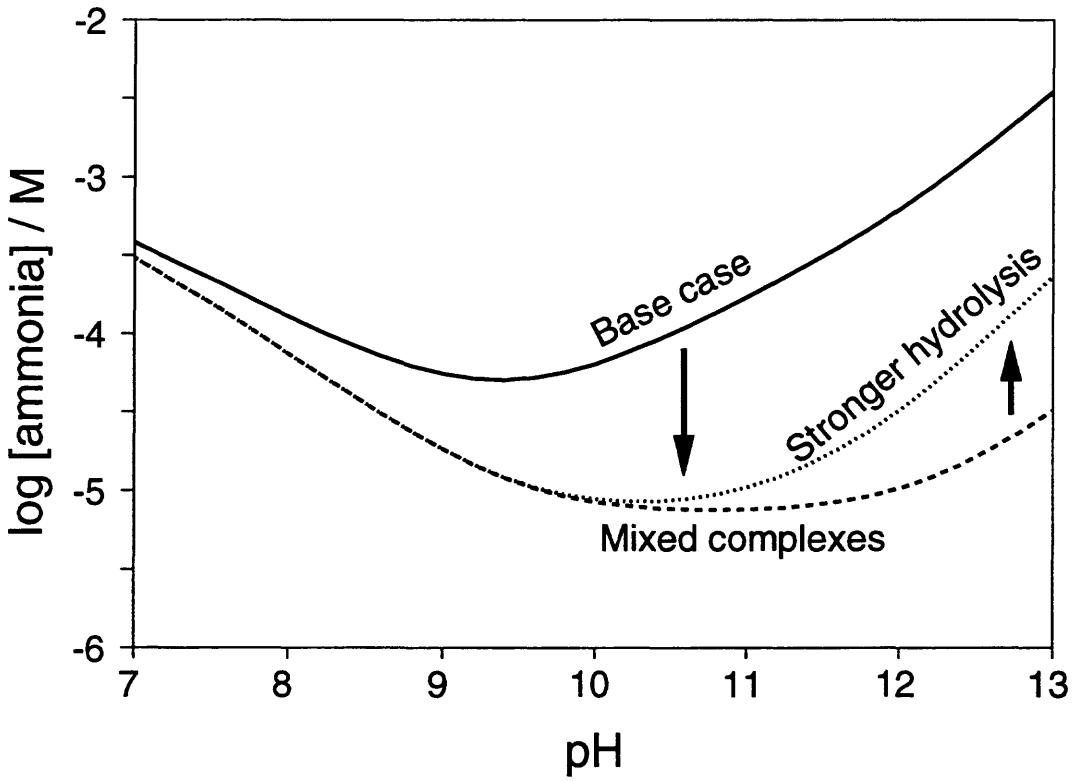

Figure 30: The concentration of ammonia needed in order to complex 50% Pd in solution (valid for [Pd]total $\leq 10^{-6}$ M). Base case (solid line): Stability data of RASMUSSEN & JØRGENSEN (1968) and NABIVANETS & KALABINA (1970), see Fig. 25. Mixed complexes (dashed line): The formation constants of the mixed complexes are estimated by analogy using hydrolysis data of WANNER (1984), see Fig. 26. Stronger hydrolysis (dotted line): The consecutive formation constants of $Pd(OH)_3^-$ and $Pd(OH)_4^{2-}$ from NABIVANETS & KALABINA (1970) increased by one order of magnitude each, see Fig. 29.

This data set is still compatible with the observation of NABIVANETS & KALABINA (1970) that "in the pH range 3 to 11 the solubility remains constant", but may be close to the upper limit of the range that would yield "constant" solubilities.

In summary, using only the published data of NABIVANETS & KALABINA (1970) and RASMUSSEN & JØRGENSEN (1968) results in a too optimistic prediction of the minimum concentration of ammonia needed to significantly influence the Pd-speciation ("Base case" in Fig. 30). Considering mixed ammonia-hydroxo complexes in the calculations lowers the minimum ammonia concentration considerably ("Mixed complexes" in Fig. 30). The probable underestimation of hydrolysis constants, on the other hand, increases the minimum ammonia concentration in the range of high pH waters ("Stronger hydrolysis" in Fig. 30).

5 GENERAL CONCLUSIONS

Oxalate and ligand X were found to be the most important ligands formed during the irradiation of **strong acidic ion exchange resins**. Oxalate has a significant influence on Ni speciation at concentrations above 10^{-4} M in common groundwaters and above 0.1 M in fresh cement pore waters. Such high oxalate concentrations will not be reached in these waters, because the precipitation of calcium oxalate solids limits the oxalate concentration in aqueous solution. For oxalate therefore no significant influence is expected on the Ni speciation in cement pore waters and common groundwaters. No further experimental investigation of this topic seems to be necessary at present.

Ligand X is predicted to show a significant effect on Ni speciations in fresh cement pore waters only if the X concentration exceeds 10^{-3} M. In very late stages of cement degradation an influence may be possible if the X concentration exceeds 10^{-4} M. Both are worst case scenarios assuming rather strong hydrolysis of NiX complexes.

For groundwaters no effect of ligand X is expected as long as its concentration stays below 10^{-6} M. If the total X concentration in common groundwaters exceeds 10^{-3} M a strong influence on Ni speciation is expected. In the range 10^{-6} M < $[X]_{total}$ < 10^{-3} M the effect of X on Ni depends on the geochemical parameters pH, P_{CO_2} and [Ca + Mg] concentration. In addition, the actual value of the estimated CaX stability constant plays an important role in this X concentration range.

It is therefore recommended, in a first step to assess the maximum X concentration expected in the near-field and in the far-field. If these expected concentrations exceed 10^{-6} M in the far-field, the stability constant of the CaX complex should be experimentally determined, as the estimated constant causes an uncertainty of predicted X concentrations up to two orders of magnitude. If the expected X concentrations are higher than 10^{-3} M in the near-field, an investigation of the hydrolysis behaviour of NiX complexes is recommended. The existence of the proposed ternary complexes $NiOHX^-$ and $Ni(OH)_2X^{2-}$ is highly speculative and their influence, if they exist at all, might be overestimated by orders of magnitude. In addition, the existence of sparingly soluble Ca-X solids, probably severely limiting the X concentration, in analogy to Ca-oxalate solids, should be investigated in this case. If in

subsequent safety assessment studies ligand X turns out to become important, the nature of ligand X should also be investigated.
The influence of oxalate as well as citrate, NTA and EDTA on the complexation of actinides and fission products in cement pore waters was investigated in detail in HUMMEL (1993). This study showed that no influence of oxalate, citrate and NTA is expected as long as their concentrations do not exceed 10^{-3} M. As already discussed, oxalate cannot reach such high concentrations due to precipitation of calcium-oxalate solids and thus, no influence of oxalate in cement pore water is expected. In analogy to the results obtained for citrate and NTA, it is concluded that ligand X also has no influence on the complexation of radionuclides other than Ni in cement pore water as long as its concentration remains below the millimolar range.

The chemical (alkaline) degradation of strong acidic ion exchange resins is negligible since the polymers belong to the addition polymers that are in general very stable to alkali.

The most important water soluble degradation products of the radiolytic degradation of **anion exchange resins** are ammonia, methylamine, dimethylamine and trimethylamine. These products do not form stable complexes with most metal cations and consequently cannot influence their speciation under alkaline conditions. A few exceptions, however, are known such as the complexation of amines with Ag^{+}, Co^{2+}, Ni^{2+}, Cu^{2+} and Pd^{2+}. Among those metals, Pd^{2+} forms the strongest complexes and thus, the Pd-ammonia system was investigated in great detail. In cement pore water (pH > 12) Pd is predicted to exist as negatively charged hydroxo complexes, $Pd(OH)_3^{-}$ and $Pd(OH)_4^{2-}$, or, if the concentration of ammonia exceeds a certain limit, as a neutral mixed ammonia-hydroxo complex $Pd(NH_3)_2(OH)_{2(aq)}$. The treshold of ammonia concentration above which Pd is significantly complexed by ammonia is about 10^{-4} M with an uncertainty of about one order of magnitude. Even rather pessimistic assumptions, which are still compatible with the qualitative and quantitative chemical observations, do not result in values below 10^{-5} M ammonia.
In groundwaters the concentration of ammonia needed to significantly influence Pd speciation always exceeds 10^{-5} M. The significant ammonia concentration, however, is not only dependent on pH as suggested by Fig. 30. Strong competition by formation of Pd-chloro and probably Pd-carbonato

complexes further will increase the limit of significant ammonia content depending on the chloride and carbonate concentration of the groundwater. Due to its rather weak hydrolysis reactions, Ag^{+} is expected also to exhibit a low treshold of ammonia concentration, whereas for Co^{2+}, Ni^{2+} and Cu^{2+} this treshold is shifted close to the molar range in cement pore waters.
Beside these amines, other (still) unknown products are formed. These additional compounds do not have important complexing properties.

For **mixed bed resins**, only small amounts of amines are produced during irradiation. A larger amount of an unknown compound, probably containing sulphur and nitrogen in its structure, is formed. These products, however, do not have complexing properties towards Eu.

In absence of a radiation field, only very small amounts of carbon could be detected in the alkaline water in equilibrium with the resins studied (for both anion and mixed bed resins). The molecular form of the carbon is unknown, but the compounds have no significant complexing properties towards Eu.

The main conclusion of this study is that the radiolytic and chemical (alkaline) degradation products of organic ion exchange resins in general will have no or only negligible influence on the speciation of radionuclides in a cementitious near field and, as such, need not to be considered in appropriate safety assessment models. Exceptions from this general statement are the strong complexing ligand X, but only if its concentration is expected to exceed 10^{-3} M, and the amine-loving metals Ag and Pd. These cases should be considered explicitely in performance assessment within the confinements outlined in this study.

6. REFERENCES

AHMED, M.T., CLAY, P.G. & HALL, G.R. (1966): Radiation induced decomposition of ion-exchange resins. Part II. The mechanism of the deamination of anion-exchange resins. Journal of the Chemical Society B, 1155-1157.

ANDEREGG, G. & MALIK, S.C. (1976): Komplexone XLVII. The Stability of Palladium(II) Complexes with Aminopolycarboxylate Anions. Helvetica Chimica Acta 59, 1489 - 1511.

ANDEREGG, G. & YAN, Q. : unpublished results, cited in WANNER 1984

BAES, C. F. Jr. & MESMER, R. E. (1986): The Hydrolysis of Cations. Krieger Publishing Company, Malabar, Florida, USA (Original Edition 1976, Reprint Edition 1986).

BAEYENS, B. & McKINLEY, I.G. (1989): A PHREEQE Database for Pd, Ni and Se. PSI-Bericht 34, Paul Scherrer Institute, Villigen, Switzerland. Also published as Nagra Technical Report NTB 88-28, Nagra, Wettingen, Switzerland.

BAEYENS, B. & BRADBURY, M.H. (1991): A physico-chemical Characterisation Technique for Determining the Pore-Water Chemistry in argillaceous Rocks. PSI-Bericht 103, Paul Scherrer Institute, Villigen, Switzerland. Also published as Nagra Technical Report NTB 90-40, Nagra, Wettingen, Switzerland.

BAEYENS, B. & BRADBURY, M. H. (1994): Physico-chemical characterisation and calculated in situ porewater chemistries for a low permeability Palfris marl sample from Wellenberg. PSI Bericht Nr. 94-19, Paul Scherrer Institut, Villigen, Switzerland. Also published as Nagra Technical Report NTB 94-22, Nagra, Wettingen, Switzerland.

BARLETTA, R.E., SWYLER, K.J., CHAN , S.F. & DAVIS, R.E. (1982): Solidification of Irradiated Epicor-II Waste Products. NUREG/CR-2969 and BNL-NUREG-51590, Brookhaven National Laboratory.

BAUMANN, E.W. (1966): Gamma irradiation of individual and mixed ion exchange resins. Journal of Chemical and Engineering Data 11, 256-260.

BERNER, U. (1990): A Thermodynamic Description of the Evolution of Pore Water Chemistry and Uranium Speciation during the Degradation of Cement. PSI-Bericht 62, Paul Scherrer Institute, Villigen, Switzerland. Also published as Nagra Technical Report NTB 90-12, Nagra, Wettingen, Switzerland.

BILINSKI, H. & SCHINDLER, P. (1982): Solubility and equilibrium constants of lead in carbonate solutions (25 °C, I = 0.3 mol dm^{-3}). Geochimica et Cosmochimica Acta 46, 921-928.

BJERRUM, J. (1941): Metal Ammine Formation in Aqueous Solution. P. Haase and Son, Copenhagen, 1941; reprinted 1957.

BJERRUM, J. (1950): On the Tendency of the Metal Ions toward Complex Formation. Chemical Reviews, 46, 381-401.

BOVEY, F.A. (1958): The Effects of Ionizing Radiation on Natural and Synthetic High Polymers. Interscience Publishers Inc., New York.

BRITTON, H. T. S. & WILLIAMS, W. G. (1935): Electrometric Studies of the Precipitation of Hydroxides. Part XIII. The Constitution of Aqueous Solutions of Silver Oxide in Ammonia, Mono-, Di-, and Trimethylamine and -ethylamine, Pyridine and Ethylenediamine; with a Note on the Dissociation Constants of the Amines. Journal of the Chemical Society, 796-801.

BROWN, P. L. & WANNER, H. (1987): Predicted Formation Constants Using the Unified Theory of Metal Ion Complexation. Organisation for Economic Co-operation and Development, Nuclear Energy Agency (OECD-NEA), Paris.

BROWN, P. L. & SYLVA, R. N. (1987): Unified Theory of Metal Ion Complex Formation Constants. Journal of Chemical Research (S): 4-5, (M): 0110-0181; and Australian Atomic Energy Commission, Research Establishment, Lucas Heights Research Laboratories, AAEC/E656.

BRUNO, J., WERSIN, P. & STUMM, W. (1992): On the influence of carbonate in mineral dissolution: II. The solubility of $FeCO_{3(s)}$ at 25 °C and 1 atm total pressure. Geochimica et Cosmochimica Acta 56, 1149-1155.

BURTON, M. & PATRICK, W.N. (1954): Radiation Chemistry of Mixtures : Cyclohexane and Benzene-d_6[1,2]. Journal of Physical Chemistry 58, 421-423.

BYRNE, R. H. & MILLER, W. L. (1985): Copper(II) carbonate complexation in seawater. Geochimica et Cosmochimica Acta 49, 1837-1844.

CHARLESBY, A. & MOORE, N. (1964): Comparison of gamma and ultra-violet radiation effects in polymethyl methacrylate at higher temperatures. International Journal of Applied Radiation and Isotopes 15, 703-708.

DAGEN A. (1980): Wirkung ionisierender Strahlung auf Bitumen und Bitumen-Salz Gemische. SAAS-253, Staatliches Amt für Atomsicherheit und Strahlenschutz , Berlin.

ESCHRICH, H. (1980): Properties and Long-term Behaviour of Bitumen and Radioactive Waste-Bitumen Mixtures. KBS 80-14.

FERRI, D., GRENTHE, I., HIETANEN, S. & SALVATORE, F. (1987a): Studies on Metal Carbonate Equilibria. 17. Zinc(II) Carbonate Complexes in Alkaline Solutions. Acta Chemica Scandinavica, A41, 190-196.

FERRI, D., GRENTHE, I., HIETANEN, S. & SALVATORE, F. (1987b): Studies on Metal Carbonate Equilibria. 18. Lead(II) Carbonate Complexes in Alkaline Solutions. Acta Chemica Scandinavica, A41, 349-354.

GANGWER, T.E., GOLDSTEIN M. & PILLAY K.K.S. (1973): Radiation Effects on Ion Exchange Materials. BNL 50781, Brookhaven National Laboratory, Upton, New York.

GMELIN (1942): Gmelins Handbuch der Anorganischen Chemie. Palladium. Lieferung 2, System-Nummer 65, 1942 (Photomechanischer Nachdruck 1968), Verlag Chemie GmbH, Weinheim/Bergstrasse.

GREENFIELD, B.F., MORETON, A.D., SPINDLER M.W., WILLIAMS S.J. & WOODWARK, D.R. (1992): the effects of degradation of organic materials in the near field of a radioactive waste repository. Materials Research Society, Symposium Proceedings 257, 299-306.

GRENTHE, I., FUGER, J., KONINGS, R. J. M., LEMIRE, R. J., MULLER, A. B., NGUYEN-TRUNG, C. & WANNER, H. (1992): Chemical Thermodynamics. Volume 1. Chemical Thermodynamics of Uranium (H. Wanner and I. Forest, eds., OECD Nuclear Energy Agency). North-Holland Elsevier Science Publishers B. V., Amsterdam.

HALL, G.R. & STREAT, M. (1963): Radiation-induced decomposition of ion-exchange resins. Part I. Anion exchange resins. Journal of the Chemical Society 5, 5205-5211.

HUMMEL, W. (1992): A New Method to Estimate the Influence of Organics on the Solubility and Speciation of Radionuclides ("The Backdoor Approach"). Radiochimica Acta 58/59, 453-460.

HUMMEL, W. (1993): Organic Complexation of Radionuclides in Cement Pore Water: A Case Study. PSI Technical Report TM-41-93-03, Paul Scherrer Institute, Villigen, Switzerland.

ILCHEVA, L. & BJERRUM, J. (1976): Metal Ammine Formation in Solution. XVII. Stability Constants of Copper(II) Methylamine and Diethylamine Complexes Obtained from Solubility Measurements with Gerhardtite, $Cu(OH)_{1.5}(NO_3)_{0.5}$. Acta Chemica Scandinavica A30, 343-350.

IRVING, H. & WILLIAMS, R. J. P. (1953): The Stability of Transition-metal Complexes. Journal of the Chemical Society, 3192-3210.

IZATT, R. M., EATOUGH, D. & CHRISTENSEN, J. J. (1967): A Study of $Pd^{2+}_{(aq)}$ Hydrolysis. Hydrolysis Constants and the Standard Potential for the Pd/Pd^{2+} Couple. Journal of the Chemical Society, 1301-1304.

KÖRNER, W. & DAGEN, A. (1971): On the radiation stability of bituminized radioactive wastes. Isotopenpraxis 7, 296-302.

KOTRLY, S. & SUCHA, L. (1985.): Handbook of Chemical Equilibria in Analytical Chemistry. Ellis Horwood Limited, Chichester, England.

LANGMUIR, D. (1979): Techniques of Estimating Thermodynamic Properties of Some Aqueous Complexes of Geochemical Interest". In Chemical Modelling in Aqueous Systems, E.A. Jenne (ed.). ACS Symposium Series 93, American Chemical Society.

LEE, J. H. & BYRNE, R. H. (1993): Complexation of trivalent rare earth elements (Ce, Eu, Gd, Tb, Yb) by carbonate ions. Geochimica et Cosmochimica Acta 57, 295-302.

MANION, J.P. & BURTON, M. (1952): Radiolysis of Hydrocarbon Mixtures. Journal of Physical Chemistry 56, 560-569.

MARTELL A. E. & SMITH, R. M. (1977): Critical Stability Constants. Volume 3: Other Organic Ligands. Plenum Press, New York and London.

MARTELL A. E. & SMITH, R. M. (1982): Critical Stability Constants. Volume 5: First Supplement. Plenum Press, New York and London.

McCONNELL, J.W. Jr., JOHNSON, D.A. & SANDERS, R.D. Sr. (1993): Radiation degradation in organic ion exchange resins. Waste Management 13, 65-75.

MOHORCIC, G. & KRAMER, V. (1968): Gases evolved by ^{60}Co radiation degradation of strongly acidic ion exchange resins. Journal of Polymer Science C, 4185-4195.

MÜLLER, H. (1853): Ueber die Palladamine. Liebigs Annalen der Chemie 86, 341-368.

NABIVANETS, B. I. & KALABINA, L. V. (1970): State of Palladium(II) in Perchlorate Solutions. Russian Journal of Inorganic Chemistry, 15, 818-821.

NAGRA (1992): Nukleare Entsorgung Schweiz - Konzept und Realisierungsplan. Nagra Technical Report NTB 92-02, Nagra, Wettingen, Switzerland.

NAGRA (1994): Endlager für schwach- und mittelaktive Abfälle (Endlager SMA). Bericht zur Langzeitsicherheit des Endlagers SMA am Standort Wellenberg (Gemeinde Wolfenschiessen, NW). Nagra Technical Report NTB 94-06, Nagra, Wettingen, Switzerland.

ÖSTHOLS, E., BRUNO, J. & GRENTHE, I. (1994): On the influence of carbonate on mineral dissolution: III. The solubility of microcrystalline ThO_2 in CO_2-H_2O media. Geochimica et Cosmochimica Acta 58, 613-623.

PEARSON, F. J., Jr. & SCHOLTIS, A. (1993): Chemistry of Reference Waters of the Crystalline Basement of Northern Switzerland for Safety Assessment Studies. Nagra Technical Report NTB 93-07, Nagra, Wettingen, Switzerland.

PERRIN, D.D. & DEMPSEY, B. (1974): Buffers for pH and Metal Ion Control, Chapman and Hall Ltd., London, England.

PLUMMER, L. N. & BUSENBERG, E. (1982): The solubilities of calcite, aragonite and vaterite in CO_2-H_2O solutions between 0 and 90 °C, and an evaluation of the aqueous model for the system $CaCO_3$-CO_2-H_2O. Geochimica et Cosmochimica Acta 46, 1011-1040.

RABENSTEIN, D. L., OZUBKO, R., LIBICH, S., EVANS, C. A., FAIRHURST, M. T. & SUVANPRAKORN, C. (1974): Nuclear Magnetic Resonance Studies of the Solution Chemistry of Metal Complexes. X. Determination of the Formation Constants of the Methylmercury Complexes of Selected Amines and Aminocarboxylic Acids. Journal of Coordination Chemistry 3, 263-271.

RAI, D., FELMY, A. R. & MOORE, D. A. (1991): Thermodynamic Model for Aqueous Cd^{2+}-CO_3^{2-} Ionic Interactions in High-Ionic-Strength Carbonate Solutions, and the Solubility Product of Crystalline $CdCO_3$. Journal of Solution Chemistry, 20, 1169-1187.

RASMUSSEN, L. & JØRGENSEN, C. L. (1968): Palladium(II) Complexes I. Spectra and Formation Constants of Ammonia and Ethylenediamine Complexes. Acta Chemica Scandinavica 22, 2313-2323.

REXER, E. & WUCKEL, L. (1965): Chemische Veränderungen von Stoffen durch energiereiche Strahlung. VEB Deutsche Verlag für Grundstoffindustrie, Leipzig, Deutschland.

RORABACHER, D. B. & MELENDEZ-CEPEDA, C. A. (1971): Steric Effects on the Kinetics and Equilibria of Nickel(II)-Alkylamine Reactions in Aqueous Solution. Journal of the American Chemical Society, 93, 6071-6076.

ROSSOTTI, J.C. & ROSSOTTI, H. (1961): The Determination of Stability Constants and other Equilibrium Constants in Solution. Mc. Graw Hill Book Company Inc., New York-Toronto-London.

SCHNABEL, W. (1978) : Degradation by high Energy Radiation. In : Aspects of Degradation and Stabilization of Polymers, H.H.G. Jellinek ed.; Elsevier Scientific Publishing Company, Amsterdam-Oxford-New York.

SCHUBERT, J., RUSSELL, E.R. & MYERS, L.S., Jr. (1950): Dissociation constants of radium-organic acid complexes measured by ion exchange. Journal of Biological Chemistry 185, 387-398.

SCHUBERT, J. & LINDENBAUM, A. (1952): Stability of alkaline earth-organic acid complexes measured by ion exchange. Journal of the American. Chemical Society 74, 3529- 3532

SCHUBERT, J., LIND, E.L., WESTFALL, W.M., PFLEGER, R. & LI, N.C. (1958): Ion exchange and solvent-extraction studies on Co(II) and Zn(II) complexes of some organic acids. Journal of the American. Chemical Society 80, 4799-4802.

SEMUSHIN, A.M., SHISTYAKOV, D.A. & KUZIN, I.A. (1979): Investigation of the influence of oxygen on the radiolysis of the sulfonic acid cation-exchanger KU-2-8. Translated from: Zhurnal Prikladnoi Khimii 52 (1979), 294-299. Journal of Applied Chemistry of the USSR 36, 268-271.

SHIGEMATSU, T. & OSHIO, T. (1959): Effect of cobalt-60 gamma radiation on ion exchange resins. Bulletin of the Institute for Chemical Research-Kyoto University 37, 349-352.

SISMAN, O., PARKINSON, W.W. & BOPP, C.D. (1963): Polymers. In: Radiation Effects on organic Materials, R.O. Bolt & J.G. Carroll eds.; Academic Press, New York & London.

SMITH, R. M. & MARTELL, A. E. (1989): Critical Stability Constants. Volume 6: Second Supplement. Plenum Press, New York and London.

SWYLER, K.J., DODGE, C.J. & DAYAL, R. (1983): Irradiation Effects on the Storage and Disposal of Radwaste containing organic Ion-exchange Media. NUREG/CR-3383 and BNL-NUREG-51691, Brookhaven National Laboratory.

VAN LOON, L.R. & KOPAJTIC, Z. (1990): Complexation of Cu^{2+}, Ni^{2+} and UO_2^{2+} by Radiolytic Degradation Products of Bitumen. PSI-Bericht 66, Paul Scherrer Institute, Villigen, Switzerland. Also published as Nagra Technical Report NTB 90-18, Nagra, Wettingen, Switzerland.

VAN LOON, L.R. & KOPAJTIC, Z. (1991): Complexation of Cu^{2+}, Ni^{2+} and UO_2^{2+} by radiolytic degradation products of bitumen. Radiochimica Acta 54, 193-199.

WANNER, H. (1984): Bildung und Hydrolyse von Palladium-Komplexen mit Pyridin, 2,2'-Bipyridyl und 1,10-Phenanthrolin. Dissertation ETH Nr. 7628, Eidgenössische Technische Hochschule Zürich, Switzerland.

WENK, M. (1993): Wachstum mikrobieller Mischkulturen unter anaeroben, alkalischen Bedingungen. Inaugural-Dissertation, Universität Zürich. Also published as Nagra Technical Report NTB 93-33, Nagra, Wettingen, Switzerland.

ZAITSEV, B. E., IVANOV-EMIN, B. N., PETRISHCHEVA, L. P., IL'INETS, A. M., BATURIN, N. A., REGEL', L. L. & DOLGANEV, V. P. (1991): Preparation and structure of alkaline-earth metal hydroxopalladates(II). Translated from: Zhurnal Neorganicheskoi Khimii 36 (1991), 134-140. Russian Journal of Inorganic Chemistry 36, 74-77.

7. ACKNOWLEDGEMENTS

The authors would like to thank S. Granacher, A. Laube and S. Stallone for their assistance with the experimental work. Special thanks goes to Prof. I. Grenthe (RIT, Stockholm) for carefully reviewing the manuscript and also to Drs. U. Berner, E. Curti, J. Pearson (PSI) and I. Hagenlocher (NAGRA) for giving useful suggestions to improve the text.
Finally we thank the Swiss National Cooperative for the Disposal of Radioactive Waste (NAGRA) for the partial financial support.